

Development of an optimisation framework for offshore grid infrastructure

Application of a capacity expansion problem on the Baltic Sea Region

Felix Jakob Fliegner

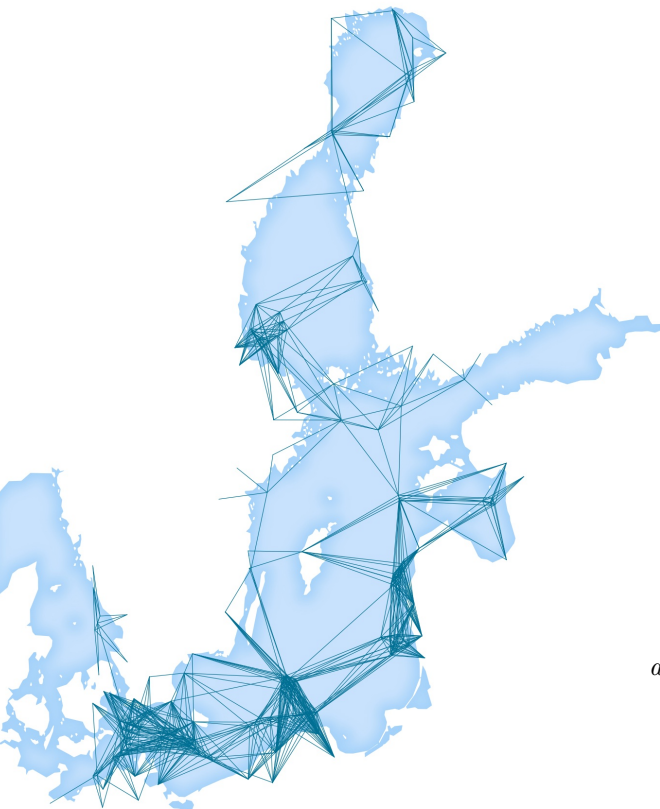
Matriculation number: 364170
Reginhardstraße 8, 13409 Berlin
fliegner@campus.tu-berlin.de
+49 151 233 859 14

Supervisors

Prof Christian von Hirschhausen (WIP, TU Berlin)
Prof Ruud Egging-Bratseth (IØT, NTNU Trondheim)
Richard Weinhold (WIP, TU Berlin)
Thomas Köbinger (System of the Future, 50hertz)
Jan Voet (System of the Future, Elia Group)

*Master thesis in the dual degree program
Sustainable Energy Systems and Markets (NTNU)
and Industrial Engineering - Electrical Engineering (TU Berlin)*

Berlin, Trondheim: 14.09.2020



Eidesstattliche Erklärung

Hiermit erkläre ich, dass ich die vorliegende Arbeit selbstständig und eigenständig sowie ohne unerlaubte fremde Hilfe und ausschließlich unter Verwendung der aufgeführten Quellen und Hilfsmittel angefertigt habe. Die Arbeit stellt ausschließlich meine eigene Forschungsarbeit dar und lässt keinen Rückschluss auf andere Positionierungen der beteiligten Partner zu. Ich unterliege keinem Interessenkonflikt.

I hereby declare that I have produced the present work independently and self-reliant, without unauthorized assistance from others and only by using the listed sources and aids. This work solely represents my view on the matter and allows no implication on strategic or other positioning of the affiliated supervising parties. I declare no conflict of interest other than my praise for the open source toolchain utilised in this project.

Berlin, 14.09.2020



Felix Jakob Fliegner

Preface

This thesis project belongs to a joined master program between NTNU Trondheim and TU Berlin. It has been drafted in collaboration with the German transmission system operator 50hertz being part of the German-Belgian Elia Group. I am thankful for the patience and confidence of my colleagues at Elia Group in Brussels and 50hertz in Berlin to let me dive into the world of offshore transmission assets. I felt the high relevance and resonance of my intermediate research results at any time. My supervisor at TU Berlin was my closest supporter, introducing me to the novel JULIA JuMP framework and giving ever helpful and cheerful tips along the way. NTNU Trondheim supported me in quite a set of individual study and research plans, I am proud that I now have something to give back to my supervisors and fellow students. Finally I would like to highlight the ever caring yet always critical support of my dear friend, who introduced me into the world of geodata processing in QGIS.

The analysis of geodata in a geographic information system for the benefit of market modelling is the underlying notion of this thesis. This discipline turned out most relevant for solving the task at hand, while being the least familiar for me. Looking beyond the academic findings, I encourage all fellows of my profession to try out crossovers with other scientific disciplines themselves. Solving a problem of our own discipline with methods from an unknown one is not just exciting, it broadens the picture for investigating the energy system of the future.

Thank you very much,

Mit herzlichem Dank,

Takk så mye,

Felix Jakob Fliegner

Abstract

The future European energy transition is dominated by offshore wind power generation. In face of a considerable power potential in the Baltic Sea and ambitions to deploy it, the question arises which future offshore topology can facilitate large scale power energy evacuation from the sea. While wind farm connections and interconnectors between countries used to be optimised separately in the past, recent studies suggest the added value of their integrated optimisation into an offshore grid.

The elementary building block of such an offshore grid is the hybrid asset, i.e. a combination of wind farm connection and market interconnection. Optimising the trajectory and strength of future hybrid assets results in a transmission capacity expansion problem with many discrete decisions to be made. It is commonly investigated with the help of tailored scenarios to limit the computational complexity of analysis. While such an approach is easily set up, it suffers from a manual identification of prospective transmission corridors and bundling of assumed wind farms, before a market model can solve the expansion problem. This thesis proposes a methodological framework which explicitly not pre-defines cluster locations, interconnector trajectories and cross zonal future transmission capacities. Instead this is endogenized into the analysis.

The contribution of this thesis is the development of a two-step optimisation framework, where a presolve in a geographic information system (GIS) enhances the common practice market modelling. Analysing the spatial density distribution and geometric relation of offshore wind farms among each other, a clustering procedure in the form of a MiniMax game is presented. Two group partitioning algorithms run against each other to create an exhaustive, yet non-redundant graph topology of permissive links and nodes. Subsequently, a mixed-integer linear market model (MILP) performs an integrated dispatch and investment optimisation on the permissive graph topology. Following an investment cost minimisation objective, it activates links and nodes wherever efficient for wind power evacuation and power market interconnection.

The developed framework is demonstrated at the example of the Baltic Sea Region for the target year 2040. Selected offshore wind farms are fixed in the Baltic Sea and given to the model for clustering and grid connection. The results reveal clustering prospects and interconnection options among wind farms and countries well beyond the commonly discussed corridors in the literature. The high-level topology optimisation creates a pan-Baltic offshore grid with a tendency towards strong DC backbones and clustered wind farms. Only a minority of wind farms is indeed connected radially. Instead, transmission paths are bundled as much as possible and mostly realised as hybrid assets. A sensitivity analysis reveals that the future Baltic offshore grid is sensitive for wind farm location assumptions and pre-defined interconnectors in the model. Not least, the capability of the onshore grid to integrate the influx of offshore wind power and the level of detail it is modelled in directly reflects on the topology results for the offshore grid.

None of the presented topology results should be interpreted as a best estimate or a ranking of future development paths. Their mere purpose is the demonstration of the novel GIS analysis approach in the context of transmission expansion studies. It is shown that it improves computational performance, enhances data uniformity and facilitates parametrised scenario building. Finally, it highlights the approach of leveraging readily available geodata for large regional scopes such as the entire Baltic Sea Region. This work stresses the relevance of a pan-Baltic offshore grid optimisation.

Keywords – Offshore Grids, GIS Analysis, MILP

Zusammenfassung

Die Zukunft der europäischen Energiewende liegt in der offshore Windenergie. Angesichts eines beträchtlichen Windkraftpotentials in der Ostsee und zahlreicher Bestrebungen, dieses zu nutzen, stellt sich die Frage, welche künftige Offshorenetztopologie die großen Mengen an erzeugtem Strom abtransportieren kann. Während Windparkanschlüsse und Interkonnektoren zwischen den Ländern in der Vergangenheit getrennt voneinander optimiert wurden, legen neuere Studien den Mehrwert ihrer integrierten Optimierung in einem Offshorenetz nahe.

Elementare Bausteine eines solchen Offshorenetzes sind hybrid assets, also die Kombinationen aus Windparkanschlüssen und Interkonnektoren in einem Übertragungssystem. Deren optimaler zukünftiger Trassenverlauf und Leistung kann in einem Kapazitätsausbauproblem beschrieben werden, bei dem viele diskrete Entscheidungen getroffen werden müssen. Zur Begrenzung des Rechenaufwandes werden solche Optimierungsprobleme häufig szenariobasiert untersucht. Diese sind zwar leicht aufzustellen, werden jedoch maßgeblich durch exogene Annahmen in ihrem Endergebnis beeinflusst. Die angenommenen Übertragungskorridore und Cluster von Windparks limitieren den Lösungsraum sehr stark, bevor ein Marktmodell das Ausbauproblem lösen kann. Die vorliegende Arbeit schlägt ein neues methodisches Vorgehen vor, welches die Clusterung von Windparks, Trassenverläufe und grenzüberschreitende Übertragungskapazitäten endogenisiert, also nicht manuell vorgibt.

Der Beitrag dieser Arbeit besteht in der Entwicklung eines zweistufigen Optimierungstools, bei dem ein geographisches Informationssystem (GIS) der sonst üblichen Marktmodellierung vorgeschaltet wird. Es analysiert die räumliche Dichteverteilung und geometrische Beziehung von Offshore-Windparks zueinander. Somit ermöglicht es eine Vorauswahl des Lösungsraumes. Dazu wird ein Clusterungsverfahren in Form eines MiniMax-Spiels vorgestellt. Zwei Partitionsalgorithmen laufen gegeneinander, um eine erschöpfende, aber nicht redundante Topologie von möglichen Knoten und Kanten zu erstellen. Anschließend führt ein gemischt ganzzahliges lineares Marktmodell (mixed-integer linear market model, MILP) eine integrierte Dispatch- und Investitionsoptimierung auf dem identifizierten Graphen durch. Mit dem Ziel der Kostenminimierung werden Leitungen auf Kanten und Plattformen an Knoten aktiviert, wo immer dies für den Abtransport von Windstrom und die Verbindung von Marktgebieten effizient ist.

Die Methode am Beispiel der Ostseeregion für das Zieljahr 2040 demonstriert. Ausgewählte offshore Windparks werden in der Ostsee fixiert und dem Modell für Clusterbildung und Netzanbindung übergeben. Die Ergebnisse zeigen Clusterungsperspektiven und Vernetzungsoptionen zwischen Windparks und Ländern auf, die weit über die in der Literatur allgemein diskutierten Korridore hinausgehen. Die abstrakte Topologieoptimierung schafft ein pan-Baltisches Offshorenetz mit einer Tendenz zu starken DC-Backbones und Windparkclustern. Nur wenige Windparks werden radial angeschlossen. Stattdessen werden die Übertragungswege so weit wie möglich gebündelt und meist als hybrid assets realisiert. Eine Sensitivitätsanalyse zeigt, dass das künftige Ostsee-Offshorenetz sensibel auf Standortannahmen für Windparks und vordefinierte Verbindungsleitungen im Modell reagiert. Nicht zuletzt wirkt sich die Fähigkeit des Onshorenetzes, die offshore Windenergie zu integrieren und die Art und Weise wie es modelliert wird direkt auf die Topologieergebnisse für das Offshorenetz aus.

Keines der vorgestellten Topologieergebnisse sollte als eine Maximalabschätzung oder eine Rangfolge zukünftiger Entwicklungspfade interpretiert werden. Sie dienen lediglich der Demonstration des neuartigen GIS-Analyseansatzes im Rahmen von Studien zum offshore Netzausbau. Es wird gezeigt, dass er die Komplexität der Lösungsfindung verringert, die Integrität der Inputdaten erhöht und die Erstellung parametrisierter Szenarien erleichtert. Schließlich wird der Mehrwert der Nutzung leicht verfügbarer Geodaten für die Analyse großer Regionen wie der Ostsee hervorgehoben. Diese Arbeit betont die Bedeutung einer gesamtbaltischen offshore Netzoptimierung.

Sammendrag

Den fremtidige europeiske energiovergangen domineres av offshore vindkraftproduksjon. I møte med et betydelig kraftpotensiale i Østersjøen og ambisjoner om å utvikle den, fremkommer spørsmålet om hvilken fremtidige offshore-topologi som kan legge til rette for utvinning av kraftenergi fra havet i stor skala. Mens vindkraftforbindelser og mellomlandsforbindelser tidligere var optimalisert hver for seg, antyder nyere studier på at integrert optimalisering til et offshore-nett vil gi en verdiøkning.

Den grunnleggende byggesteinen for et slikt offshore-nett er hybrid assets, dvs. en kombinasjon av vindkraftforbindelse og markedssammenkobling. Optimalisering av retningen og styrken for fremtidige hybrid assets resulterer i et utvidelsesproblem for overføringskapasitet, med mange distinkte beslutninger som må tas. Dette undersøkes ofte ved hjelp av skreddersydde scenarier for å begrense beregningskompleksiteten i analysen. Selv om en slik tilnærming er enkel å sette opp, rammes den av en manuell identifisering av potensielle overføringskorridorer og sammenbinding av antatte vindparker, før en markedsmodell kan løse utvidelsesproblemet. Denne rapporten foreslår et metodisk rammeverk som eksplisitt ikke forhåndsdefinerer gruppeområder, sammenkoblingsbaner eller fremtidige overføringskapasiteter på tvers av soner.

Bidraget fra denne rapporten er utviklingen av et to-trinns optimaliseringsrammeverk, hvor en forhåndsløsning i et geographic information system (GIS) forbedrer den vanlige markedsmodelleringen. Med analyser av romtetthetsfordelingen og den geometriske relasjonen til offshore vindmølleparker seg i mellom, presenteres en grupperingsprosedyre i form av et MiniMax game. To gruppepartisjoneringsalgoritmer kjøres mot hverandre for å skape en uttømmende men ikke-overflødig graf-topologi av tillatelige sammenkoblinger og noder. Deretter utfører en mixed-integer linear market model (MILP) en integrert forsendelses- og investeringsoptimalisering på den tillatende graf-topologien. Etter en målsetning om minimering av investeringskostnader, aktiverer den koblinger og noder der det er effektivt for overføring av vindkraft og sammenkobling av kraftmarkedet.

Det utviklede rammeverket demonstreres med Østersjøregionen for målåret 2040 som eksempel. Utvalgte havparker er satt til Østersjøen og tilføres modellen for gruppering og nettilkobling. Resultatene viser grupperingsutsikter og alternativer for sammenkobling blant vindparker og land langt utover de korridorene som ofte diskuteres i litteraturen. Topologioptimaliseringen er på høyt nivå og skaper et pan-baltisk offshore-nett med en tendens til sterke DC-ryggrader og grupperede vindparker. Det er faktisk kun et mindretall av vindparkene som er tilkoblet radielt. I stedet samles overføringsbaner i så stor grad som mulig og realiseres i hovedsak som hybrid assets. En sensitivitetsanalyse avslører at det fremtidige baltiske offshore-nettet er sensitivt for lokale forutsetninger for vindparker og for forhåndsdefinerte sammenkoblinger i modellen. Ikke minst reflekteres landnettets evne til å integrere tilstrømmingen av offshore-vindkraft direkte på topologieresultatene for offshore-nettet.

Ingen av de presenterte topologieresultatene skal tolkes som et beste estimat eller en rangering av fremtidige utviklingsveier. Deres hensikt er å demonstrere den nye GIS-analyse-tilnærmingen i sammenheng med utvidelsesstudier. Det har blitt vist at dette forbedrer beregningsytelsen, forbedrer dataens ensartethet og tilrettelegger for parametrisert scenariobygging. Til slutt fremhever den tilnærmingen hvor man utnytter lett tilgjengelige geodata for store regionale områder slik som hele Østersjøregionen. Dette arbeidet understreker relevansen av en pan-baltisk offshore nettoptimalisering.

Contents

1	Introduction	1
1.1	Research Question	1
1.2	Previous work on offshore transmission expansion planning	2
1.3	Scope of analysis	4
2	Input data	6
2.1	Framing the Baltic Sea Region	6
2.1.1	Geographic and jurisdictional overview of the Baltic Sea	6
2.1.2	Optimal wind power sites in the Baltic Sea	8
2.2	High-level offshore grid technology screening	12
2.2.1	Building blocks of an offshore grid infrastructure	13
2.2.2	Parametrisation for the optimisation problem	15
2.3	Initial setpoint of the analysis	17
2.3.1	Generation capacity and fuel types	17
2.3.2	Climate year and availability time series	18
2.3.3	Start grid	21
3	Methodology	22
3.1	Pre-Processing in GIS	24
3.1.1	GIS analysis tasks	24
3.1.2	Added value of GIS analysis	25
3.1.3	Elementary building blocks of GIS analysis	26
3.1.4	Spatial analysis in GIS	28
3.1.5	Geometric clustering in GIS	30
3.2	Power Market Description	36
3.2.1	Building blocks of the optimisation model	36
3.2.2	Definition of a linear cost function	38
3.2.3	Completing the objective function	40
3.2.4	Constraining the linear transport problem	40
3.3	Post-Processing	44
4	Results	46
4.1	Presolving topology and dispatch	47
4.1.1	GIS topology output	47
4.1.2	Warm start for market model	53
4.2	Base case topology optimisation	55
4.2.1	Grid topology result	55
4.2.2	Concentration of grid infeed	59
4.2.3	Utilisation and redundancy	62
4.2.4	Investment cost breakdown	66
4.3	Sensitivity of topology and dispatch	67
4.3.1	No preset interconnectors	69
4.3.2	Wind farms connected national and radial only	71
4.3.3	Strong onshore grid	73
5	Discussion	77
5.1	Contribution of this analysis	77
5.2	Limits of the proposed framework	78
5.2.1	Accuracy of GIS analysis	78
5.2.2	Accuracy of market model	80
5.3	Rescope and further research need	82
6	Conclusion	85
	References	87

List of Figures

1.1	Bundling wind energy evacuation and market interconnection into a hybrid asset.	2
2.1	Overview map of the Baltic Sea Region.	7
2.2	Wind power potential nomenclature. – Adapted from [75]	8
2.3	Wind power capacity potential and ambitions to deploy it in the BSR.	9
2.4	Map of selected maritime activities in the BSR.	10
2.5	Map of wind farms in the BSR in context of the existing power grid.	11
2.6	Elementary building blocks of offshore transmission assets.	13
2.7	Building blocks of offshore grids.	15
2.8	Share of fuel types in each country and total installed capacity.	17
2.9	Capacity factor time series for selected sites in the Baltic Sea.	18
2.10	Measurement sites for capacity factor time series in the Baltic Sea.	19
2.11	Reservoir water levels in Scandinavia 2012 and simplified inflows.	20
2.12	Weekly mean demand per country relative to each countries peak demand.	20
2.13	Assumed nominal transfer capacities [GW] in the BSR.	21
3.1	Two options for a graph topology setup for optimisation.	23
3.2	GIS in the context of a generic toolchain for offshore grid studies.	23
3.3	Toolchain developed for this thesis.	24
3.4	Reducing combinatorial complexity with GIS analysis.	26
3.5	Layer based display and processing of spatial information in GIS.	27
3.6	Creation of the permissive graph topology in two steps in GIS.	28
3.7	Elements of spatial analysis in GIS.	29
3.8	Elements of geometric clustering in GIS.	31
3.9	Spatial distribution of offshore wind farms and reachability relations within clusters.	31
3.10	Observations from partitioning with k-means, DBSCAN and buffer analysis.	33
3.11	Elements of MiniMax partitioning with redundancy filtering in GIS.	34
3.12	Link types created with geometric clustering.	35
3.13	Building blocks of the optimisation problem in Julia. – Adapted from [81]	38
3.14	Discrete decision making in Julia for node and link activation.	38
3.15	Three steps to maintain solvability of the market model.	44
4.1	Overview on results categories.	46
4.2	Map of geometric clustering results and hub node creation.	48
4.3	Map of permissive links in the Baltic Sea Region.	50
4.4	Permissive link types in the Baltic Sea Region.	51
4.5	Daily mean demand Baltic Sea Region for 2040.	53
4.6	Daily mean RES generation and total demand Baltic Sea Region for 2040.	54
4.7	Map of topology results – Base case.	56
4.8	Map of wind concentration and distribution of energy landing per substation – Base case.	60
4.9	Net-infeed and total wind farm generation per jurisdiction per year	61
4.10	Map of mean power flow per link – Base case.	63
4.11	Map of utilisation per link – Base case.	64
4.12	Ratio of total installed wind farm capacity and total landing capacity per jurisdiction.	65
4.13	Cost breakdown of offshore grid investments – Base case.	66
4.14	Sketched sensitivity analysis overview	67
4.15	Map of topology results – No interconnectors sensitivity.	70
4.16	Number of wind farms per connection type (total: 71).	71
4.17	Map of topology results – Radial sensitivity.	72
4.18	Offshore wind curtailment	73
4.19	Map of topology results – Strong grid sensitivity.	74
4.20	Cable lengths and strengths	75
5.1	Benchmark link creation – Åland to Denmark path.	79

List of Tables

2.1	Cost assumptions and technical parameters for offshore transmission assets.	16
2.2	Commodity price assumptions.	18
4.1	Yearly BSR energy outputs from copper plate model in TWh/ year	53

List of abbreviations

BSR	<i>Baltic Sea Region</i>
DBSCAN	<i>Density Based Clustering and Application with Noise (GIS analysis algorithm)</i>
CAPEX	<i>Capital Expenditures (investment cost)</i>
EEZ	<i>Exclusive Economic Zone</i>
ENTSO-E	<i>European Network of Transmission System Operators for Electricity</i>
GIS	<i>Geographic Information System</i>
HVAC	<i>High Voltage Altering Current</i>
HVDC	<i>High Voltage Direct Current</i>
IC	<i>Interconnector</i>
MILP	<i>Mixed Integer Linear Program</i>
MSP	<i>Marine Spatial Plan</i>
MVAC	<i>Medium Voltage Altering Current</i>
NTC	<i>Nominal Transmission Capacity</i>
OWF	<i>Offshore Wind Farm</i>
POC	<i>Point Of Connection onshore (landing point, onshore substation)</i>
RES	<i>Renewable Energy Sources</i>
TIN	<i>Tee-in hub (interface of a platform into an interconnector)</i>
TSO	<i>Transmission System Operator</i>
TYNDP	<i>Ten Year Network Development Plan</i>

Nomenclature

Category	Symbol	Description	
Sets & Indices	$n \in N$	Set of all nodes in the model	
	$n \in N^{\text{POC}}$	Subset of nodes: substation as onshore point of connection (POC)	
	$n \in N^{\text{OWF}}$	Subset of nodes: offshore wind farm (OWF)	
	$n \in N^{\text{TIN}}$	Subset of nodes: Tee-in hub (TIN)	
	$h \in H$	Set of all states (time steps) in the analysis	
	$g \in G$	Set of all generators	
	$s \in G^{\text{S}}$	Subset of generators: storages (battery and hydro)	
	$v \in V$	Set of voltage types	
	$l \in L$	Set of all links in the model	
	$l \in L_n$	Subset of links: starting and ending links at n	
	$l \in L_n^{\text{from}}$	Subset of links: starting links at n (<i>from</i> -node)	
	$l \in L_n^{\text{to}}$	Subset of links: ending links at n (<i>to</i> -node)	
	$l \in L_n^{\text{IC}}$	Subset of links: starting and ending links at n , while belonging to an interconnector (IC)	
	Parameters	$mc_{g,h}$	Marginal cost of g in h [€/MWh]
$d_{n,h}$		Demand at n in h [GW]	
$ni_{s,h}$		Natural inflow at reservoir s in h [MWh]	
\hat{p}_g		Generation limit of g [GW] (generation capacity)	
\hat{c}_s		Charging limit of s [GW] (charging capacity)	
\hat{w}_s		Storage capacity limit of s [GWh]	
a		Annuity factor, defined as $\frac{(1+i)^d * i}{(1+i)^d - 1}$, where $i \dots$ discount rate, $d \dots$ lifetime	
t		Length of time step h , such that: $t = \frac{\text{hours of the year}}{ H }$	
M		A sufficiently large number	
$mu_{n,v}^{\text{pwr}}$		Cost deduction for power dependent platform cost at n of type v when located onshore [%]	
$mu_{n,v}^{\text{fx}}$		Cost deduction for fixed platform cost at n of type v when located onshore [%]	
$mu_{n,v}^{\text{act}}$		Cost markup for platform cost n of type v when located in an icing risk zone [%]	
... for links		len_l	Length of l [km]
		$ntc_{l,v}$	Pre-existing link capacity on l of type v [GW]
		$\widehat{ntc}_{l,v}$	Link capacity limit on l of type v [GW]
... for cables		$\widehat{k}_{l,v}$	Cable capacity limit on l of type v [GW]
		$c_{l,v}^{\text{len,pwr}}$	Length and power dependent cost per cable on l of type v [M€/km]
		$c_{l,v}^{\text{len}}$	Length dependent cost per cable on l of type v [M€]
		c_v^{fx}	Fixed cost per cable of type v [M€]
		$c_{l,v}^{\text{fx}}$	Fixed cost for activating one cable on l of type v [M€], where $c_{l,v}^{\text{pwr}} := len_l \cdot c_{l,v}^{\text{len,pwr}}$
	$c_{l,v}^{\text{pwr}}$	Power dependent cost for activating one cable on l of type v [M€/GW], where $c_{l,v}^{\text{pwr}} := len_l \cdot c_{l,v}^{\text{len,pwr}}$	
... for nodes	$\widehat{k}_{n,v}$	Capacity for one unit of equipment at n of type v [GW]	
	$c_{n,v}^{\text{pwr}}$	Power dependent cost of activating n of type v [M€/GW]	
	$c_{n,v}^{\text{act}}$	Fixed cost for building a platform at n of type v [M€/GW]	
	$c_{n,v}^{\text{fx}}$	Fixed cost for activating one unit of equipment of type v at n [M€]	
Variables	$K_{l,v}$	New link capacity on l of type v [MW]	
	$K_{n,v}$	New node capacity at n of type v [MW]	
	$P_{g,h}$	Generation of g in h [MW]	
	$C_{s,h}$	Storage charging of s in h [MW]	
	$W_{s,h}$	State of charge (water level) of s in h [MWh]	
	$\Theta_{l,v,h}$	Economic power flow on l of type v in h [MW]	
	$\Phi_{n,v}$	Binary, indicating, whether n is activated of type v or not	
	$\Upsilon_{l,v}$	Integer, number if cables built on l of type v	
	$\Upsilon_{n,v}$	Integer, number of units of equipment built at n of type v	

1 Introduction

Europe is entering the next phase of its energy transition. Following the notion of the European Commission's Green Deal, ever more states realise the immense resource potential of offshore wind energy [25]. National governments adjust their ambitions on the installation of offshore wind power capacity in their jurisdiction accordingly to make them a central pillar in contribution to the Paris Climate Agreement [78]. While Latvia and Poland, for instance, have no experience with offshore wind as of date, they settled marine spatial plans which would allow installation of more than 15 GW of installed wind power until 2040 [53, 51]. Meanwhile, the recently published final report from the Baltic Energy Market Interconnection Plan (BEMIP) by the European Commission identifies a wind power resource potential of above 90 GW for the entire Baltic Sea Region [11]. This potential faces a status quo of installed wind power in the Baltic Sea of below 3 GW in 2020 [82]. The future of offshore wind in the Baltic Sea is hence just taking off.

The European Network of Transmission System Operators for Electricity (ENTSO-E) acknowledges this shift of attention towards the sea. The Ten-Year Network Development Plan (TYNDP) foresees an increased transmission need from North to South, i.e. from the generation centres in the northern Seas towards the main consumption in continental Europe [18]. Following this notion at the example of the Baltic Sea and adding high amounts of offshore wind power capacity to it, leads to an unprecedented transmission need from the wind farms to the shores. Conventional radial connection systems linking wind farms directly with the shoreline would ultimately lead to scattered offshore systems dominated by long parallel cables and high total installed transmission capacity across the water body.

The challenge evolves whether a more advanced connection concept for the Sea can identify synergies in wind farm connections and power market interconnection. Parallel transmission paths could be bundled into one common network, realising savings in cable length, power rating and installation costs. In addition, neighbouring wind farms could be clustered into groups with hub platforms at their centre, resulting in a more centralised and lean offshore grid infrastructure. ENTSO-E identifies such an approach as a fundamental pillar for the future offshore grid development [19]. The interconnection of countries and the evacuation of wind energy from the sea should no longer be seen as two separate optimisation problems but rather combined in one holistic view.

1.1 Research Question

In the face of an optimisation need for the future offshore grid, the question arises which configuration of it is most beneficial and what measures are taken into account when analysing its optimality. It should be analysed to which extent the development of an offshore grid made of hubs and clusters is beneficial compared to conventional individual radial connections of wind farms without clusters. This thesis projects this subject into the Baltic Sea Region by raising the following research question:

Which high-level grid topology is most beneficial to tap large amounts of the wind energy potential in the Baltic Sea Region?

Purpose of this report is to develop a methodology which can identify future transmission prospects for wind farms and interconnectors in a bottom-up created topology graph. Acknowledging the high computational complexity of solving such a large scale problem, it attempts to enhance the commonly chosen approach of transmission capacity expansion optimisation in a market model with an additional element in the toolchain. This element is denoted as GIS pre-processing and describes the analysis of readily available geodata in a Geographic Information System (GIS).

The thesis demonstrates the concept for the novel toolchain at the example of the Baltic Sea Region. The output is a set of spotlights of possible topology configurations, which help to understand the performance of the tools and their limits given the selected set of parameters and input data. On the contrary, the analysis does explicitly not strive to identify a best estimate of the future Baltic Offshore Grid. Nor does it attempt to rank or value the obtained topology results for probability of realisation or indeed socio-economic feasibility. The report should thus be understood as a descriptive analysis of the characteristics of the future offshore grid coming from the performed analysis, and the added value of GIS analysis in the context of transmission expansion planning.

1.2 Previous work on offshore transmission expansion planning

Leveraging overlaying transmission needs

One of the first comprehensive investigations of the future European offshore grid is the TradeWind study from 2009 [28]. Its purpose is to layout the power market and power grid for 2030 to integrate 120 GW of offshore wind power into the network. The comparison of direct radial versus meshed connections of wind farms reveals high annual savings when realising an interconnected offshore network as opposed to independent wind farm connectors and interconnectors.

The OFFSHOREGRID consortium picks up on this finding and differentiates various topology types that describe an offshore grid [2]. Offshore transmission assets are grouped as the set of cables, platforms and platform equipment necessary to transmit energy through the sea. If such assets serve a dual purpose of transmission, i.e. both evacuation of generated wind power from the sea and interconnection of market areas, they are called hybrid assets [32]. Refer to the sketch in figure 1.1 for illustration. The contribution from OFFSHOREGRID is an estimation of tipping points from where the construction of hybrid assets is superior to two separate installations of a wind farm (radial) connection and a market area (inter-) connection. Such tipping points can either be defined by absolute distance or power parameters or described as relations of wind farm capacities and cable capacities.

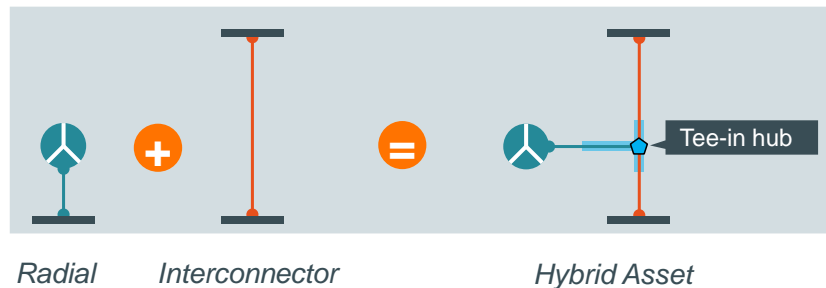


Figure 1.1: Bundling wind energy evacuation and market interconnection into a hybrid asset.

The geometric parametrisation of tipping points from one connection regime to another allows SVENDSEN the application of a pre-processing of “allowable” connections of wind farms to the shoreline or predefined hubs nearby [68]. He defines the hubs as additional platforms in the sea which collect wind power from nearby wind farms and transmit it on a stronger cable to the shore or indeed another hub. The locations are obtained with the help of an iterative k-means clustering based on a distance and power threshold. If wind farms are close enough to a hub in question and the hub does not cluster “too much” power already the connection is called allowable and thus given to the market model. The model then performs a mixed-integer linear optimisation of all allowable connections, activating the most optimal ones with respect to the objective function.

Distributional effects of offshore grids

While SVENDSEN assumes a neutral welfare maximising party performing the investment decision, KONSTANTELOS et al. investigate the cost-benefit distribution between countries that results from market interconnection [47]. Three interconnection case studies in the North Sea are analysed, and the added value of cross-national cooperation is once again confirmed on a global level. Country-wise the costs and benefits are, however quite different, resulting in the risk that some of the interconnection projects might be impeded if no fair cost-sharing and benefit allocation regime can be found.

EGERER et al. validate the notion of increased welfare with the increased interconnection of market areas [16]. Analysing three development scenarios for the North and Baltic Sea offshore grid they find that meshing the offshore grid, hence making it a unilateral undertaking, imposes unbalanced allocation of consumer and generator rents. Remaining at status quo of mainly radial connections or bilateral contracts for point to point connections is seen suboptimal from a European perspective. Additionally, they emphasise that unregulated business is unlikely to provide sufficient transmission capacity which stresses the rationale of an offshore regulatory framework for making the offshore grid a reality. GERBAULET & WEBER and MEEUS further elaborate on the difficult task of finding the well-balanced market framework for optimal future offshore grid investments [31, 50].

While interconnectors have strong distributional effects on the European energy market, they are to some extent residual to other investment decisions themselves. VON HIRSCHHAUSEN argues that grid investment follows investment decisions into generation [36]. It is residual to the extent, that location concentration and size of generators imply which transmission infrastructure is required to evacuate it. Notice that in the offshore context, the positioning of wind farms, therefore, is of crucial influence on the obtainable offshore topology. With SVENDSEN'S clustering approach in mind, this reveals that the offshore topology optimisation is not just a matter of well-calibrated hub identification and market modelling but also a matter of well-funded assumptions on location and realisation probability of future wind farm projects.

Technical obstacles for offshore grids

Beyond the regulatory and economic disputes for offshore grid development, the technical availability of the components required to operate and control the future grid is challenging its realisation as well. VAN HERTEM & GHANDHARI layout obstacles on the way towards a European multi-terminal high voltage DC (HVDC) grid from a technical point of view [79]. They emphasise the superiority of DC systems over AC systems for the comparative cost advantage of long-distance and high power transmission. On the contrary, switching and transformation of voltage levels are much more complex and expensive to realise on the DC side than for AC systems. In fact, as of date, no multi-terminal HVDC grid has ever been realised. DC links are usually implemented as point-to-point connections with AC-DC converters on each side. This drives total investment into DC links and limits the operational flexibility of the entire grid. For the offshore grid, AC dominated systems are not foreseen by most studies. Hence DC maturity and interoperability in multi terminals must be given for their realisation.

The PROMOTION study consortium started in 2015 to address the multiple barriers of future offshore grid development in a unilateral research and development framework [71]. Its major outcome as of July 2020 is a deployment plan for the future North Sea offshore grid towards 2050. Based on technology improvements being realised or assumed in the upcoming decades a roadmap is drafted, how an offshore grid infrastructure could be realised in a stepwise manner. Particular focus is put on secure system operation and interoperability of components. Based on the simulations, a clustering of wind farms into centralised hubs or even large energy islands appears efficient.

The PROMOTION results suggest that a paramount criterion in offshore grid development should be the

minimisation of cable lengths. Meshing for creation of redundant paths is seen less relevant in this context. Additionally, a plea for standardisation is made. Converters and platforms should be created in 2 GW units, which is considered enough to cluster nearby wind farms into one common centre node.

The Interreg project BALTIC INTEGRID sketches a similar deployment plan for the Baltic Sea Region [7]. While the focus is more on the regulatory side, it investigates the technology readiness of DC components as well. The ambition of the project is to explore the potential of a meshed Baltic Offshore Grid towards 2050. The findings suggest that the realisation of several hybrid assets and indeed, a pan-Baltic backbone represent a sound basis ensuring that up to 35 GW of wind power can be landed efficiently. The reduced spatial impact of clustered wind farms and bundled transmission paths is emphasised and also illustrated at reduced overall cable lengths.

Significant challenges are according to BALTIC INTEGRID the legal status of the cables and hub platforms which cluster wind farms from foreign jurisdictions and the so-called purpose priority of the cable utilisation. The study points out that on a hybrid asset, temporal congestion might require prioritisation of power flows. It raises the subject of legal definition: Is the hybrid asset defined as an interconnector, with some additional wind infeed if possible? Or does the cable mainly serve a connection purpose for the wind farm and is available for interconnection of market areas only during low wind infeed? Finally, the consortium suggests to reconsider already announced interconnection projects for suitability of a hybrid asset. If the trajectory of planned interconnectors bypasses planned wind farms an investigation of bundling opportunities of both assets is proposed. Such bundling is denoted as tee-in since the link from the wind farm, and the bypassing interconnector describe a “T” (c.f. figure 1.1).

1.3 Scope of analysis

This thesis acknowledges the introduced selection of literature in this discourse as a point of departure for the analysis. While some studies are further investigated for retrieval of input data, other sources help to frame the discussion in the final section of the report. In agreement with almost all literature findings, this thesis attempts to validate the added value of an interconnected offshore grid. It shall be demonstrated on the less intense studied Baltic Sea Region for the target year 2040. It is chosen in favour of 2050 for its better match with the TYNDP scenario time horizon.

The Baltic Sea Region proves a relevant choice of analysis for its conceivable increase in offshore activities towards 2040. While the region is historically well interconnected, the TYNDP reveals high ambitions to connect the Baltic states both to the Nordics and central Europe. With high dominance of hydro reservoirs in the North and high demand in the South, the region is likely to experience increased North-South flows in the future [18]. Bidirectional use of the offshore grid is also attractive to tap the “blue batteries” [36] in Norway, Sweden and Finland respectively. For the narrow water body, distances to opposite shorelines are short, which makes cross border interconnection attractive and opens up various options for linking several hubs to each other.

Following the notion of SVENDSEN’s pre-processing, this thesis spotlights the combinatorial nature of offshore transmission assets. The concept of allowable link identification is expanded with the help of a thorough GIS analysis. This shift in complexity comes at the cost of a simplified representation of the physical reality of the offshore grid. It is simplified into a transport model without physical power flow and contingency analysis. Indeed no operational feasibility analysis will be conducted. In consequence, the topology optimisation follows a high-level approach, without investigating interoperability or actual offshore grid planning. The onshore grid is aggregated into zones and not co-optimised. Besides, the socio-economic reality is kept abstract to the extent that individual cost-benefit analysis and regulatory barriers are kept out of scope. In consequence the results from this thesis do not allow direct conclusions concerning welfare and distributional effects resulting from increased power market interconnection.

Given the scope of the analysis, the optimality criterion is a minimisation of capital expenditure cost (CAPEX) of offshore transmission investments. Since the onshore grid remains untouched, the parametrisation of both GIS analysis and market modelling can be investigated separately from onshore influences on the model. This underlines the methodological aspiration of this work as opposed to a strategic analysis or indeed offshore grid forecast.

The remainder of this thesis report is structured as follows. The input chapter 2 frames the Baltic Sea Region, introduces the elementary building blocks of offshore grid infrastructure and lists all parameters and data being used. Chapter 3 presents the toolchain and provides a thorough introduction into GIS analysis, market model description and sensitivity analysis. The results are presented in chapter 4 and prepared for discussion in chapter 5. The report closes with a brief conclusion.

2 Input data

Purpose of this chapter is to specify the scope of analysis. It introduces all required input data, which is entirely retrieved from publicly available sources. In some cases, simplifications need to be made to limit the complexity. They are outlined and justified, for subsequent chapters to reference this line of argument where applicable.

First, the Baltic Sea Region is framed for the context of this thesis. The focus is drawn to the optimal wind power siting, and the sources used to fix the wind power sites for this analysis. Second, the elementary building blocks of an offshore grid are introduced. The level of explanation is equivalent to the level of analysis, i.e. no technical classification and detailed technology screening are conducted. The chapter closes with displaying the assumptions on the model parameters and time series data.

2.1 Framing the Baltic Sea Region

2.1.1 Geographic and jurisdictional overview of the Baltic Sea

The Baltic Sea is an arm of the North Atlantic Ocean, which separates the Scandinavian Peninsula from the rest of continental Europe. It stretches over 1600 km from its most southerly point at the coast of Poland to its northern tip at the Swedish coast near the Arctic Circle. With an average width of 190 km, it is a comparatively narrow sea, which is about half the size of the North Sea [1]. The water body is divided into sub-regions, as shown on the map in figure 2.1.

The scope of analysis stretches over all regions of the Baltic Sea. The water body is structured into jurisdictional zones, namely territorial and exclusive economic zones (EEZ). While the former one denotes an expansion of the national territory, the latter one does only define the formal right of the state to regulate maritime activities [77, 76]. Observe that for the narrow water body of the Baltic Sea, international waters do not exist. The activities analysed in this thesis address wind power evacuation mainly from the EEZ.

Bathymetry and seabed

The average sea depth of the Baltic Sea is 54 m, with few extremes above 200 m below sea level east and north west of Gotland respectively. Figure 2.1 maps the bathymetry of the Baltic Sea. The main part of the water body is shallow, especially the region around the Danish archipelago and the southern coastline. Seabed sediments in the Kattegat, Danish Straits and Baltic Proper include mostly sand and mud. This challenging grounding condition for wind turbines coexist with less than 30 m sea depth. Offshore Finland and Sweden, hard bottom complexes and hard clay dominate the slightly deeper seabed with still less than 40 m in most areas [1]. At first sight, the Baltic Sea, therefore, provides large areas suitable for wind turbine installation with respect to grounding and construction.

Ice conditions

The far North-South extend of the Baltic Sea leads to significant temperature differences in the region, which result in different ice conditions. Three main regions of different icing conditions can be identified. The first one denotes high risk of icing, i.e. ice cover is to be expected even during years with average temperature conditions. The Gulfs of Bothnia and Finland belong to this region. The second category further south experiences icing only during severe winters, denoted as medium icing risk. This region is mostly limited to the coastlines of mid Sweden, Estonia, Latvia and Lithuania. The third region describes the remainder of the Sea with low or no icing risk [69]. The map in figure 2.1 illustrates the sea ice risk zones of the Baltic Sea.

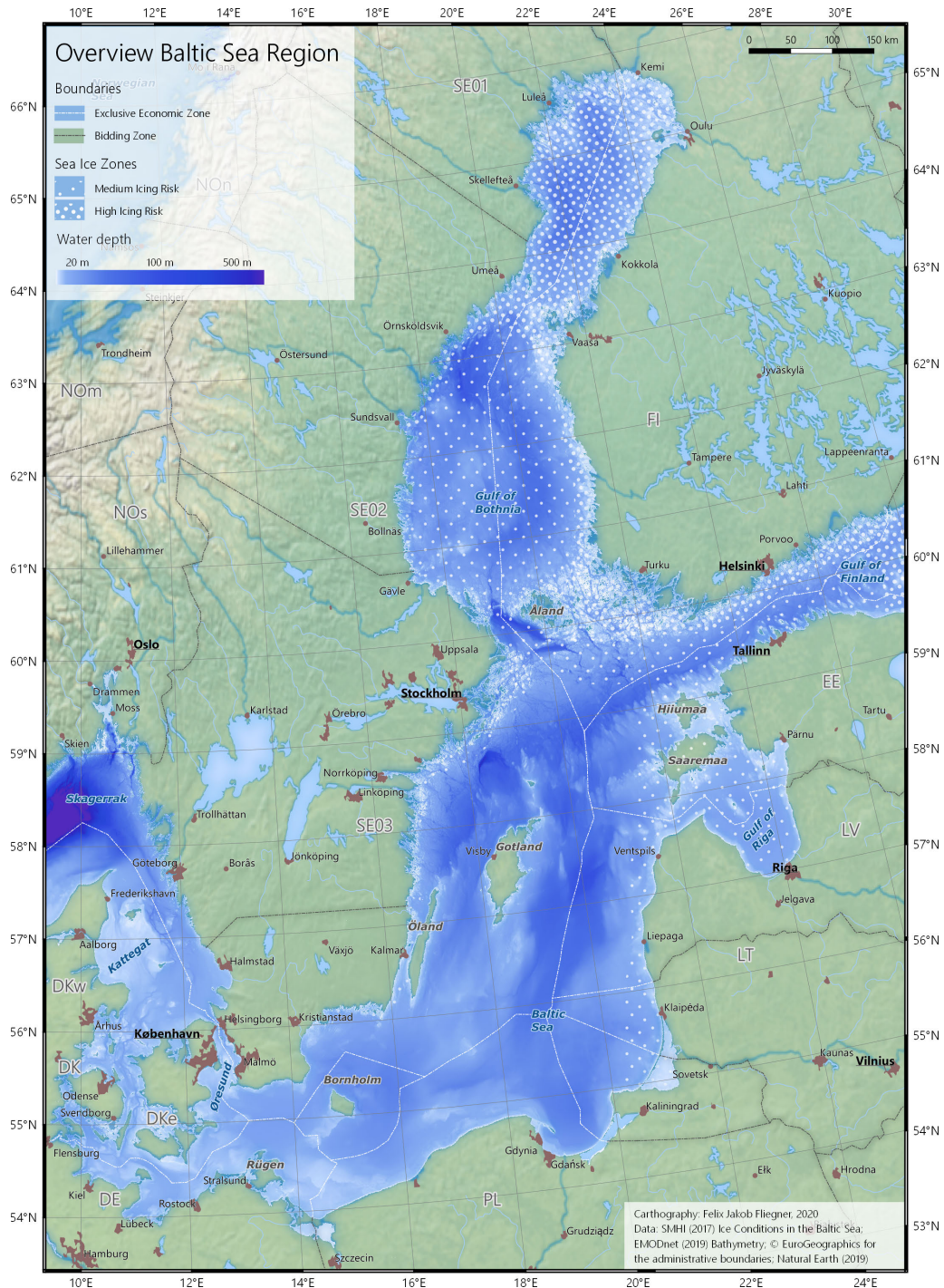


Figure 2.1: Overview map of the Baltic Sea Region.

Icing can either occur as ice coats in the form of pack ice. Ice coating of blades effects power generation efficiency and overall material fatigue. Even with de-icing measures in place the overall performance of a wind farm in cold climate is reduced. It can also result from forced downtime due to inaccessibility for longer periods in time [65, 62]. The model accounts for this performance loss by reducing the capacity factors for wind farms in regions for high and medium icing risk by 5 % and 10 % respectively [11]. Pack ice imposes material stress on all fixed foundations in the sea. It requires enforcing all installations for cold climate conditions at higher investment costs. Besides, the resulting short summer season limits schedules for installation and maintenance, which drives logistics costs. Such CAPEX mark-ups for platform installations in medium and high risk zones are given to the model as 4 % and 7 % respectively [11].

2.1.2 Optimal wind power sites in the Baltic Sea

This thesis does not attempt to estimate the wind power potential for the Baltic Sea bottom up. Potential sites for wind farms are retrieved from literature and pre-processed to validate them (c.f. section 3.1). The selection of the sources is based on the type of resource potential they estimate. For this analysis, it is desirable to obtain actual wind power sites that are feasible with respect to both, meteorological and spatial conditions. Following the nomenclature of the potential definitions by the German Environment Agency (Umweltbundesamt), this is best framed by the so-called realisable wind power potential [75]. It is related to other potential types in the VENN diagram in figure 2.2.

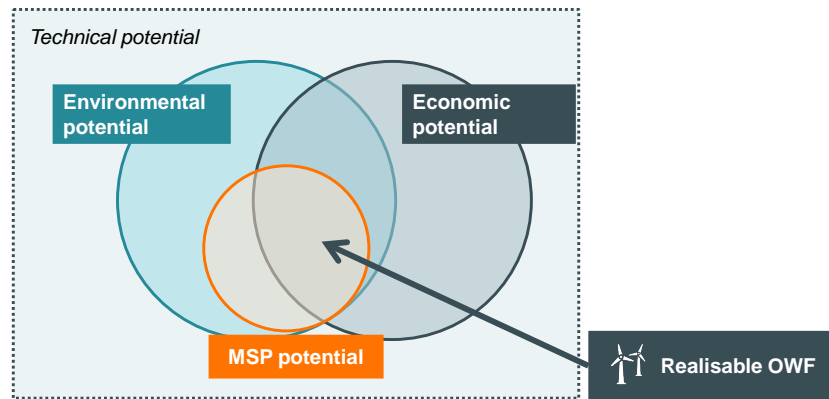


Figure 2.2: Wind power potential nomenclature. – Adapted from [75]

The realisable potential of wind power sites is influenced by technical feasibility, environmental compatibility, and economic viability. Observe a partial overlap of these potentials in figure 2.2. For a selected site to be realisable, it needs to satisfy all criteria simultaneously. Any announced and planned offshore project belongs to this subset. In order to receive permission, be constructed or in operation, one additional criterion needs satisfaction: The wind farm is required to be inside a wind energy priority area according to the respective national marine spatial plan (MSP). It is not a resource potential as such but rather a regulatory boundary condition, which can be translated into a resource potential. It also partially overlaps with the other dimensions of wind power potential in figure 2.2.

MSP as primary source for wind power site estimation

Wind priority areas as outlined in national MSP allow an estimation of the conceivable wind power potential per EEZ. Each EU member state is obliged to draft a national MSP by 2021 that maps all human activities in marine waters today and identifies the most effective future uses [26]. It shall take into account all land-sea interactions, environmental, economic, social and safety aspects. Particular focus is drawn towards cross border coherence of spatial planning and the identification of synergies in energy excavation. While Denmark and Germany previously had spatial planning regimes in place for the other Baltic Sea Region states, new drafts have been created. This thesis considers their latest status as of July 2020 and retrieves them from [10, 52, 51, 60, 46, 35, 29, 12]. From the wide spectrum of maritime activities the MSP covers, only the wind power priority areas are of interest for this thesis. They are considered as an essential input for the analysis both for their high institutional ranking (EU directive) and superiority with regards to permitting. Hence this source is a primary input for the data validation and pre-processing outlined in chapter 3.

MSP priority areas for offshore wind energy are identified in the context of the natural and anthropogenic context in which the wind farms will be constructed. These areas result from a thorough site screening, which takes sea depth, seabed conditions, wind conditions, grid connection options into account. Besides, other maritime activities are considered and synergies with them are accounted for, when defining

minimum competing interest areas in the water body. For each wind farm cluster, environmental impact assessments are conducted or prescribed [23]. Economic feasibility is not taken into account. That is, the identified areas satisfy all constraints for permitting, but do not suggest economic feasibility as such. The resulting wind power potential is thus a true subset of the environmental potential while only partly overlapping with the economic potential (compare with figure 2.2).

In consequence, the total wind power potential from all MSP clusters describes an upper limit for the deployment of wind farms in the Baltic Sea. Higher than this it will not be. Outside an MSP cluster, a wind farm is unlikely to receive permission. This thesis assumes most clusters to be populated with wind farms by 2040. Hence, it takes an optimistic stance towards offshore wind power development, which supports the notion of a need for an optimised offshore grid infrastructure. Notice that this approach does not imply any judgement on the likelihood of reaching that capacity. The assumptions purely serve as boundary conditions for the model to demonstrate its performance.

Offshore wind power potential identified in MSP

The wind power potential listed in the recent MSP drafts accumulates to 45 GW in the Baltic Sea. It is aggregated country-wise in figure 2.3 in relation to other wind power potentials: The currently installed capacity and the technical potential identified in [11]. Data from the Ten-Year Network Development Plan (TYNDP) 2020 scenario report *National Trends* scenario [20] is also provided. It reflects the latest ambitions of member states on RES targets set by the European Union [22]. *National Trends* is one of three TYNDP storylines by ENTSO-E envisioning the future towards 2040. It is compliant with the European Commission long-term strategy for decarbonising Europe’s energy sector. The scenario is created bottom-up based on existing drafts from the national energy and climate plans (NECP) by individual member states [27]. This bottom-up story building is suitable for comparison since it reflects the official ambitions of each member state on renewable energy (RES) targets, including offshore wind power.

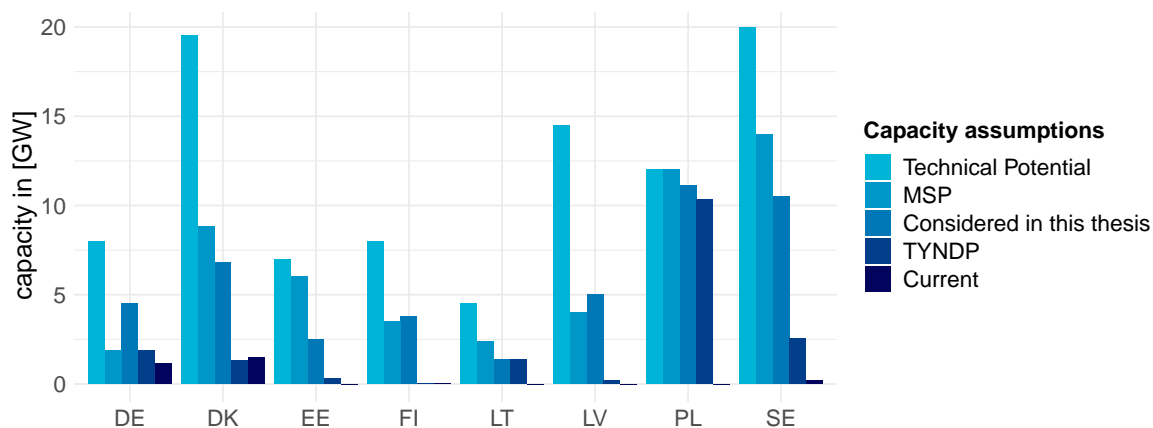


Figure 2.3: Wind power capacity potential and ambitions to deploy it in the BSR.

Figure 2.4 illustrates the country-wise distribution of the MSP wind power potential. Notice the cross border coherence of the MSP priority areas. Several states identify adjacent clusters, which the analysis in this thesis can leverage for clustering. In cases where the MSP only lists areas without defining the targeted generation capacities per cluster, the power potential is estimated with an average wind farm density of 5 MW/km^2 from the BALTIC LINES study [43].

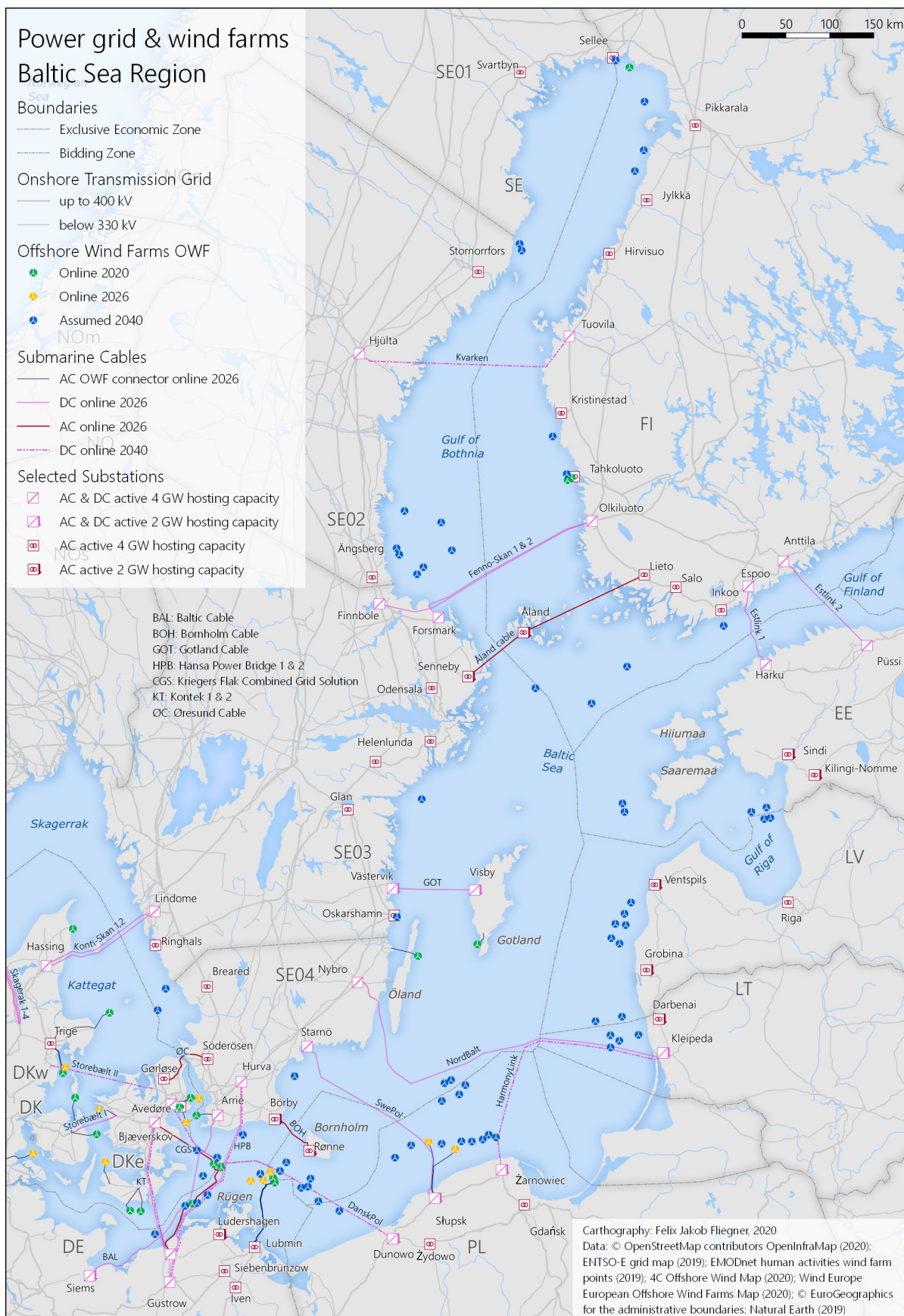


Figure 2.5: Map of wind farms in the BSR in context of the existing power grid.

Allocating wind farms across the water body

When optimising the offshore grid topology for 2040 one cannot say for sure, which potential wind farm areas will be populated. The MSP priority areas for wind only allow a best estimate on focus areas. This thesis allocates the identified 45 GW across MSP areas with the help of various sources. They include open databases such as the European Marine Observation and Data Network (EMODnet)¹, Wind Europe interactive offshore maps² and 4C Offshore maps³ which list actual wind farm projects either in operation, construction or planning phase. For this thesis, only the latter ones are of interest. For an outlook further into the future, wind power potential studies conducted in the Baltic Energy Market and Interconnection Plan (BEMIP) [11] and in the Interreg project BALTIC INTEGRID [7] are chosen as reference. The resulting dataset of considered wind farms is presented in the map of figure 2.5. Observe that the MSP framework only applies to the EEZ. Territorial waters still experience wind farm development outside priority areas. In Sweden, Lithuania and Latvia, for instance, several near coast wind farms are part of the dataset. Most other states do not show wind farms in territorial waters.

The procedure of pre-processing and allocating these sites is called spatial analysis and is presented in section 3.1. In addition to mere wind power sites and MSP clusters, it takes into account selected geo-data to enhance the analysis. This thesis considers shipping routes, marine protected areas and regions with icing risk. Bathymetric information, seabed conditions and wave patterns could also be included, but are excluded in this scope for reasons of simplicity.

Once, the wind farm nodes are identified, their location and capacity is fixed for the remainder of the analysis. The focus is drawn to an optimised transmission infrastructure to evacuate their generated wind power. Doing so requires input knowledge on the nature and parameters of such offshore transmission assets. It is developed in the next section.

2.2 High-level offshore grid technology screening

Scope of this thesis is the optimisation of offshore transmission assets. They are defined as the set of components required to evacuate the generated electricity from the wind farms to a substation onshore [32]. The offshore system boundary for this analysis is the aggregated wind farm. While the platform and optional converter or transformer equipment are in scope, the topology inside the wind farm and the turbines are out of scope. As seen from the model, each wind farm is depicted as a generation node with a predefined availability time series and fixed marginal cost. The system boundary onshore is defined similarly. Necessary converters and transformers for the required throughput of power are accounted for.

A thorough investigation of the physical strength and power handling capability of the onshore grid is outside the system boundary of this analysis. Instead the onshore grid is aggregated into onshore bidding zones, where the selected nearshore substations are modelled as internal nodes inside a zone. To reflect upon their physical limit of power throughput this thesis adopts the notion of hosting capacity from [70]. Substations being connected to the highest voltage level of up to 400 kV are assumed to have a hosting capacity of 4 GW. In case a transmission line of lower voltage is connected to a substation it is assumed to have a hosting capacity of 2 GW for the lower power throughput the connected onshore grid would allow at the reduced voltage level. The classification of the considered substations is shown in figure 2.5. Note that this classification is solely based on visual inspection of the ENTSO-E grid map⁴ and does not result from a pre-analysis of a grid model. For its high impact on the final results this assumption is lifted in a sensitivity analysis.

¹<https://www.emodnet.eu/>

²<https://windeurope.org/about-wind/interactive-offshore-maps/>

³<https://www.4coffshore.com/offshorewind/>

⁴retrieved from <https://www.entsoe.eu/data/map/>; assumptions for Poland adjusted in accordance with [42]

2.2.1 Building blocks of an offshore grid infrastructure

Offshore transmission assets

The set of components of offshore transmission assets contains offshore platforms, onshore substations and cables linking them [48]. Offshore platforms can be further distinguished into cluster hubs, which cluster a set of wind farms nearby and tee-in hubs creating an interface to link cables with an interconnector [2]. A wind farm is also modelled as a platform. Each platform and substation can either be interpreted as a node in the market model or as a physical point in a set of geo-data. In both cases, the referred physical object remains the same. Hence, this terminology is used synonymously in the respective parts throughout the thesis.

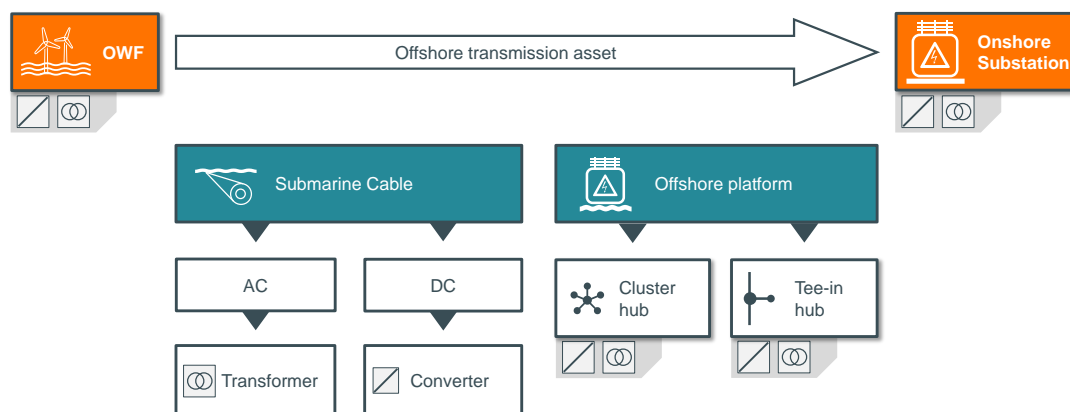


Figure 2.6: Elementary building blocks of offshore transmission assets.

Platforms are connected with other platforms via cables. They can either inject AC power or DC power into the system. Cables can either be built as high voltage direct current (HVDC) or high voltage altering current (HVAC) cables. Compare with figure 2.6 how these elementary building blocks are semantically related to each other. The choice of cable voltage type defines the type of power equipment required on the linked nodes. If an AC cable is to be built both, start and end node need to be AC active. This requires the respective capacity of an AC transformer being installed at both ends. Vice versa with DC cables and AC/DC converters at each end. Observe this in figure 2.6 with the indicated converter and transformer icons below each platform type. The concept of active elements as opposed to permissive elements is explained in chapter 3. Notice that activated equipment is only required when transformation and conversion are indeed required. If the power flow leaves a node in the same voltage type as it entered no conversion or transformation takes place. This distinction is implemented in the model to avoid over-investment and will be further explained in section 3.2.4. For short distance clustering of wind farms into a common centre point (cluster hub), a third cable type is considered. It is operating at lower AC voltage and is therefore denoted as medium voltage (MVAC) cable.⁵

AC and DC components

The distinction between AC and DC systems is relevant in the face of different performance strengths and weaknesses of both systems. AC systems, on the one hand, provide the lowest losses on short distances and require less platform equipment which saves large amounts of CAPEX upfront. On the contrary, a considerable amount of reactive power is generated, the longer the cable gets, or the more power is transmitted via the cable. This requires costly reactive power compensation until it outweighs the initial investment savings [49, 66]. DC systems, on the other hand, require fewer cables than equivalent AC

⁵Medium voltage in this context is not comparable to the medium voltage level for the onshore grid. It only signals a lower voltage rating compared to the HVDC and HVAC cables.

systems. Reactive power is not an issue, since only active power is transmitted. This does indeed allow a more efficient power flow control and frequency decoupling of system areas. In theory, there is no distance limit for DC power transmission. The most prominent downside of DC links is their high cost for installation and significant spatial platform requirements for converter equipment, power electronics and protection [49, 48].

The issue of protection is pronounced in the context of multi-terminal offshore grids. Direct linking of lines requires switching gear to protect individual branches in case of short circuit failures. In case of AC links, such equipment is readily available. DC breakers are however not available to date at the required power ratings [79]. This analysis considers grid topologies, which could require a DC circuit breaker in operation. It is assumed available for the target year without investigating alternatives if it should not be available. This underlines the notion of a high-level topology analysis without claiming a technical simulation or indeed, operational feasibility analysis. Refer to [72] and [68] for further work on DC circuit breaker development and how to model components which are not yet existent.

In conclusion, AC systems perform well over short distances and with medium power flow. DC systems, as a complement, perform well over large distances and with high power flow. Both transmission tasks arise in this analysis. Therefore both technologies are considered. In the literature, common break-even distances between HVAC and HVDC cables are between 50 and 80 km cable length [79]. The model enforces this distance limit indirectly via the cost function. Following the notion of necessary compensation equipment and high losses, the cost function for AC systems starts at a low offset but escalates steeper than the DC system cost function, which starts with a higher offset but less steeper slope. Eventually a tipping point is reached between AC and DC systems, purely based on accumulating costs. The concept is further explained in section 3.2.2. The parameters of that cost function are presented in the next section.

The MVAC technology can be depicted as an extreme case of “short distance” transmission. When wind farms are located close to a hub (both, cluster and tee-in), the voltage level can be chosen lower, saving on transformer and cable cost. MVAC cables are usually not assumed longer than 20 km [66]. In contrast to the length limit for the high voltage systems, this parameter is directly enforced by the model. It is used during pre-processing (c.f. GIS analysis).

This is the lowest level of detail this thesis can reach out to. Any technological and operational analysis of single components or indeed, topologies needs to be neglected for the sake of feasibility in the context of this thesis project. The author stresses the importance of follow-up analysis on the results from the viewpoint of system operation and actual grid planning.

Creating simple and complex offshore topologies

Offshore topologies of various complexity are obtained when stacking the elementary building blocks to larger systems. The underlying notion is always the same: generated wind power shall be brought to the shoreline and injected into the onshore grid. Besides, exchange capacity between countries shall be provided via interconnectors, reaching from one shore to the next. Both can either be done directly or with the help of intermediate nodes (platforms).

While the connection between two nodes is realised with a (submarine) cable, in more general terms this thesis denotes this connection as a link. A link is the carrier of all technical and geographical information relevant to define this connection. It defines capacity, start node, end node and length. E.g. a DC link carries a number of DC cables of same length, realising the galvanic connection of two platforms at a rated capacity. For the remainder of this analysis the concept of links is used to describe relations among nodes and points.

The base case for an offshore grid is represented by direct links from start to destination. A wind farm is directly linked to shore, and an interconnector directly links to shorelines. Several wind farms in a region

share a common onshore point, but each has its own offshore transmission system. Such a connection system is also labelled radial. Interconnectors are built in parallel. To date, it is common practise to build interconnectors separately from offshore wind farm connection systems [2]. This setup is the departure point for this analysis and is depicted in the first column of figure 2.7.

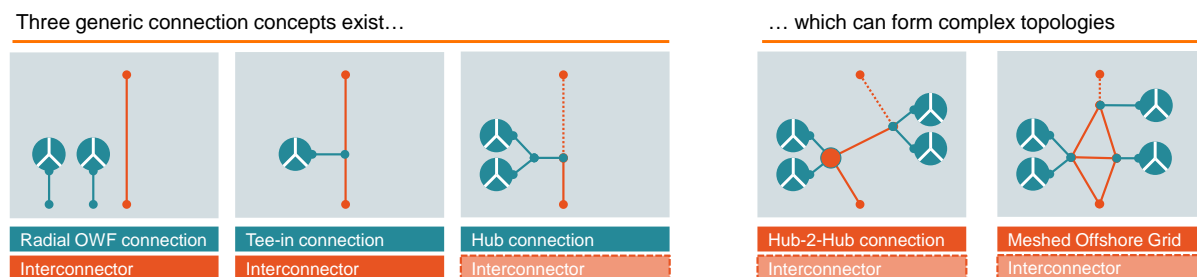


Figure 2.7: Building blocks of offshore grids.

The next best optimisation potential of the radial setup is the acknowledgement of overlapping corridors. While maintaining the corridor of an interconnector, the nearby wind farm can tee-into that system. This creates synergies with respect to reduced cable investment and operation. Each time the wind farm does not feed into the grid, the very same cable system can still serve as an interconnector [2]. Conversely, the interconnector allows the wind farm to trade in two regions as opposed to just one in the base case. These synergies are best framed in the concept of hybrid assets [72]. “hybrid” alludes to the dual purpose of the cable. It is no longer a mere interconnector. Instead, it is indeed a wind farm connector and interconnector at the same time. Compare with figure 2.7 for illustration.

Reflecting on the proximity of some wind farms to each other, clusters might be identified. They share a common cluster hub in the centre with transformers and converters for all wind farms nearby. The wind farms are linked with so-called hub-spoke cables to the hub platform. The name alludes to the spoke-like layout of cables from surrounding wind farms terminating in one common centre point (hub). A stronger cable then evacuates the collected infeed to shore. This hub can either operate standalone (cluster hub) or as a hybrid asset (tee-in hub) with an interconnector nearby. Expanding on this notion of clustering, one can indeed connect several hubs with each other. When such connections are redundant “true” offshore meshes result from it. Such an offshore grid is also called multi-terminal [71]. Some nodes might be bigger than others and sometimes even placed on natural or artificial islands. Notice that cable ratings and hub equipment ratings can be asymmetrical, meaning that some links turn out to be bigger than others. It is at the core of this thesis to identify such asymmetrical configurations of stacked building blocks.

2.2.2 Parametrisation for the optimisation problem

The above-listed considerations on a simplified grid topology with simple building blocks allow a parametrisation of the optimisation problem mostly based on cost parameters. The underlying notion is that the discussed performance benefits and limits are reflected in higher or lower investment cost, respectively.

The cost parameters in the model include fixed costs which occur in discrete units and variable costs which scale with power units, length units or both. In the model, discrete units are either cables (MVAC, HVAC or HVDC), platforms (wind farm, cluster hub and tee-in hub) or equipment being installed on platforms or onshore substations (transformers and converters). Recall figure 2.6 for illustration. Counting discrete units requires some technical parameters. They include maximum power rating per unit and in case of the MVAC cables a maximum cable length per unit. The parameters are introduced in this section, and their purpose in modelling is presented in section 3.2.1.

Cable parameters in the model

Populating a link with a cable causes costs, independent of its actual length, size or power rating. They are called fixed costs and represent, for instance, planning and permitting costs. They scale discrete with each unit of cable being installed. In this analysis, miscellaneous additional installations at each end of a cable are also subsumed in this parameter. Depending on the cable length, transportation, trenching, and laying costs apply. Hence, a length-dependent variable cost parameter is included in the analysis. Since the length of the cables is known upfront, these costs will later be included in the fixed cost term as well. Finally, the third cost parameter addresses the actual power rating of the cable. It scales continuously with the installed capacity and represents conductor type, cross-sectional area and insulation [68, 49, 80]. Annual operation costs are priced into the initial investment and not separately modelled.

The cost parameters are implemented in a cost model with the help of a technical capacity limit of one cable unit [13]. Each time a capacity shall be installed on a given link, the model tests, how many cables it would need to satisfy this capacity request. This results in counting cables for the fixed costs and counting power units for the variable costs. It allows a linearised, yet reasonable approximate cost modelling with a sloped stepwise linear cost function [40, 68]. Refer to section 3.2.1 for an introduction into the cost model and the variables being involved. Table 2.1 lists the required parameters required for this.

Notice that the power-dependent cost parameters for the short distance MVAC cables are lower and the length-dependent cost parameters are higher when compared with the HVAC counterpart. It follows the observation of cost savings on the logistics and trenching side. On the contrary, building short distance cables increases the relative effort of installing miscellaneous equipment compared to the actual cable. Hence this parameter is lifted above the HVAC parameter. Besides, a length limit is enforced for the MVAC cables following the initial considerations on technical performance.

Table 2.1: Cost assumptions and technical parameters for offshore transmission assets.

Parameter	Symbol	Unit	MVAC	HVAC	HVDC
Cable length and power cost	$c_{l,v}^{\text{len,pwr}}$	M€/ GW/ km	0.34	0.97	0.19
Cable length cost	$c_{l,v}^{\text{len}}$	M€/ km	1.4	1.29	0.8
Cable fixed cost	c_v^{fx}	M€ p.u.	2	4	4
Node power cost	$c_{n,v}^{\text{pwr}}$	M€/ GW	n/a	30	120
– deduction onshore	$mu_{n,v}^{\text{pwr}}$	%	n/a	-8	-26
Node equipment cost	$c_{n,v}^{\text{fx}}$	M€ p.u.	n/a	60	40
Node fixed cost	$c_{n,v}^{\text{act}}$	M€ p.u.	n/a	26.52	175.96
– deduction onshore	$mu_{n,v}^{\text{fx}}$	%	n/a	-50	-80
– markup sea ice high	$mu_{n,v}^{\text{act}}$	%	n/a	+7	+7
– markup sea ice medium	$mu_{n,v}^{\text{act}}$	%	n/a	+4	+4
Equipment power limit	$\hat{k}_{n,v}$	GW	1.6	1.6	2
Cable power limit	$\hat{k}_{l,v}$	GW	0.4	1	2
Link length limit	n/a	km	20	n/a	n/a
POC limit high hosting capacity	$\widehat{ntc}_{l,v}$	GW	n/a	4	4
POC limit low hosting capacity	$\widehat{ntc}_{l,v}$	GW	n/a	2	2
Lifetime	d	years	40	40	40
Discount rate	i	%	5	5	5

Node parameters in the model

The cost nomenclature for the nodes distinguishes between power-related and non-power related costs as well. Building a platform is assumed with nodal fixed cost independent of platform size and power rating of the installed equipment. The only distinction is made for the voltage type. Offshore converter platforms for AC-DC conversion tend to get much larger than less complex AC-AC transformer platforms [80].

Platform fixed costs are further subject to a cold climate CAPEX mark-up as elaborated above. Sea depth and seabed conditions at each platform location are not accounted for in this thesis. For now, one general cost term applies to all locations. It is, however, possible to implement individual terms at a later stage into the framework.

For the power rating of a node, two additional parameters are required, namely power-dependent node cost and fixed node equipment cost. While the power-dependent node cost represents transformer and converter ratings, the fixed equipment cost applies for each discrete unit of converters and transformers being installed, independent of their actual capacity rating [13, 44]. Note the similarity to the consideration for cable costs from above. Compare with table 2.1 for the numbers.

In summary, one final observation can be made from the cost parameters. While the cable costs are higher for the AC systems, the DC systems have much higher nodal costs. For this reason, HVDC transmission systems become more attractive for long-distance transmission. This tipping point enforces the earlier mentioned break-even distance between AC and DC systems, without explicitly defining it as a constraint. Instead, it serves as a validity check for the model results, if indeed no “long” AC cables are built.

2.3 Initial setpoint of the analysis

The analysis requires a set of initial values to start the optimisation. This includes data on generation capacity, time series for RES, demand and water inflow in reservoirs, and nominal transfer capacities of the start grid. The data sets are implemented in a power market model, where each country is aggregated into its market area(s).⁶ They cover all BSR states, excluding Russia but including Norway. The remainder of continental Europe is aggregated into one WEST node (representing Belgium, France, Luxembourg, The Netherlands and United Kingdom) and one SOUTH node (representing Austria, Czech Republic, Italy and Switzerland). For this study, the target year 2040 is analysed.

2.3.1 Generation capacity and fuel types

Assumptions for generation in the simulation model are based on the TYNDP 2020 scenario report *National Trends* scenario [20]. Since its storyline is developed bottom-up from national ambitions, it allows updating selected values (here: offshore wind power capacity) without interfering with the overall storyline too much. The assumed capacities per fuel type are summarised in figure 2.8. The values for wind power are deducted for their offshore share. The installed capacity of offshore wind per country is overwritten by the allocation of 45 GW of wind among the BSR states.

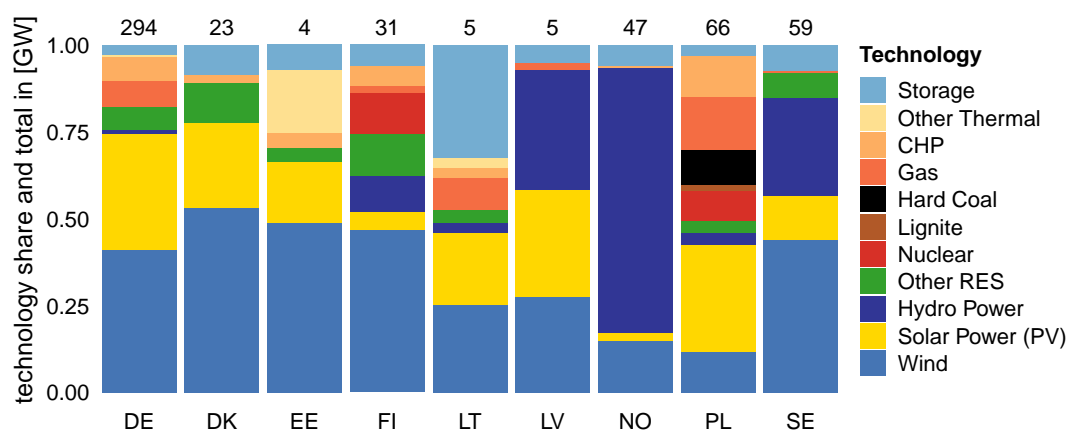


Figure 2.8: Share of fuel types in each country and total installed capacity.

⁶Aggregation of Norway into three market areas follows the TYNDP methodology.

Commodity price projections for 2040 are also taken from the TYNDP. They are converted to marginal cost with the help of efficiency assumptions and a CO₂ price of 100 €/t CO₂ as listed in the TYNDP. The data is summarised in table 2.2.

Table 2.2: Commodity price assumptions.

Category	Power price in €/MWh	Efficiency
Nuclear	14.13	33 %
Lignite	51.67	35 %
Hard Coal	108.91	35 %
Gas	88.31	40 %
Other Thermal	205.99	35 %

2.3.2 Climate year and availability time series

Time series data for the analysis is retrieved based on the climate year 2012. It is commonly chosen for the German grid planning process (Netzentwicklungsplan) [3]. From a German perspective, this year is a suitable choice for simulating the future grid. A cold spell characterises it in February, which enforces a high-load situation in the model. Wind availability and solar radiation are close to mean values, while two weeks are characterised by very low wind infeed. The Scandinavian reservoir levels are slightly above mean. In summary, the climate year provides a set of variable weather and load conditions to challenge the optimal grid topology in various ways.

RES availability time series

The model considers availability time series for solar power (photovoltaic) and wind power generation. They result from a reanalysis of satellite measurements (MERRA by NASA) in a resolution of 1 hour and approximately 40 km × 40 km. The reanalysis has been conducted by Pfenninger and Staffel [67, 58], who provide the data open access for a wide range of climate years.⁷ Onshore PV and wind are aggregated into one RES time series per country.

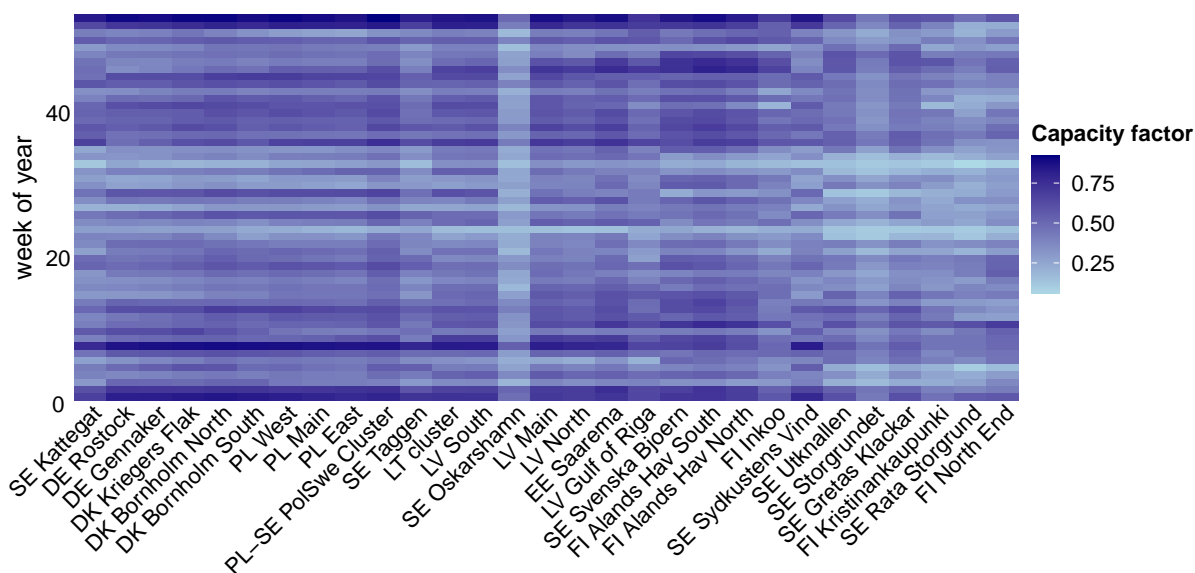


Figure 2.9: Capacity factor time series for selected sites in the Baltic Sea.

⁷<https://www.renewables.ninja/>

For the offshore wind farms, 29 clusters are identified, where each cluster receives its time series based on its mean coordinates. Figures 2.9 and 2.10 summarise a heat map plot for the capacity factors for the entire year aggregated on a weekly level and the cluster locations. Given the high share of intermittent generation from renewables in each country, the concurrence of infeed is a critical indicator to be aware of. It describes to which extent infeed from wind power plants in one region correlates with the infeed in another region. Neglecting future investment decisions and grid states, first derivations can be drawn from the raw weather data. It suggests that wind infeed in the Baltic Sea is highly simultaneous. Either most clusters produce at once or hardly any. The outliers are the nearshore locations or clusters, which are far off. In some weeks of the year, this concurrence is less pronounced. The offshore grid will therefore need to deal with simultaneous infeed in some hours and hardly any infeed in others while satisfying the onshore load at any time.



Figure 2.10: Measurement sites for capacity factor time series in the Baltic Sea.

Water inflow time series for reservoirs

Hydro reservoir storage levels are modelled with a simplified inflow time series. For the climate year 2012 weekly storage levels and total annual generation are collected for all reservoir storages. The observation from the storage level statistics of Scandinavia in figure 2.11 is, that the storage level at start and end of the year are equal [56, 17]. Hence total annual generation equals total annual inflow. The inflow is however not evenly distributed among the weeks. During summertime the inflow reaches its maximum, resulting from bulk snow melting. In winter hardly any water accumulates in the lakes, since most water is frozen or “stored” as snow in the mountainous catchment areas of each reservoir. The mean weekly inflow is therefore redistributed among the weeks with help of a relative inflow time series. It describes the inflow per week in relation to a weekly mean inflow. E.g. during the summer season the inflow is up to four times larger than average, while in winter it is up to ten times smaller. Compare with the bars in figure 2.11 for the resulting water inflow time series.

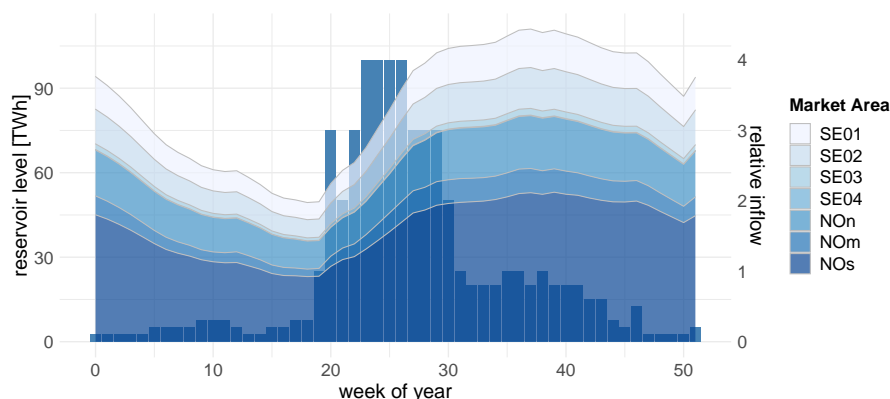


Figure 2.11: Reservoir water levels in Scandinavia 2012 and simplified inflows.

Demand time series

Electrical load data used for the simulations stems from a historical time series from the ENTSO-E data portal and power statistics. The open power system data platform⁸ has been used to retrieve the load time series for all nodes for the climate year 2012 [57]. While this historical time series neglects future developments on the demand side, it is consistent with the generation time series and the overall conditions of the chosen climate year. To account for this error, the time series is scaled up to fit the total yearly demand per country in 2040 as listed in the TYNDP scenario report. Flexible demand is excluded from the analysis. Refer to the discussion chapter for the impacts on the analysis it may have.

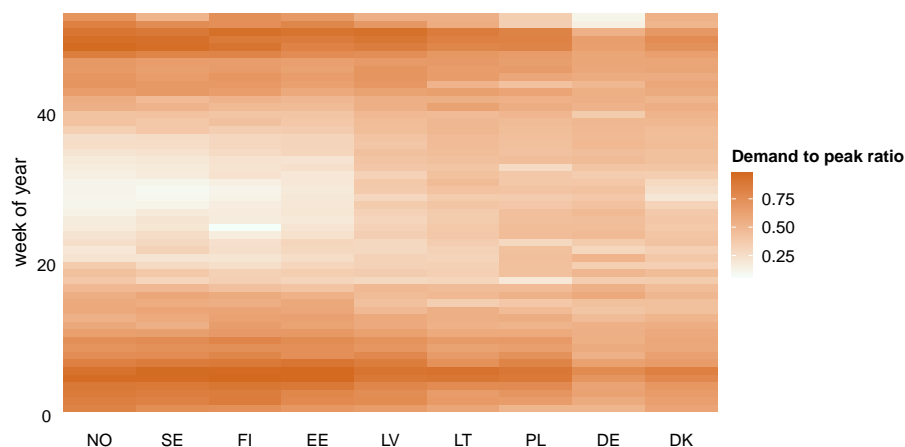


Figure 2.12: Weekly mean demand per country relative to each countries peak demand.

Figure 2.12 displays the development of the total demand throughout the year. It shows the aggregated load on a weekly level related to the peak load in each country. In such a way, the high absolute differences in demand among the BSR states become comparable. This pre-analysis allows the identification of extreme situations. Such extremes are characterised either by high-wind-high-load or by low-wind-high-load grid states. The first one challenges the grid infrastructure to transmit bulk power infeed over long distances to bulk consumption centres. Optimal connection of each wind farm to the benefit of the grid is desirable in such a situation. The second grid state shifts the attention towards the mere interconnection task of the grid. In such a situation the share of thermal generation is highest, hence the purpose of the transmission grid is to dispatch as much cheap electricity as possible. Notice the hidden dual purpose of the offshore grid infrastructure, which has been introduced earlier in this chapter. When

⁸<https://open-power-system-data.org/>

3 Methodology

The following chapter is dedicated to introducing and justifying the choice of tools for the task at hand. It is structured in three steps, where each step applies selected concepts from graph theory, geographic information system analysis (GIS analysis), and power market modelling. Concatenation of the individual steps leads to a toolchain. A few preliminary considerations are made before it is presented.

The notion of active and permissive graph elements

Transmission capacity expansion studies like this one require an initialised set of nodes and lines to start with. Such an analysis is denoted as brownfield approach [41] where the start grid is commonly organised in a mathematical graph topology.⁹ At this level of detail, the topology distinguishes between two types of graph elements, namely nodes and lines. A node can either aggregate an entire market area (e.g. Germany) into one element, with demand, generation and power exchange with neighbouring nodes. Alternatively, a node can also represent one individual landing point (point of connection, POC), offshore hub or an offshore wind farm (OWF). A link connects two nodes with each other. It can either represent an individual power cable, e.g. from a wind farm to shore. Alternatively, it aggregates all cables with their nominal transmission capacity (NTC), e.g. all interconnectors between Germany and Poland.

In the context of offshore transmission expansion, such a start grid hardly exists. Only substations along the shoreline, the onshore bidding zone nodes, and some interconnectors frame the otherwise “empty” water body (c.f. section 2.1). Even wind farms exist on a few selected sites only. Besides, these wind farms are always connected radially (i.e. directly) to shore, which leads to their aggregation into the onshore bidding zone. The unbuilt but considered graph elements, namely offshore wind farm nodes, hub nodes and new interconnector links represent the new building blocks of the graph topology. In order to distinguish and organise them, the concept of active and permissive graph elements is introduced here.

An active graph element is available for the optimiser to schedule power flows across it. That is, a link has at least one cable system installed, or a node is built with a platform and offers transformer or converter capacity when required. All elements in the start grid are active. Grid expansion is described with permissive elements. A permissive element is not active, but the optimiser is aware of its existence, i.e. feasibility with respect to predefined permissive rules (c.f. section 3.1) is ensured. Such an element can be activated at a given cost to become part of the expanded grid.

In more general terms, transmission capacity expansion optimisation in this thesis describes an informed search on a predefined graph, which contains pre-solved (active) elements and optional (permissive) elements [64]. It is an informed search since the optimiser knows all available options up front, including all cost parameters and constraints. It is also a discrete search since each element has at least two disjunct statuses to be decided on: activate or not. Note that this generalisation does only hold in light of the framed input parameters and viewpoint of this thesis.

Obtaining a graph topology to perform the optimisation in

Creating the graph topology from scratch is now either a question of scenario building or GIS analysis. This simplified choice is illustrated in figure 3.1. Scenario building, on the one hand, requires sophisticated input knowledge and careful balancing of different storylines in order not to bias the result into an otherwise suboptimal high-level grid topology. It is, however, a light approach, which might overcome missing input data. Such an approach is commonly chosen [16, 31, 30, 34].

⁹Unless otherwise and explicitly stated in this report, “topology” is used in reference to graph theory and not the system operation of the transmission grid.

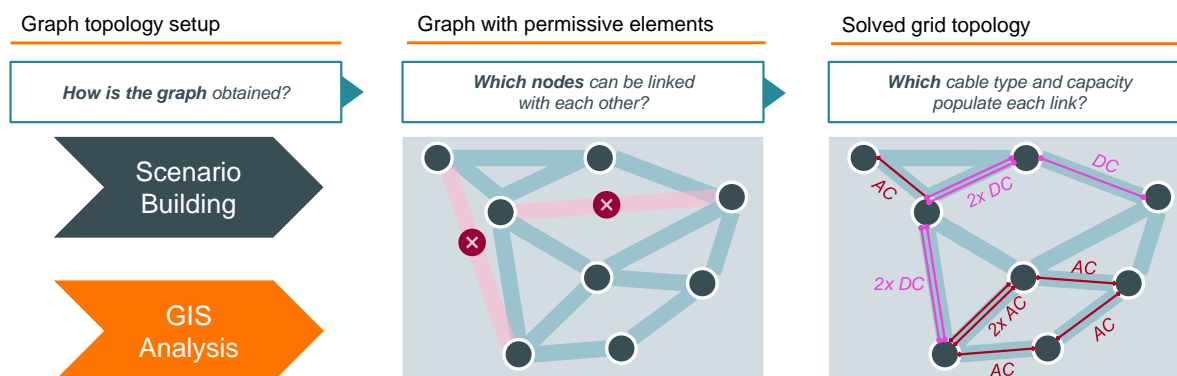


Figure 3.1: Two options for a graph topology setup for optimisation.

A GIS analysis, on the other hand, offers a purely analytical approach to obtain a graph topology with permissive elements bottom-up. The choice and quality of input data are crucial, but once the data is uniform, the topology creation outperforms any heuristic approach. The striking difference to the manual approach is that it is much better performant and able to consider large amounts of extra constraints. Besides, no redundant graph elements are generated as will be demonstrated in this chapter.

Once a graph topology is created, an optimiser can decide which elements are indeed going to be activated. Depending on the level of detail of the expansion planning, different voltage types and cable numbers can be considered. Refer to the final step in figure 3.1 for illustration. Display of the optimised graph topology alongside selected performance indicators of the represented transmission grid is again possible with the help of a GIS.

Development of a toolchain for the analysis

For this thesis, an enhanced toolchain with GIS topology setup and GIS post-processing is introduced. Its position in a generic toolchain is shown in figure 3.2. It is a novel approach, which will be in focus for the upcoming sections. It does not attempt to question the existing and commonly applied steps of analysis. The mere purpose is to demonstrate a proof of concept and showcase potential gains from this methodology.

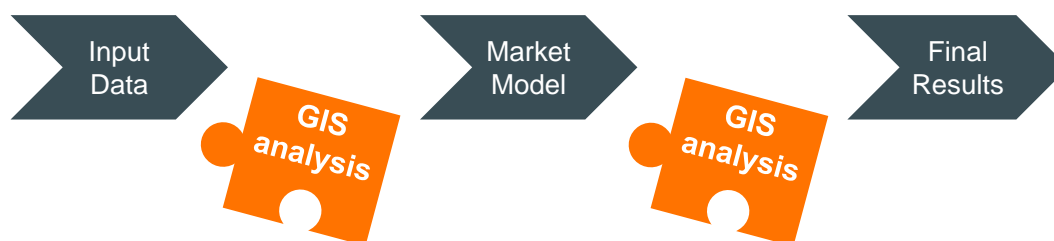


Figure 3.2: GIS in the context of a generic toolchain for offshore grid studies.

The analysis is structured in three steps: The first one is dedicated to the analytical graph topology setup in GIS. Second, an optimal high-level grid topology is obtained inside that graph with the help of a market model. Finally, the results are processed again in GIS, sensitivities are conducted, and selected results are further investigated. The resulting toolchain is depicted in figure 3.3.

Notice the twin-part division of the initial transmission capacity expansion problem. While the market model (step 2) performs the actual optimisation based on a constrained objective function, the pre-processing (step 1) prepares the graph for the optimiser to iterate over. Such an approach creates an extra dimension of methodological complexity and thus, sensitivity towards the result. On the contrary, it

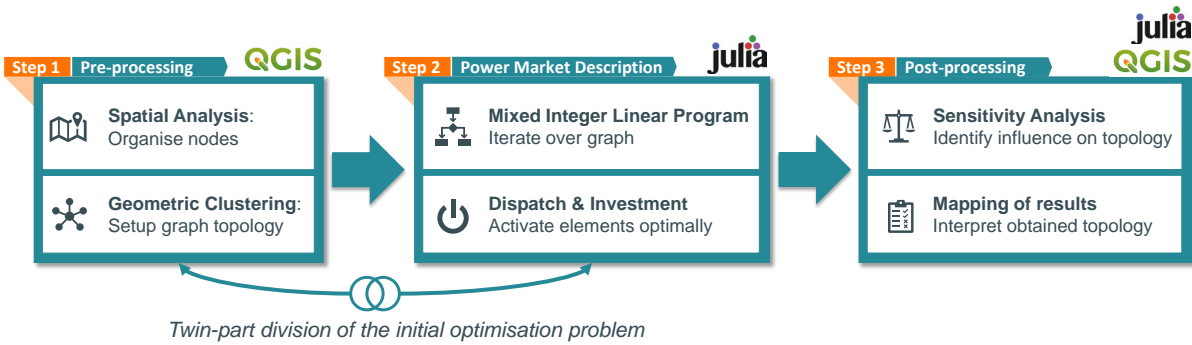


Figure 3.3: Toolchain developed for this thesis.

facilitates the setup of a consistent graph topology for the market model to iterate over. In fact, different parametrisation of the pre-processing can be used to create different graph topologies to investigate. In consequence, several scenarios with customised graphs could be analysed. This thesis sticks with just one parametrisation for the primary analysis and identifies sensitivities in the final step of the toolchain.

3.1 Pre-Processing in GIS

For an efficient set up of the optimisation problem, input geo-data needs to be acquired, validated, and structured. This is done in the first step of the toolchain presented in figure 3.3. It is depicted as pre-processing since it aims beyond the mere structuring and preparation of parameters and sets. In fact, the identification of permissive elements is already pre-solving the broader optimisation problem. Since most data in this analysis is linked to a geographic reference, a GIS is used for this step in the toolchain.

The purpose of pre-processing is threefold. First, it organises and filters the nodes, which is done via spatial analysis. Second, it sets up a graph topology based on geometric clustering. Finally, pre-processing improves the computational performance of the optimisation procedure in step two of the toolchain.

For this thesis project, the open-source GIS QGIS¹⁰ is used for processing of all geo-data. Geo-data is stored in standardised SQLite databases. Geopackages and CSV-files are used for data exchange. A particular strength of QGIS is its flexibility in handling a wide range of geo-data file formats. Besides, it offers an interface with Python, which allows automating workflows. QGIS is licensed under GNU general public license. This project uses the long-term release 3.10 “A Coruña”.

3.1.1 GIS analysis tasks

A GIS is a computer-aided system for modelling and processing of spatial tasks. It handles import, management, analysis, and presentation of spatial information [9]. In this thesis, it is set up to handle two fundamental analysis tasks. They include spatial analysis such as spatial queries (Where is something and what is nearby?) and geometric clustering with the help of problem-solving (Where is the best location and which optimal path links them?) [54]. Each task requires selected GIS analysis steps and creates results ready for processing in subsequent steps of the GIS analysis or in the market model. An elaborated description of the applied GIS methods to conduct the analysis is presented in sections 3.1.4 and 3.1.5. The following section delves further on that aspect and derives the added value of pre-processing in a GIS in the context of transmission capacity expansion optimisation.

¹⁰<https://qgis.org/en/site/index.html>

3.1.2 Added value of GIS analysis

Validate input data: spatial analysis

Identifying potential wind power sites is beyond the scope of many expansion studies. Distributing wind farms across the water but is subject to a resource pre-analysis and taken from other studies (c.f. section 2.1.2). Hence, the quality of input data on wind farms is a crucial element in data preparation.

Visual analysis and the intersection of points in GIS can help to gain trust in the integrity and consistency of the data sources. In addition to wind power sites, all other spatial elements in the water body can be visualised and used for cross-checking. In some cases, this may lead to the exclusion of an otherwise proposed wind farm (e.g. when a wind farm point is located in a protected area). This element of pre-processing is called spatial analysis is introduced in section 3.1.4.

Structuring the solution space: geometric clustering

One rationale of offshore grid development is the leveraging of synergies when planning and operating offshore transmission assets. One prominent synergy is the reduced total cable length when combining several cable systems into one higher-rated (back-)bone. When combining several cables into one system, economics of scale and economics of scope apply [72]. Larger cables tend to get cheaper per power rating and length and several offshore wind farms can be connected with just one cable system. Further synergies may arise from the operation of interlinked terminals (multi-terminal or modular offshore grids) [2]. Finally, the development of hybrid assets increases the operational flexibility and usage rate, which improves economic efficiency, especially on the OPEX side [7].

Geometric clustering can help to identify such terminal locations. Its task is to partition the set of wind farms by spatial relation to each other. Next, it identifies common centre points for the identified clusters. They can later serve as offshore hubs in a hub-spoke design. Finally, geometric clustering allows identification of permissive links. In other words, not every node is linked with every other node. Specific link types can be generated based on selected input parameters. For instance, hub-spoke links share different characteristics than radial links. The different types of element classes for structuring links and nodes, and the procedure to classify them is further elaborated in section 3.1.5.

Limiting the size of the solution space: Reducing complexity

Capturing a large water body of the Baltic Sea with any kind of grid infrastructure results in a large solution space with a high number of nodes under consideration. Consider a fictional setup of just four wind farms requiring at least one connection to the shoreline (one optimal path per wind farm). Imagine four onshore substations in reach. Besides, two hubs shall be part of the permissive element list. Without any further pre-analysis, an optimiser would need to assume all nodes being equally classified and adjacent to each other. The given set of $n = 10$ nodes would hence result in a number of links L equal to

$$L = \frac{n(n-1)}{2} = 45 \text{ .}$$

If per link l , one cable can be built or not (one decision variable per link) the combinatorial number of all link combinations grows exponentially resulting in

$$\sum_l^L \binom{L}{l} = 2^L = 3.5 \times 10^{13} \text{ .}$$

Even for a modest set size of nodes, this reaches prohibitively high numbers of combinations. In practice, this number rises even further since per link more than one cable can be built and indeed more than one decision variable needs to be solved. Each node or link which can be eliminated from the initial set of permissive elements, therefore, reduces the size of the solution space and computational complexity substantially. In figure 3.4 the number of generated links can be reduced from 20 000 in the complete graph with all combinatorial links to 1300 in the reduced graph with permissive links. Observe the exponential savings on the combinatorial complexity and the visual clearance of the offshore grid options.

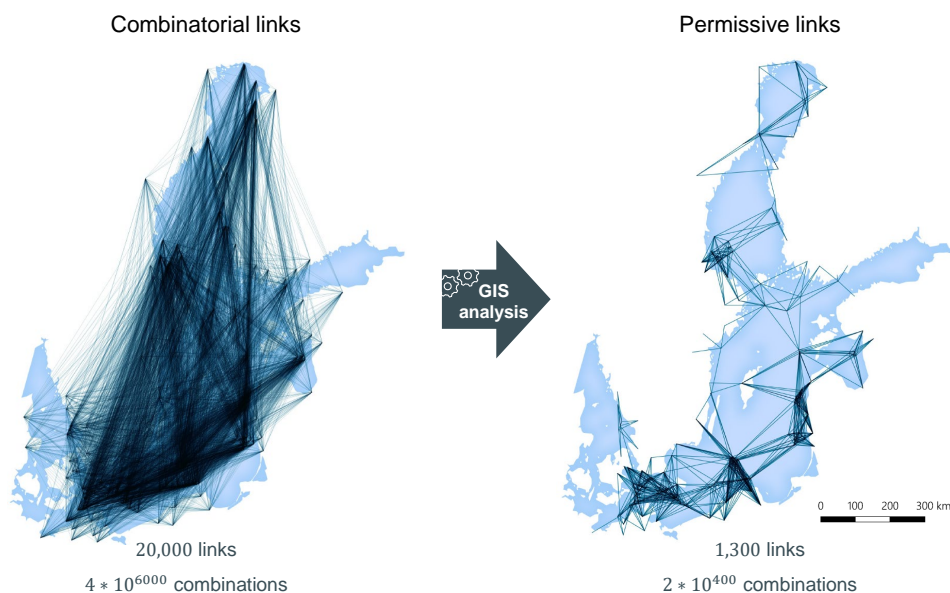


Figure 3.4: Reducing combinatorial complexity with GIS analysis.

Being aware of the rationale behind GIS pre-processing the upcoming sections introduce the elementary building blocks of GIS analysis. The methodology for the spatial analysis and geometric clustering are developed respectively.

3.1.3 Elementary building blocks of GIS analysis

Spatial information represents geo-data which projects an extract of the real world into a geographic model. The GIS is the working environment to populate and use such a model. It is organised in layers where each layer contains one type of information. Geo objects hold this information. A set of layers referring to spatial information in a given region can be displayed on top of each other to create a map [9]. Data processing refers to simultaneous or sequential manipulation of sets of layers in so-called processing tools. The result is usually a new layer, containing processed information, which itself can serve as a new input for subsequent processing [54]. Figure 3.5 sketches this elementary mechanics of GIS. The spatial data type of a selected layer constraints the processing tools available for analysis. This analysis deals with geometry and topology information stored in vector and raster layers.¹¹

Geometric and topological information

A geometry describes real world-objects in a dataset in size, shape and relative position to each other. Carriers of that information are the elementary building blocks of the geometry type, namely pixel, point, line or shape. Spatial information such as adjacency, distance or overlap is assigned to them. This relational description can be projected into an absolute one with the help of a coordinate reference system [9].

¹¹The wording “raster layer” and “raster data” is used synonymous in this thesis. Likewise with vector data.

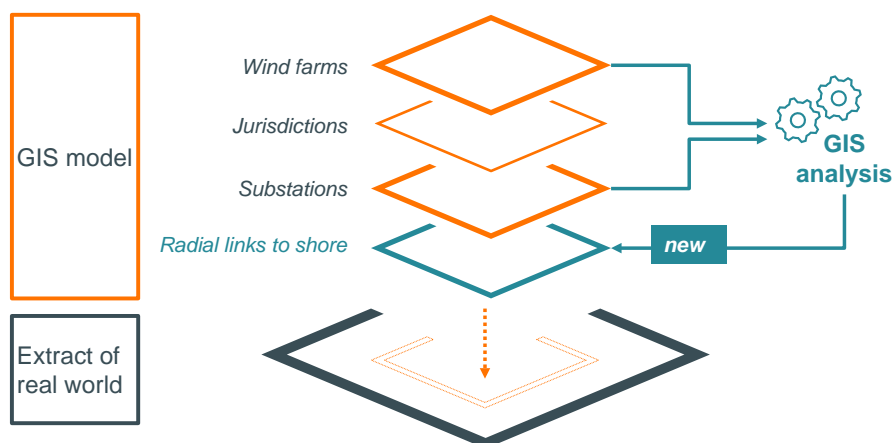


Figure 3.5: Layer based display and processing of spatial information in GIS.

For this thesis, EPSG: 3025 is used as coordinate reference system.¹² It is used since it allows statistical mapping at all scales and accurate measurements in meters. As opposed to true angular or true longitudinal area representation, it offers a true area representation. This is desired in the context of spatial clustering based on distance and density. The coordinate system is cartesian with two axes, namely northing and easting. The prime meridian is Greenwich. All coordinates in this thesis use it for reference.

The concept of topology in the context of GIS refers to the mathematical discipline of graph theory. A topology describes abstract relations of geo-objects among each other. In graph theory, they are also denoted as points. In contrast to geometry, it is only relevant if a pair of points is neighboured or reachable via intermediate objects. The type and metrics of that relation are not tracked. Carriers of the topological information are the lines, linking pairs of points with each other. When two points are linked, they are called adjacent. A chain of lines creates a path, where a closed path is known as loop or mesh. A desirable strength of topology is that it remains unchanged, even when processing tools change the geometric organisation of a given data set [9].

The topology is a result of the transformation of the GIS model into an abstract mathematical graph, which requires structuring and classification of geo-data. The result is a light data structure to perform search and optimisation. This transformation requires structuring and classification of geo-data. It is the fundamental building block of pre-solved solution space and plays a core role in the GIS analysis developed in this thesis when handling vector and raster data.

Vector data and raster data

Discrete units, depicted as points describe the geometry of vector data. Several points can serve as intermediate nodes of lines or polygons (shapes). The points are also carriers of the topological information, e.g. a point can have the attribute “starting of a line” or “bordering of a shape” to indicate adjacencies. Lines and shapes are then described as ordered sets of points. A set of points belonging to one layer is stored in an attribute table where each row represents a geometry (point, line or shape). The columns are populated with attributes framing each geometry. Frequently used attributes are, for example, a unique identifier and coordinates or any other kind of geo-reference [9]. For instance, all offshore wind farms considered in this analysis are organised in one vector layer. Each wind farm is a point geometry with, among others, identifier, country ID and installed capacity. Other vector layers in the model include the transmission grid with interconnectors (line geometry), nearshore substations (point geometry) and bidding zones (shape geometry).

¹²<https://epsg.io/3035>

Raster data use pixels as their primary unit. A raster is a continuous layer similar to an image, where each pixel carries various information, depending on the number of channels being attached to it (analogous to the columns in the attribute table). Raster layers cannot distinguish between points, lines or shapes. Therefore no logical connection between the elements exists beyond the mere location in the raster. An externally defined coordinate reference system, however, creates a geo-reference of the raster data [9]. In this analysis, information such as bathymetry of the Baltic Sea or shipping density is depicted as raster data.

Processing tools

With the help of processing tools, GIS analysis of various complexity can be conducted. They take one or more layers as inputs and process the attached attribute data and geometries based on predefined parameters to create one or more output layers. A graphical modeller stacks several processing tools into more complex structures, which allows sequential or parallel processing. Each tool applies a selection of analysis methods. In this thesis, methods dealing with geometry, topology, statistics and sets are applied. The stacking of tools enabling spatial analysis and geometric clustering is described in the following sections. Both processes aim at creating the graph topology for the optimiser to iterate over. This is summarised in figure 3.6.

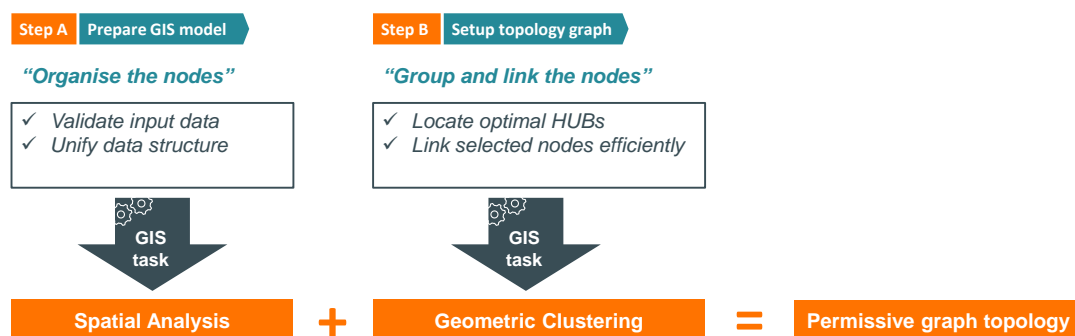


Figure 3.6: Creation of the permissive graph topology in two steps in GIS.

3.1.4 Spatial analysis in GIS

The purpose of spatial analysis is the setup of a consistent and complete data set on offshore wind generation in the BSR. Wind energy evacuation from the sea via offshore cables and nodes is the core element of this analysis. Any offshore topology needs to reflect on the regional distribution and cumulated capacity of the wind farms. When estimating the number of wind farms and their cumulated capacity for the target year, various sources are tapped (c.f. Input data screening). Pre-processing ensures that a final set of wind farms considered in this analysis is both robust and well balanced.

This analysis does not attempt to identify wind power sites bottom up. It solely bases its input on announced, proposed or permitted projects in the time horizon towards 2040. The approach arguably influences the quality of the final result. On the contrary, for a proof of concept study, it is less critical where precisely the wind farm data comes from, as long as the framework can handle such data consistently. In either case, collected data (c.f. section 2.1.2 for elaboration on wind farm data) requires validation, exclusion and enhancement.

Data collection and ranking

In the first step of spatial analysis, wind power sites are collected and classified into three groups. They are labelled as *commissioned* when they are in production by 2021. *Planned* projects include wind farms,

which are currently under construction or in a mature status of planning and permission. This category can track the commissioning date, if available. For the classification, it is, however only relevant, that this type of wind farm is likely to be online between 2022 and 2030. Finally, *proposed* wind farms are all residual projects with any kind of status ranging from mere power potential studies, early concepts to proposed priority areas.

While all three categories are included in the initial data set, it is only the third category (*proposed*) which will be further investigated. The timestep of 2040 forces this analysis to assume all commissioned and planned projects being online at their current capacity. In fact, they are subsumed with respective onshore bidding zone node and do not show up on the GIS analysis outputs. They are only included for illustration in the final step again. Dismantling of wind farms at any point in time is not considered for simplicity.

Data validation and exclusion

For each concrete wind farm project, at least two independent data sources are required for it to be included in the analysis (data validation). For those regions, not having concrete proposed projects but maritime priority areas for offshore wind energy, estimations are performed. Refer to section 2.1.2 for the respective input data screening.

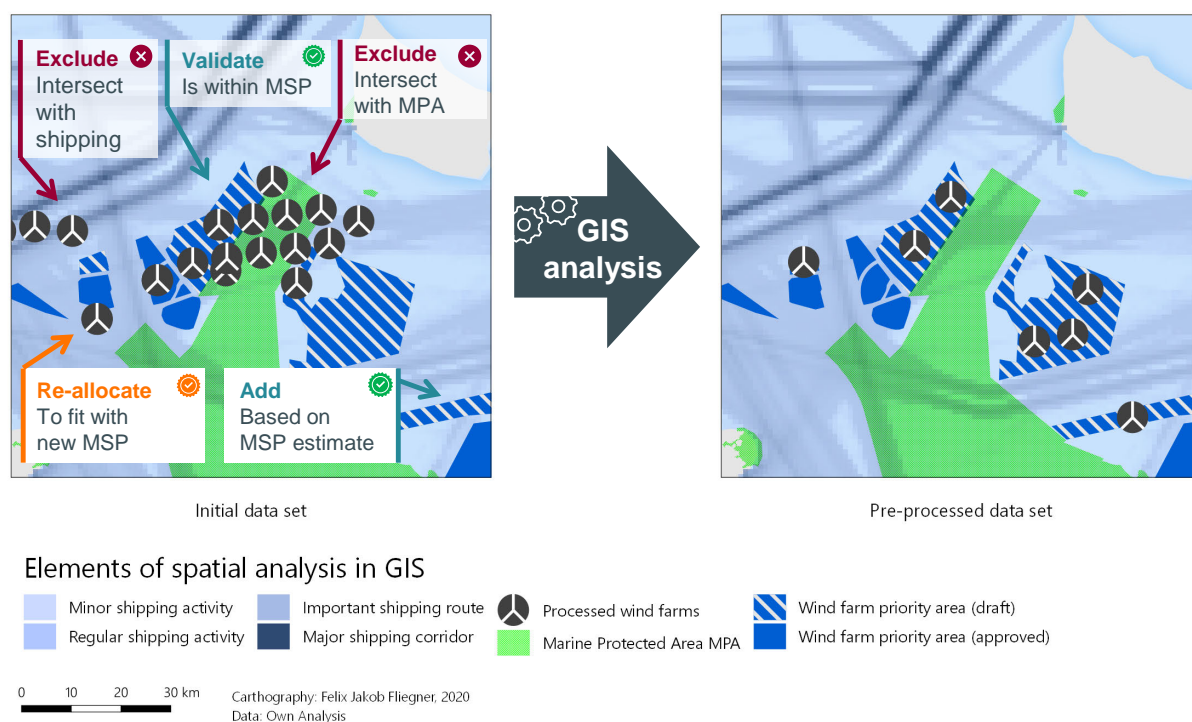


Figure 3.7: Elements of spatial analysis in GIS.

The procedure of estimated wind power sites follows a stepwise spatial selection process. The most relevant criterion for validation is the Marine Spatial Plan (MSP) by each state. An example is shown in figure 3.7. For its high level of institutional anchoring on EU level, MSP is considered the dominating source in case of data conflicts. Outside the MSP offshore wind priority areas, no wind farms are included, even if some sources might suggest them (data exclusion). Such a validation procedure is conducted in GIS with the vector intersection of wind farm locations (point geometry) with MSP (shape geometry). Inside the MSP areas, wind farms up to a cumulated capacity limit are included. This benchmark can be calculated based on the MSP area size, and the average power density of offshore wind farms. In some cases, power density or power limits are explicitly stated in the MSP. In GIS, this process requires a

point-in-polygon-counting.

The second criterion for power site estimation is at least one source proposing a wind farm location. The fallback source in this analysis is the comprehensive list of identified wind power sites in the BEMIP study [24]. For projects in the territorial zone, the validation with the help of MSP clusters is not feasible since MSP does not apply there. In those places, the additional intersection of wind farm points is done with other information layers in the GIS.

This thesis considers two additional types of layer information for enhanced spatial selection. The first type represents marine protected areas (MPA), namely UNESCO heritage areas (UN level), Natura2000 protected areas (EU level), and national parks or otherwise managed areas (national level). In figure 3.7 they are shown as green shapes. Second, shipping routes are displayed as a density raster counting the ships per cell and year. This raster is rendered in shades of blue in figure 3.7.

Interference with either of these layers results in the exclusion of a proposed or suggested wind power site. In some cases, manual visual inspection is performed. Wind farm locations are then shifted in the neighbourhood to satisfy all exclusion criteria while keeping them in the model. A prominent example is the Bornholm Energy Island initiative by Ørsted and the Danish energy agency [12]. While the BEMIP study proposes a wind farm distribution which interferes both with shipping routes and protected areas, the later published MSP draft by the Danish energy agency now allows re-allocation of the identified points.

Data enhancement

The final step in spatial GIS analysis addresses the attribute data of each wind farm included in the analysis. In case it is located in an area of medium or high sea ice risk (c.f. section 2.1), its cost parameters are incremented accordingly. Besides, the screening of markups based on sea bed condition or sea depth belongs to the same category of spatial analysis and pre-processing. Both of them are, however, excluded from this analysis for simplicity. The final result of the spatial analysis in GIS is a consistent set of offshore wind farm points. The set can be processed further in geometric clustering and the setup of the graph topology for the market model.

3.1.5 Geometric clustering in GIS

Structuring the solution space for permissive links and nodes results in the ranking and classification of geo-objects. The objective of geometric clustering is to achieve this structuring by aggregation of geo-data from various layers into one graph topology. The points of that graph represent permissive links, connecting pairs of points. Points are either wind farms, substations (both onshore and offshore) or bidding zone nodes.

While most nodes exist before geometric clustering, permissive hub nodes and all permissive links need to be created. In other words, geometric clustering takes two steps. First, it identifies all permissive hubs by employing classification methods. This step is also denoted as point creation and is introduced first. Second, it links the hubs and all other nodes in the model with each other guided by geometric and technologic parameters. This procedure is denoted as link creation and completes the graph. Figure 3.8 sketches the entire procedure, which is explained subsequently.

Leveraging density and reachability

Identifying prospective hubs for clustering wind farms into groups needs to reflect the nature of spatial wind farm distribution across the water body. Four generic types of spatial distribution exist, which are exemplified in figure 3.9. In some places, wind farms are close to each other and may form compact

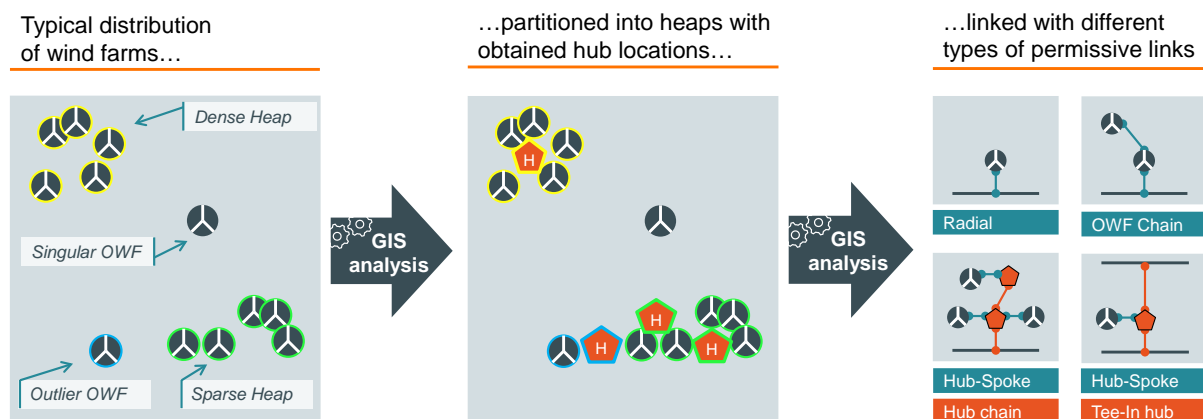


Figure 3.8: Elements of geometric clustering in GIS.

groups. Such groups are easily distinguishable from their surroundings by visual inspection. In other places, wind farms may occur loosely chained, which makes the identification of groups ambiguous. An extreme case of remoteness is a singular wind farm with no prospect of clustering. Most challenging for clustering are outliers, which blur the boundary between loose groups and singulars. An outlier is a wind farm which is not close enough to its neighbours to be regarded as part of a cluster. At the same time, it could be linked to that cluster with the help of one intermediate hub node. In other words, it is neither a group member nor a singular. The concept of density best frames this notion of compact groups, scattered chains, singulars and outliers. Clustering wind farms is now a question of division based on density features.

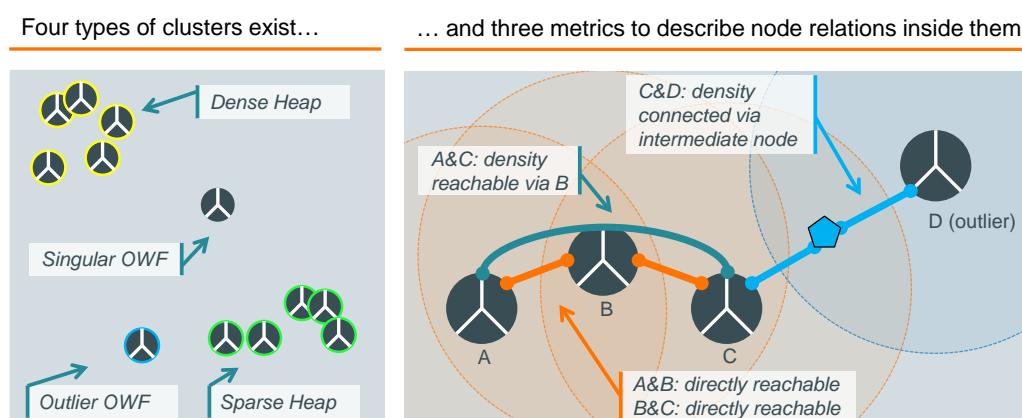


Figure 3.9: Spatial distribution of offshore wind farms and reachability relations within clusters.

For a group, the typical density of wind farm nodes is considerably higher than outside that group. In areas of noise (only singular wind farms) the density is lower than in any of the clusters. The separation between compact and scattered groups can be formalised with the concept of reachability.

Two nodes are *directly reachable* if the connecting link is not longer than a defined threshold (c.f. buffer circles in figure 3.9) [21]. If all nodes in a set of wind farms are directly reachable to each other, this set is a compact group. When the distance is measured Euclidean, the shape will be close to a circle.¹³ It will be called dense heap for the remainder of this analysis. For a dense heap, one global centre point can be found, which links all surrounding nodes in a hub-spoke design.

If the group happens to be chained, the reachability condition may only hold for selected pairs of group members. Follow this in figure 3.9 (green link). While B is directly reachable from A and C, A and C

¹³Unless otherwise and explicitly stated Euclidean distance is meant with distance measurements in the entire thesis.

cannot be linked directly without violating the threshold. Since B is a common neighbour of A and C and a member of the same heap, they can still be labelled as *density reachable* (via B). Such a group is usually not dense and can take any arbitrary shape [21]. It will be called sparse heap for the remainder of this analysis. An important observation with sparse heaps is the absence of a shared centre point, which is directly reachable by all group members. Instead, several sub-centres can exist, which again link nodes in a hub-spoke design.

Outliers can be linked to both dense and sparse heaps or indeed to each other. In contrast to the sparse heap, this does require an additional intermediate node. This node can be depicted as yet another sub-centre, just on the edge of a heap. As such, it does not belong to the heap but allows linking one or more outliers to it. Observe that the heap definition still holds: The nodes are at least density reachable, while the outlier is still not density reachable. It is however reachable with the help of a new external (i.e. non-member of the heap) created node. This type of connection is known as *density connected* [21] and is illustrated blue in figure 3.9.

Partitioning algorithms for heap identification and topology setup

Processing tools which divide a given dataset into heaps are also denoted as partitioning algorithms. In this analysis, two of such algorithms are applied: k-means and DBSCAN (Density-Based Clustering and Application with Noise). When applied in combination, they share three desired features of clustering algorithms, for which they are considered suitable in this context. First, they require minimum domain knowledge to determine the input parameters. Second, the discovery of clusters of arbitrary shape is ensured. Third, they run efficiently on large data sets.

K-means clustering belongs to the statistical domain of spatial GIS analysis methods. It is a minimum distance classification, which partitions a multivariate dataset into k disjunct clusters. Once the clusters are identified, centres of gravity of each cluster can be calculated [9]. The parameter k defines the number of clusters to be obtained. In this analysis, k-means is repeated with incremental k until all members of a cluster are directly reachable from their centre of gravity. From that point on this centre is labelled as *permissive k-means hub*. An example is shown in figure 3.10a (yellow clusters).

The incremental approach avoids arbitrary pre-definition of k . Minimum distance classification is well performant in the identification of small and dense heaps. It does, however, fail to recognise sparse heaps, i.e. such scattered areas are randomly divided into sub-clusters. Besides, k-means does not allow assignment of one wind farm to more than one hub. It is, however, desirable to identify all directly reachable hubs nearby. To address this lack of accuracy, DBSCAN is introduced.

DBSCAN applies the spatial GIS analysis of classification as well. It follows the concept of maximum likelihood classification but uses a different kind of indicator than probability. Clusters are identified based on the regional analysis of density in a given data set. For each point of the set, at least one more wind farm must be directly reachable, in order to satisfy the cluster condition. Otherwise, the node is either outlier or singular. The cluster is complete when all density reachable nodes have been found [21]. Finally, sub-centres are created such that each hub node groups a non-redundant subset of the heap. They are denoted as *permissive DBSCAN hub*.

Similar to k-means, no pre-set apart from the mere distance threshold is required. DBSCAN performs even without an outer loop, testing when to abort. Finally, heaps of any shape are identified with a slight bias towards sparse heaps. The identification of sub-centres requires an additional iteration of DBSCAN and buffer analysis with a redundancy test, which makes the procedure more complicated. A positive side effect of the sub-centre analysis is, however, that outliers are included and automatically linked via intermediate nodes. The concept of DBSCAN with buffered post-processing is sketched in figure 3.10b (green and blue clusters).

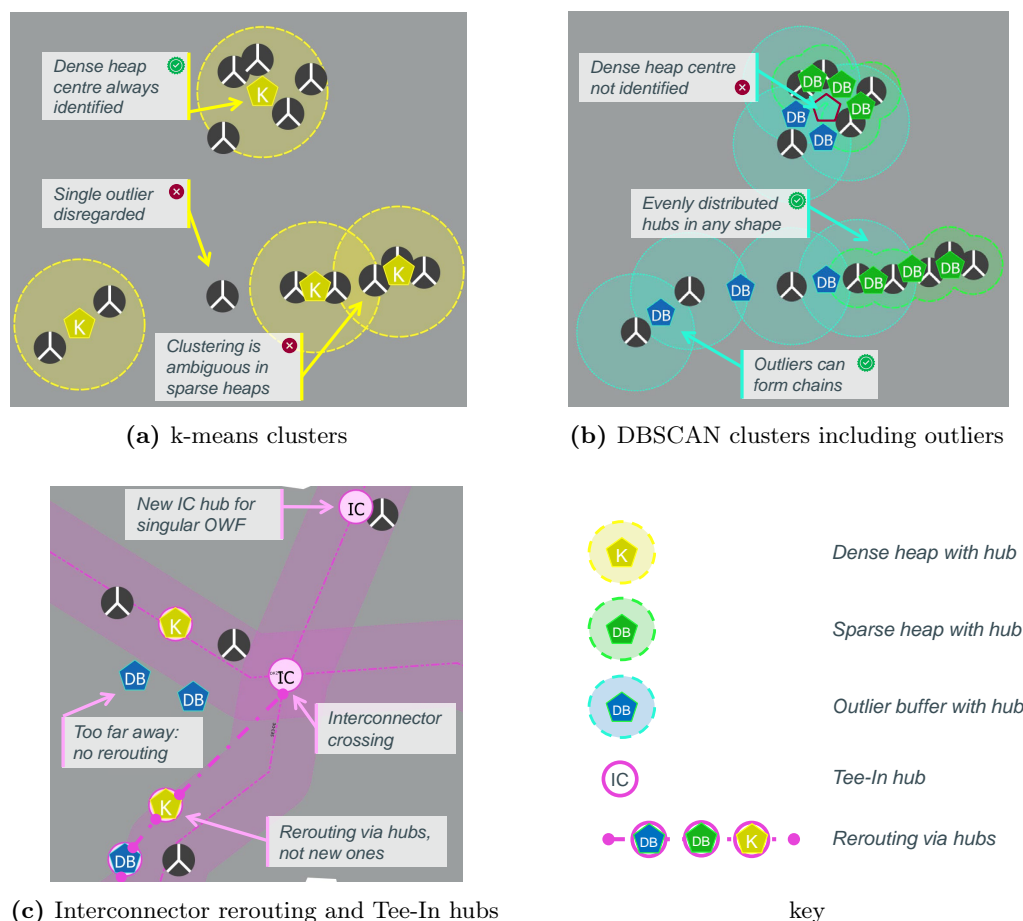


Figure 3.10: Observations from partitioning with k-means, DBSCAN and buffer analysis.

Interconnectors can be regarded as outliers in this process. I.e. the buffer analysis around heaps can not only identify surrounding density connected wind farms but also lines. In case an interconnector passes by an existing heap, it is rerouted via the closest hub node. If the interconnector passes by a singular wind farm, a new node is created on the interconnector. Finally, two interconnectors may intersect, which creates an opportunity of an offshore switchyard. The result is, in all three cases, a split interconnector line with an intermediate hub node. Since it serves as a plug, it is denoted as *permissive Tee-In hub*. Figure 3.10c depicts all three cases (pink nodes).

MiniMax game to obtain permissive hub nodes

This thesis proposes a simultaneous partitioning with k-means and DBSCAN. Both algorithms are applied to the same graph before a final redundancy test ensures the overall integrity of the resulting set of permissive hubs. This approach is denoted as MiniMax game [64] as shown in figure 3.11. k-means performs well in limiting the number of hub nodes (Mini-game). At the same time, DBSCAN creates a non-redundant and non-random enhancement of the clusters, including outliers (Max-game). In other words, once k-means is finished, DBSCAN searches both for outliers near k-means hubs and adversely shaped sparse heaps. When DBSCAN terminates, each OWF is either singular, outlier or member of one or more heaps. Interconnectors are linked to heaps or outliers, where permissive.

The enhancement of MiniMax is threefold. First, it ensures that wind farms are linked with all reachable hubs nearby (negating the pitfall of k-means). Second, it creates permissive cluster options for smaller sub-clusters, and it identifies outliers. Finally, it limits the total number of permissive hubs both with the help of k-means clustering and final redundancy testing.

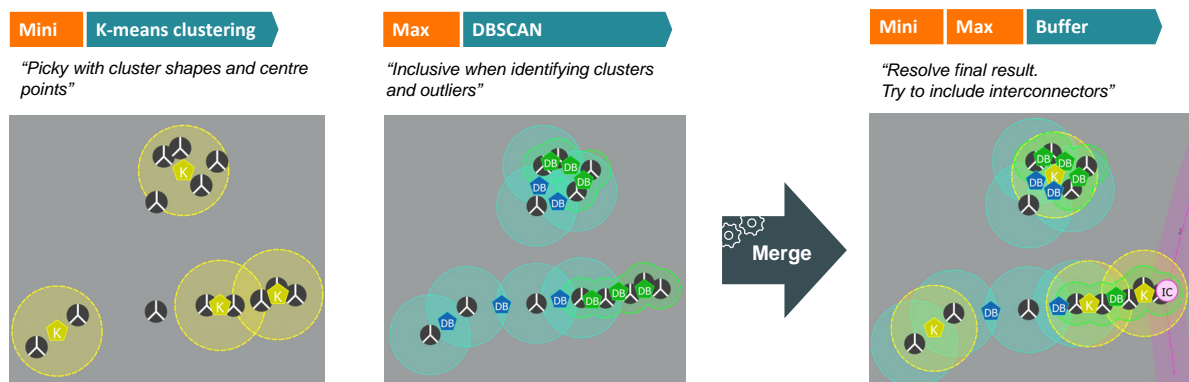


Figure 3.11: Elements of MiniMax partitioning with redundancy filtering in GIS.

Node creation summary

In summary, four types of spatial wind farm distribution can be distinguished. Singulars, sparse heaps, dense heaps and outliers. MiniMax partitioning identifies them. It describes a joined clustering of k-means and DBSCAN with buffer post-processing. As a result, it obtains both global and local centre points which can serve as hub-spoke connectors for all wind farms nearby. A take-away from this algorithm is the Tee-In clustering of wind farms or hubs into interconnectors nearby. Once all nodes are generated, the GIS can continue in the topology setup, by adding links.

Link creation for completing the graph

Once all wind farms are assigned to clusters with respective hub locations, the graph can be finalised. It takes advantage of the spatial information and cluster information of all previous processes. Guided by a parametrisation, links are either created or not. Figure 3.12 summarises all link types considered in this analysis. Read the graph cumulative from left to right. For instance, a radial hub link (third column) is a subset of a hub chain (fourth column), which itself could contain tee-in hubs, if linked to more than one shoreline (fifth column). Similarly, the last wind farm in the OWF chain (column two) is denoted a clustered wind farm. It is first hub-spoke connected to another node (similarly to the wind farms in column three) before the path continues radially to the shoreline. In other words, it is important to understand here that both, wind farms (grey circles) and hub platforms (orange pentagons) can act as intermediate hubs in a chain or as central hubs of hub-spoke layouts. The results discussion revisits this observation.

Link types obtained from geometric clustering

The base case for link generation is the **radial OWF link**. It connects one wind farm with one onshore substation. Either the prospective substation is located within the same jurisdiction, creating a national radial connection. Or the radial connection crosses borders and links a given wind farm to a foreign onshore grid. The former case is also known as business-as-usual since this is the procedure in offshore grid planning up to date. The latter one takes already one step towards European integration. The rationale is, that connecting wind farms to foreign shorelines might be desirable either for leveraging reduced cable cost (shorter distance) or higher market value of the generated electricity (higher wholesale prices). The GIS analysis creates permissive links by identifying the three shortest links from each wind farm to shore.

The number three is arbitrarily chosen. As a rule of thumb, it should be higher than one, to give the model some decision room. It is, however, desirable to make it not much higher than one since creating random links contradicts the purpose of GIS analysis. Alternatively, a circumference of some kilometres

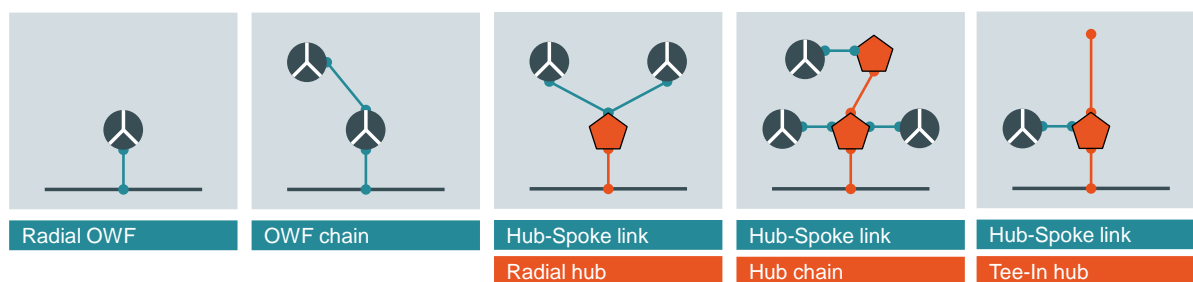


Figure 3.12: Link types created with geometric clustering.

could be defined around each wind farm. All onshore substations lying in that area are then permissive radial connection points. This thesis steps back from this approach since it generates overwhelmingly redundant links in areas with high substation density.

The next best connection prospect for a given wind farm is creating an **OWF chain**. It links one wind farm with the next one, before connecting the entire chain with the onshore grid. This follows the rationale that a given wind farm always entails an offshore substation. Making this platform bigger, enabling it to handle throughput from surrounding wind farms as well, is assumed feasible in the scope of this analysis. The GIS analysis creates permissive links by searching for neighbour wind farms within a circumference of 200 km.

200 km is chosen for the Baltic Sea Region since it reflects the average distance from the shoreline to the jurisdictional EEZ borderline (in “the middle” of the water body) The reasoning here is, that a chain requires linking of at least two wind farms. In the most extreme case, this arbitrarily chosen pair would be located oppositely located in the water body. If they were further away from each other, their optimal connection solution would likely be a radial or a different cluster. Trial and error test run of the GIS analysis revealed that prospective wind farm chains beyond 200 km are indeed not activated in any model run in the market model. Therefore, they can be excluded from the solution space without pruning an optimal solution.

Clustering of wind farms and connecting the cluster with a central link requires **hub-spoke links**. They link wind farms belonging to one cluster to a common central node, which is denoted as hub. Such hub could serve as a modular offshore grid platform¹⁴ with a hub-spoke layout or as a Tee-In node being connected to an interconnector. Such hub-spoke connectors can be sized a bit smaller, for their limited distance they need to cover. The smaller cable dimension reduces cost significantly (c.f. section 2.2.2). This creates a trade-off in cost for the optimiser to make. It can either leverage from the cheap hub-spoke cables, requiring an expensive central platform. Alternatively, it builds longer cables while saving on smaller platforms. The distance limit reflects the technical constraint of high compensation and transmission losses beyond that distance at this voltage level.

In practice, hub-spoke cables could, of course, get longer if more expensive measures were taken to safeguard operation. Since operational aspects are, however, not considered in this analysis, it sticks with the mere 20 km limit. Regarding the sensitivity of that parameter to the resulting size and shape of wind farm clusters in the BSR, tests revealed that distances of 15 km or up to 30 km do not alter the final graph topology significantly. It is, however, advisable to cross-check this parameter for other model runs again since it introduces a substantial cost trade-off into the model.

Finally, hub nodes can either be interconnected among each other, creating **hub chains**. Alternatively, they can be linked to the shoreline, resulting in (central) **radial hub links**. The rationale behind this and the parameters are similar to radial wind farm links and wind farm chains, respectively.

¹⁴first proposed by Elia in <https://tyndp.entsoe.eu/tyndp2018/projects/projects/75>

3.2 Power Market Description

The core element of the optimisation framework is a market model based on a constrained objective function. In figure 3.3 it is depicted as power market description which reflects the focus of optimisation. The model receives the topology generated during pre-processing and interprets this graph as a power market involving several bidding zones (nodes) with nominal transfer capacities linking these zones (lines).

The purpose of the market model is threefold. First, it abstracts the reality of the physical power grid. Second, it replicates the electricity market by describing an economic dispatch problem. Third, it makes investment decisions, which activate permissive nodes and links in the initial graph to solve the initial problem for optimality. The following sections elaborate on how these objectives are to be met.

The model setup is written in the Julia programming language enhanced by the algebraic modelling library JuMP [8, 15]. It is a high-level dynamic programming language for numerical computing like Python in combination with Pyomo. One advantage of Julia over Python is its higher performance with respect to computation time [81]. This analysis uses Version 1.4.1, which is available open-source and licensed under MIT license.¹⁵

3.2.1 Building blocks of the optimisation model

For the task at hand, a transmission capacity expansion problem is setup. On the one hand it seeks a sufficiently detailed representation of the existing grid and future changes to it. On the other hand, it tries to focus the complexity on the discrete decision making of capacity expansion. Both desired outputs result in a trade-off between simple models with linearised physical constraints and more sophisticated models with a more accurate depiction of the physical reality. While the first one reduces computational complexity, its results are not accurate for final network expansion decisions or indeed estimations on operational feasibility. Conversely, the latter approach quickly becomes computationally infeasible to solve, which would require tighter pre-processing (reducing the graph) or manual scenario building [5].

Centre of complexity

This analysis gives preference to a linearised description of the physical reality of transmission capacity expansion planning. It underlines the approach of this thesis, not aiming at an offshore grid deployment plan but rather a pre-feasibility study to investigate high-level topology configurations in the big picture. In other words, the output of this analysis can be regarded as a relaxation of the real physical optimisation problem. It draws the focus of attention towards high-level discrete decision making as opposed to a detailed technical simulation. A hypothetical fourth step in the toolchain could perform such an analysis to investigate the operational and economic feasibility of the obtained high-level offshore topology.

The combinatorial nature of expansion options defines the focus of complexity in the analysis. Each graph element of the pre-processed topology can either be active or not. Initially, most elements are not active but labelled as permissive. The permissive rules are laid down by the GIS pre-processing and topology setup. The optimiser of the model now iterates over the permissive topology by testing combinations of link and node activations for feasibility. The feasibility criteria are laid down by the constraints of the model (c.f. section 3.2.4). An optimal solution is found, when no other combination of active links and nodes performs better with respect to the objective function. Only active elements can contribute to the optimal solution since they can perform transmission and switching tasks. Such tasks are required for power transmission from nodes with generation surplus to nodes with demand surplus. Since the combinatorial options in the model drive computational complexity, concessions (i.e. simplifications) need to be made at other parts of the model to keep the entire problem solvable.

¹⁵<https://julialang.org/>

A significant simplification in this analysis is the constraint of the physical power flow on active links by mere nominal transmission capacity (NTC). The power rating of grid elements is set as the paramount criterion for the optimiser. Other physical parameters, which also influence the power flow, are neglected: nodal voltage differences and line impedances. Note that this simplification is still in agreement with KIRCHHOFF's current law while neglecting KIRCHHOFF's voltage law and OHM's law.

It is a valid simplification in the face of a stable power system operation. Neither dynamic instability nor contingencies will be part of the analysis. Hence voltage limits can be assumed within tight limits, without modelling them. In the absence of voltage angles, modelled power flows can deviate from real power flows. They may lead to line congestion which would otherwise not show up or on the contrary suggest feasibility of a line flow which could suffer from loop flows [4]. Finally, neglect of line losses is likely to result in underestimated investment cost since lossless lines can be dimensioned smaller [6]. The notion of a high-level descriptive analysis justifies all beforementioned simplifications since no cost-benefit analysis or indeed investment decision support is envisaged here.

Setup of a transport model

Reflecting on the focus of complexity, a problem formulation as a transport model is considered sufficient for this analysis. Similar formulations for equivalent problems agree with this approach [5, 63]. The central idea of a transport model is a linearised representation of properties of links and nodes. Power can flow on links from one node the next, when it is active and when the NTC is not exceeded. Since voltage angles are not accounted for, the power flow optimisation becomes purely economic. In other words, the model does not determine a real optimal power flow but an economic optimal power flow instead.

The economic model is split into two parts: economic dispatch and investment. The first part of the model abstracts the power flow into the economic realm and enables a replication of the power market. It optimises the economic dispatch of power plants, resulting in a cost minimisation problem. It sets up a merit order, where units are dispatched until demand is met. Preference is given to cheap units with marginal cost close to zero, which benefits all renewable sources (including all offshore wind farms). The market model further enforces nodal energy balance, where the sum of all infeed (generation and import via links) equals withdrawal (demand, storage, and export via links). Exchange with neighbouring bidding zones is also considered. The first-hand outputs of this model part are production levels of generation units, state of charge of storages (namely filling levels of hydro reservoirs), nodal market-clearing prices and power flow on all active links.

The second part of the transport model addresses the activation of graph elements. The model receives an initial start grid (some elements activated) and can expand this grid by activation of additional graph elements. Such an activation induces costs and forces the model into a trade-off. It can either increase transmission capacity between countries or by connecting wind farms at the cost of activating a required combination of permissive graph elements. Alternatively, if it refuses to do so, it loses cheap electricity in the merit order and transmission capacity. In other words, investments in the activation of graph elements improve the objective value as long as savings on the dispatch side outweigh the induced cost of investment. The output of this model part is a set of activated links and nodes with a capacity rating, which expand the initial graph and the grid it represents. A schematic representation of the transport model setup is depicted in figure 3.13.

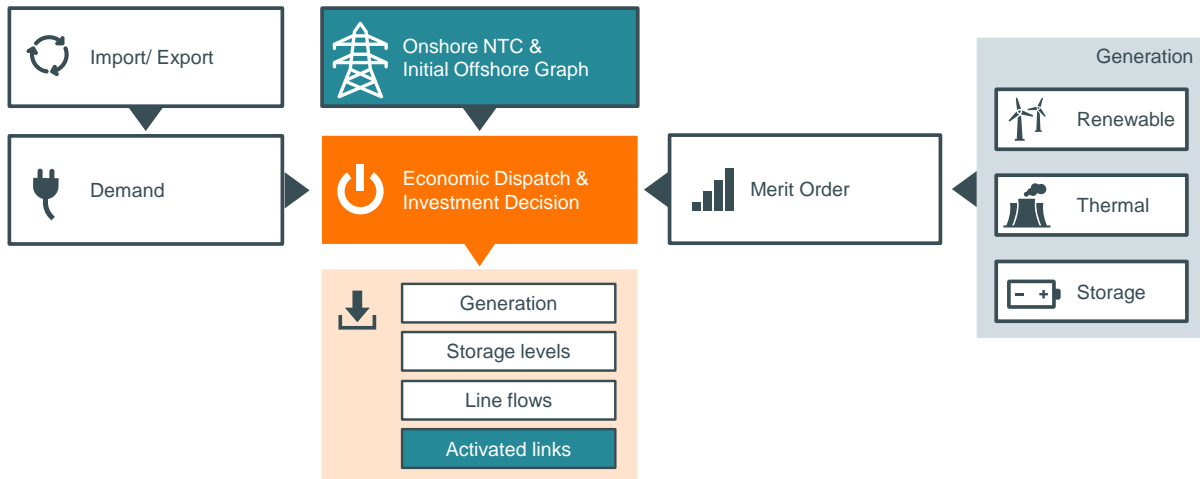


Figure 3.13: Building blocks of the optimisation problem in Julia. – Adapted from [81]

3.2.2 Definition of a linear cost function

Investment optimisation results in discrete decision making for individual graph elements. Only active elements can be part of a feasible solution. Mere activation of an element can be understood as a fixed cost investment decision. The impact of its activation and therefore final cost depends on its power rating, making it a variable cost investment. Both cost types need to be reflected in the cost function.

Discrete decision making

Each link and node in the offshore water body is depicted as an individual graph element. Link activation reflects the decision by the optimiser to install a given capacity on that link. This requires the introduction of integer variables. For each link, it tracks the number of discrete cable systems required to satisfy the capacity request. For instance, a 1.7 GW capacity request might result in fixed cost equivalent to two 1 GW systems, reflecting the discrete nature of feasible investments. Offshore node activation usually requires the installation of an offshore platform. This one-time investment is tracked with the help of a binary variable, denoting its existence or not. No scaling in size or shape is tracked here for simplicity. If that platform equipment serves a conversion task (transformation on the AC side or conversion between AC and DC), the same logic with integer power rating of the installed equipment as with the cables applies.

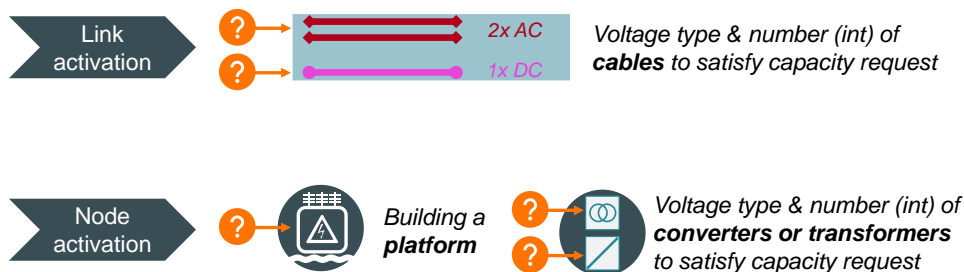


Figure 3.14: Discrete decision making in Julia for node and link activation.

In consequence, each link and node element introduces two integer variables into the model. Each node element additionally introduces one more binary variable. Figure 3.14 summarises the discrete decision making in the model. A cost function assigns predefined cost parameters (c.f. section 2.2.2) to permissive nodes and links during activation.

Linearised cost function

A linear cost function is the core element of a linear model. It is commonly used in the context of market modelling for three main benefits. First, it simplifies computational complexity. Since the problem is a MILP already, its complexity is driven by discrete decision making. Any simplification in the remaining model towards linearisation, therefore, facilitates performance and sometimes even solvability. Second, the amount of required input data can be limited. Collecting realistic and consistent cost data can be difficult. Making the model ever more detailed requires more data, which at some point adds more uncertainty to the result than is gained from the finer granularity. Besides, a linear cost model can still leverage more detailed data when calibrating the linear parameters. Third, a linear cost model is regarded as a reasonable approximation to the real costs in the context of high-level topology optimisation [68].

Based on [40] a linear cost model is defined. It reflects the discrete (fixed cost) and continuous (variable cost) notion of activating a node or link, respectively.¹⁶ The model separates a link, node and markup term, which are called respectively to accumulate the cost for a given investment decision. The combination of fixed and variable cost terms results into a step-wise sloped linear cost function.

Link activation results in investment cost equal to:

$$cost(l, v) = \underbrace{K_{l,v} \cdot len_l \cdot c_{l,v}^{len,pwr}}_{\text{variable}} + \underbrace{\Upsilon_{l,v} \cdot (len_l \cdot c_{l,v}^{len} + c_v^{fx})}_{\text{fixed}}, \quad \text{where } \Upsilon_{l,v} = \left\lceil \frac{K_{l,v}}{\widehat{\kappa}_{l,v}} \right\rceil. \quad (3.1)$$

The variable link activation cost is defined by a length- and power dependent parameter $c_{l,v}^{len,pwr}$. Consequently it scales with the link length len_l and link capacity $K_{l,v}$, where the latter represents one continuous decision variable per link $l \in L$ and voltage type $v \in V$. Fixed link activation costs are made of a length dependent term $c_{l,v}^{len}$ and a length independent term c_v^{fx} . Depending on the requested capacity rating for a link, discrete cost steps are enforced. They are accumulated in the integer decision variable $\Upsilon_{l,v}$. The integer value can be depicted as ceiling value of the requested capacity $K_{l,v}$ related to the rated capacity $\widehat{\kappa}_{l,v}$ of one cable.

Node activation follows a similar notion and results into:

$$cost(n, v) = \underbrace{K_{n,v} \cdot c_{n,v}^{pwr}}_{\text{variable}} + \underbrace{\Upsilon_{n,v} \cdot c_{n,v}^{fx} + \Phi_{n,v} \cdot c_{n,v}^{act}}_{\text{fixed}}, \quad \text{where } \Upsilon_{n,v} = \left\lceil \frac{K_{n,v}}{\widehat{\kappa}_{n,v}} \right\rceil. \quad (3.2)$$

Observe a split of the fixed cost term into two parts. While the first one mimics the approach from the link activation with help of the integer decision variable $\Upsilon_{n,v}$, the second one $\Phi_{n,v}$ enforces a one time payment for building the platform. C.f. to figure 3.14 for clarification.

The nodal activation cost are further adjusted with help of a markup function, defined as:

$$markup(n, v) = K_{n,v} \cdot mu_{n,v}^{pwr} + \Phi_{n,v} \cdot mu_{n,v}^{act}. \quad (3.3)$$

Two types of calibrations are feasible in the model. The first one is a power dependent cost deduction $mu_{n,v}^{pwr}$ for nodes, which are not built offshore. This may represent nodes located on an island or onshore. The second term $mu_{n,v}^{act}$ addresses a markup for investments inside regions with sea ice risk (c.f. section 2.1 for elaboration).

The markup function could also be applied for link specific cost adjustments or for benchmarking otherwise unknown cost. For instance, the high uncertainty entailed by investments into DC circuit breakers could

¹⁶C.f. section for a summarised model nomenclature.

be parameterised as an additional markup term. Refer to [74] for a suggested approach. This thesis steps back from this approach for reasons of simplicity.

3.2.3 Completing the objective function

The beforementioned trade-off between dispatch cost and investment cost is enforced by a cost minimisation problem. Consequently the objective function is a minimisation which calls the cost functions from equations (3.1), (3.2) and (3.3). For the final objective function two additional considerations are made.

The first one is the necessity of discounting investments. The obtained dispatch cost are scaled to an entire year with help of the step length parameter t . It scales up the step length of the “hour” $h \in H$ for each model run that is shorter than one year. The parameter is defined as $t := \frac{6870}{|H|}$ for a normal year.¹⁷ Observe that if $|H| = 8760$, one hour in the model does indeed represent one hour in reality and the sum of all represents one year. For a daily ($|H| = 365$) or six-hourly ($|H| = 1460$) analysis instead, t stretches the “hourly” time steps accordingly. Conversely the investment cost, being applicable for the entire lifetime of the asset, are scaled (discounted) to one year as well. This is done with the annuity factor $a := \frac{(1+i)^d \cdot i}{(1+i)^d - 1}$, where i is the discount rate and d is the asset lifetime [37]. In that way, both cost categories become comparable and can be handled in one equation.

The second consideration is a simplification of the cost parameters. The length- and power dependent variable cost parameter for the link activation is pre-processed into a solely power dependent parameter for convenient use with power variables: $c_{l,v}^{\text{pwr}} := \text{len}_l \cdot c_{l,v}^{\text{len,pwr}}$. Similar with both fixed cost parameters: $c_{l,v}^{\text{fx}} := \text{len}_l \cdot c_{l,v}^{\text{len}} + c_v^{\text{fx}}$. This pre-processing is simple, since the link lengths are known from beginning on and the resulting fixed cost can be computed during model setup as opposed to calculation during the optimisation.

The objective function results in:

$$\begin{aligned}
 \min \quad & t \cdot \sum_{\substack{g \in G \\ h \in H}} mc_{g,h} \cdot P_{g,h} && \text{dispatch} \\
 & + a \cdot \sum_{\substack{l \in L \\ v \in V}} \left(c_{l,v}^{\text{pwr}} \cdot K_{l,v} + c_{l,v}^{\text{fx}} \cdot \Upsilon_{l,v} \right) && \text{link activation} \\
 & + a \cdot \sum_{\substack{n \in N \\ v \in V}} \left(c_{n,v}^{\text{pwr}} \cdot K_{n,v} + c_{n,v}^{\text{fx}} \cdot \Upsilon_{n,v} + c_{n,v}^{\text{act}} \cdot \Phi_{n,v} \right) && \text{node activation} \quad (3.4)
 \end{aligned}$$

Note that for ease of reading, the markup function is not displayed.

3.2.4 Constraining the linear transport problem

Various constraints are necessary to enforce an economic dispatch with investment. In addition, the physical reality of the grid needs to be reflected, i.e. limits of power flows, generation capacity and storage levels are imposed. Finally, some non-linearities, resulting from the combinatorial decision making require linearisation. The following section lists and briefly explains the constraints applicable for the linear transport problem.

¹⁷The chosen climate year 2012 is a leap year, resulting in 8784 time steps in the model.

The objective function in equation (3.4) is subject to:

$$\underbrace{\sum_{g \in G_n} P_{g,h}}_{\text{generation}} - \underbrace{\sum_{\substack{l \in L_n^{\text{from}} \\ v \in V}} \Theta_{l,v,h} + \sum_{\substack{l \in L_n^{\text{to}} \\ v \in V}} \Theta_{l,v,h}}_{\text{flow}} - \underbrace{\sum_{s \in S_n} C_{s,h}}_{\text{storage}} = d_{n,h} \quad \forall n \in N, \forall h \in H \quad (3.5)$$

$$P_{g,h} \leq \hat{p}_{g,h} \quad \forall g \in G, \forall h \in H \quad (3.6)$$

$$\Theta_{l,v,h} - K_{l,v} \leq ntc_{l,v} \quad \forall l \in L, \forall v \in V, \forall h \in H \quad (3.7)$$

$$-\Theta_{l,v,h} - K_{l,v} \leq ntc_{l,v} \quad \forall l \in L, \forall v \in V, \forall h \in H \quad (3.8)$$

$$C_{s,h} \leq \hat{c}_s \quad \forall s \in G^S, \forall h \in H \quad (3.9)$$

$$W_{s,h} \leq \hat{w}_s \quad \forall s \in G^S, \forall h \in H \quad (3.10)$$

$$W_{s,h-1} - P_{s,h} + C_{s,h} + ni_{s,h} - W_{s,h} = 0 \quad \forall s \in G^S, \forall h \in H \setminus \{1\} \quad (3.11)$$

$$K_{l,v} \leq \hat{k}_{l,v} \cdot \Upsilon_{l,v} \quad \forall l \in L, \forall v \in V \quad (3.12)$$

$$K_{n,v} \leq \hat{k}_{n,v} \cdot \Upsilon_{n,v} \quad \forall n \in N, \forall v \in V \quad (3.13)$$

$$K_{l,v} \leq \hat{ntc}_{l,v} \quad \forall l \in L, \forall v \in V \quad (3.14)$$

$$\left| \sum_{\substack{l \in L_n^{\text{to}} \\ v \in V}} \Theta_{l,v,h} - \sum_{\substack{l \in L_n^{\text{from}} \\ v \in V}} \Theta_{l,v,h} \right| \leq K_{n,v} \quad \forall v \in V, \forall h \in H \quad (3.15)$$

$$\sum_{l \in L_n} \Upsilon_{l,v} \leq M \cdot \Phi_{n,v} \quad \forall n \in N \setminus N^{\text{TIN}}, \forall v \in V \quad (3.16)$$

$$\sum_{l \in L_n \setminus L^{\text{IC}}} \Upsilon_{l,v} \leq M \cdot \Phi_{n,v} \quad \forall n \in N^{\text{TIN}}, \forall v \in V \quad (3.17)$$

$$C_{s,h}, K_{l,v}, K_{n,v}, P_{g,h}, W_{s,h} \geq 0 \quad (3.18)$$

$$\Upsilon_{l,v}, \Upsilon_{n,v} \in \mathbb{N} \quad (3.19)$$

$$\Phi_{n,v} \in \{0; 1\} \quad (3.20)$$

While equation (3.5 - 3.11) constrain the economic dispatch, equation (3.12 - 3.17) enforce investment cost accumulation for each graph element to be activated. The applicable number range for constrained decision variables is defined in equation (3.18 - 3.20). Note that the power flow variable $\Theta_{l,v,h}$ is the only unrestricted variable. It can take both, positive and negative values to reflect the direction of power flow across lines and track injections into nodes with the adequate sign. The following paragraphs elaborate on the listed constraints.

Constraining the economic dispatch

The strongest binding constraint is the nodal energy balance in (3.5). It accumulates all generation and import flows as injection into a node n and balances this against all exports, charging of storages and demand. This is done for each time step h . The complexity of that constraint increases with the number of time steps under consideration.

Equation (3.6) limits generation per generator to its rated capacity. Similarly, (3.9) limits the power a storage can charge with in addition to a cap for the total storage capacity in (3.10). The power flow $\Theta_{l,v,h}$ is restricted to the available NTC by (3.7) and (3.8). Some lines offer this from the beginning (denoted with a non-zero $ntc_{l,v}$). The restriction can be lifted inside the model by adding capacity in $K_{l,v}$.

Enforcing investment cost

Adding link capacity reflects the core concept of the transport model. It needs to track which capacity is added for each link and voltage type. This is enforced with the help of the integer variable $\Upsilon_{l,v}$ in (3.12). It counts the number of cables required on a link l to enable a certain capacity increase $K_{l,v}$ at voltage type v . Each cable contributes with a rated capacity $\widehat{\kappa}_{l,v}$ to the total capacity expansion. With increasing values for $\Upsilon_{l,v}$, and $K_{l,v}$ the objective function accumulates fixed and variable investment costs respectively. This enforcement of link activation cost implements the previously introduced sloped step-wise link cost function from equation (3.1) in the model.

Link capacity increase is limited for some links by $\widehat{ntc}_{l,v}$ in (3.14). It is introduced to reflect the capability of the onshore grid to handle large influxes of offshore wind energy at very few substations. While no onshore grid expansion and indeed power flow analysis is conducted in this thesis, a rough parametrisation of onshore substation hosting capacity limits is implemented. The (virtual) links that connect a selected onshore substation with a market area node have such a limit imposed (c.f. section 2.2.2). In table 2.1 it is denoted as POC limit. Observe that this limit reflects a nodal capacity limit, which is implemented as a link limit for better performance in the model. Offshore links have no such limit imposed.

Node capacity increase is the second important concept of the transport model. It reflects the notion that offshore platforms need to be built, when switching, transformation, and conversion of power flows is required. The division between variable and fixed cost for the power related cost is similar to the elaboration on the link activation. While $K_{n,v}$ leads to variable cost accumulation in the objective function, $\Upsilon_{n,v}$ increments fixed costs. In that way, the sloped step-wise node cost function from equation (3.2) is implemented in the model.

The power related costs are enforced in (3.15).¹⁸ For each node and hour it is tracked whether injected power leaves a selected node in the same voltage type or not. If the absolute value returns zero, no power is assumed to be transformed or converted. Hence no equipment needs to be installed beyond switch yards and misc. If the absolute value is non-zero, power is either generated, consumed, or just converted or transformed. In that case, transformer and converter equipment is required for the delta. Since this equation is investigated for each hour it implicitly imposes a maximum value constraint on the equipment rating $K_{n,v}$. Note, that this kind of procedure oversimplifies the real nature of power conversion and power flow. The absolute value function does not account for all conversion and transformation tasks, that take place unnoticed by the nodal energy balance. Hence this procedure can only estimate the lower bound of required equipment installation. In light of a high-level approximation this level of detail is considered sufficient.

For each node, non-power related costs apply for the construction of a platform. In this model they are simplified into one binary variable $\Phi_{n,v}$. It is switched on with help of the “big M ” approach in (3.16) as soon as at least one discrete unit of node equipment $\Upsilon_{n,v}$ is required. Note, that M needs to be sufficiently large in order not to constrain the model, once it is activated.

For each platform, which is part of an interconnector, one special consideration applies. When an interconnector is routed across such Tee-In hubs (c.f. section 3.1.5), the links belonging to that interconnector will have initial NTC values assigned. This enforces transmission capacity to be built at no cost, which reflects the reality as seen from the model: The interconnector is built in any case, whether an offshore grid follows or not. The mechanics of the model now enforce each intermediate node of the interconnector to be activated at a node activation cost. This is however only correct, if the platform indeed serves a purpose beyond hosting an interconnector cable. The creation of node sub sets of N in equation (3.16) and (3.17) allows this distinction. While node activation cost in general, only applies to

¹⁸The absolute value function requires translation into two separate constraints to be solvable in an MILP. Here, it is aggregated into one term for better readability.

nodes which are not a Tee-In hub ($n \in N \setminus N^{\text{TIN}}$), node activation cost at a Tee-In hub does only apply if at least one link is active, which is not part of an interconnector ($l \in L_n \setminus L^{\text{IC}}$).

In conclusion, the power flow decision variable $\Theta_{l,v,h}$ drives activation cost for new links and nodes in the model. It either pushes up link capacity constraints, resulting in cables to be installed. Or, it requires node equipment to be installed for conversion and transformation of each unit of power flow that enters a node on a different voltage type than it leaves. Since the power flow is residual to the dispatch per time step, model complexity increases substantially with long time horizons under consideration.

Time coupling of constraints

Another driver for complexity is the level of detail for the modelled storages. The model considers two types of storages, namely pumped hydro and reservoir storages. While the former can be charged actively at the cost of power consumption ($C_{s,h}$), the latter is mostly charged via natural inflow at no cost ($ni_{s,h}$). Battery storages are subsumed under the first type of storage, since they behave similarly while having a much smaller storage capacity.

Equation (3.11) enforces a time coupling of storage levels from one time step to the next. It obtains the state of charge¹⁹ for a given time step $W_{s,h}$ recursively from the previous time step, while subtracting generation and adding charging (pumping or natural inflow) to it. For sake of simplicity initial and final storage levels are kept at 50%. The charging capacity is limited to the power rating \hat{c}_s of the pumps (3.9) and a storage can store energy up to its energy limit \hat{w}_s (3.10).

Generation from reservoirs can be interpreted as a dispatchable renewable energy source with limited energy availability. Storage of energy is not resulting in a demand from the power grid with later re-feeding but from a shift of available energy (natural inflow) from one time step into a future time step. During each time step the reservoir is charged with some energy. In consequence, production is enforced, when the storage capacity limit is reached. Spillage of energy is not allowed. Observe that this is indirectly enforced via (3.10).

Modelling of reservoirs with fixed inflow time series and fixed start and end values for pumped hydro storages maintains perfect foresight in the model. Storage dispatch is thus less stochastic than it would be in reality with unknown inflow and price development throughout the year. Nevertheless, for a yearly model run the storage level modelling leads to complex time coupling of several thousand time steps.

Measures to maintain solvability

Both, time coupling of constraints and the combinatorial activation options for offshore transmission assets challenge the computational solvability within the resources of this master thesis. This challenge is addressed with two measures, namely a sequential optimisation in three steps and a time series reduction from the entire climate year down to a representative set of time steps. The measures are summarised in figure 3.15, along with the most relevant results from each step.

In the first step, a warm start is prepared for the market model. It aims at usable estimations for the storage and reservoir dispatch for the main model to fix. For the warm start the Baltic Sea Region is modelled with infinite transmission capacity, i.e. a copper plate assumption. No investment decisions are made and the dispatch can be optimised centrally. In that way the model can identify the reservoir and storage dispatch in an “ideal world”, while satisfying constraint 3.11. This model run is performed in a six-hourly resolution. The obtained schedules are saved and fixed for the second step.

The second step of analysis performs the actual optimisation of investment decisions. It receives the warm start schedules for storages and reservoirs, hence does not optimise them in accordance with

¹⁹For the high dominance of hydro storages it is denoted as water level $W_{s,h}$ measured in MWh.

constraint 3.11 anymore. The time coupling complexity is, therefore, removed from the main optimisation. It does, however, now face the combinatorial complexity of link activation. In order to solve this model, the time resolution is further reduced to 25-hourly steps. This results in analysing the first hour of day one, the second hour of day two and continues in that pattern until the end of the year. The resulting set of time steps is much less complex to solve and still represents the chosen climate year in its seasonal, weekly and hourly characteristics. Note that this approach oversimplifies the nature of grid investment. Due to exponential increase in data storage and computation power needs, this thesis cannot provide higher resolution results. For an alternative strategy of time series reduction refer to [31]. They apply a k-means time clustering for selection of “representative hours” of the year.

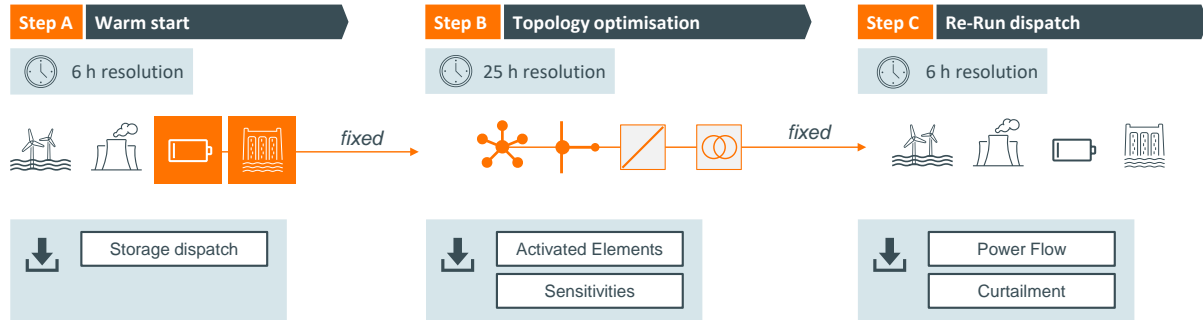


Figure 3.15: Three steps to maintain solvability of the market model.

In a third step a yearly model run (six-hourly resolution again) is conducted on the obtained topology results from step two. Now, the time coupling of storages is included in the model again and the final dispatch of wind farms and all other power plants is obtained. This model run forms the basis for the power flow and link utilisation results.

The sequential and simplified market modelling supports the objective of demonstrating feasibility of the proposed toolchain. Further investigation beyond this project is, however, advised to validate the obtained results against a yearly model run. Any investment decision being obtained is, therefore, only optimal in light of the reduced time horizon under consideration.

3.3 Post-Processing

Post-Processing is the final step in the toolchain (c.f. figure 3.3). Its purpose is the mapping of model results and aggregation of selected offshore grid performance indicators. The focus of result processing is drawn to the investigation of the previously introduced trade-off between investment into new transmission capacity (i.e. connecting wind farms and market areas) and economic dispatch (i.e. creating a merit order with many renewables inside).

Trade-off investment against dispatch improvement

Investigating this trade-off requires an analysis of how much wind energy is not delivered. It is signaled by curtailment of offshore wind farm production. Visualising power flows and link utilisation rates further reveals concentration of load flow and risk of congestion. Finally, wind farms might be connected at reduced capacity, resulting in slightly undersized cable transmission systems compared to the rated capacity of the wind farm. The most extreme case of undersizing is indeed not connecting the wind farm at all. In this case the wind farm generation is spilt. It represents a situation, where the cost of activating additional transmission capacity does not outweigh the benefits from integrating cheap wind energy into the market. The rationale for each of the listed reasons for not delivered wind energy is subject of result discussion in chapter 5.

In face of the wide range of link types and topology options under consideration, the question arises where possible tipping points exist between different link types. The OFFSHOREGRID study [2] identifies two major tipping points to consider. They include the break-even distance from wind farm to shore beyond which a tee-in connection into an interconnector is beneficial compared to a parallel radial cable. And the break-even distance between hubs below which a hub-to-hub connection (hub chain) is beneficial compared to a parallel interconnector. Expanding this concept, this thesis also investigates tipping points for clustering beyond which clustering of wind farms outperforms their individual radial connection.

Since each of the depicted tipping points represents a separate optimisation problem, the output of this analysis can only hint towards striking tipping points. Counting the number of wind farms being clustered or chained gives a first impression on how easily the tipping points are reached or not. Some tipping points might not be visible at first sight, since the obtained topology is fixed for one shot and no scenarios are investigated. In addition, thorough investigation of operational feasibility and economic viability is required to validate any of these findings. It is however possible to conduct a sensitivity analysis on the input parameters, to identify value drivers and major biases for the findings.

Sensitivity analysis

The purpose of sensitivity analysis is to identify the most influential parameters for the model result. Referring to the previous elaboration on GIS pre-processing, the permissive rules for graph creation are sensitive with respect to the obtained graph and the permissive elements it may contain or not (c.f. section 3.1.5). This thesis does not generate several graphs to optimise in Julia. It does, however, discuss briefly how changes in the permissive graph topology impact investment decisions. Three sensitivities are selected for further analysis. They address the topological nature of the model in favour of technical or economic parameters. While the latter ones are sensitive inputs as well, they are out of scope of this methodological thesis.

To investigate the imposed bias of pre-activated links in the model the first sensitivity removes all interconnectors from the picture. In other words, the offshore topology is not pre-defined and all permissive links and nodes have equal chance for activation. Interconnectors might still be realised and can be compared with the predefined interconnectors from TYNDP. This sensitivity provides insights on the impact of ex-ante topology prioritisation and selection.

In a second sensitivity, the model is forced to connect all wind farms nationally and radially. This reflects the status quo of today's offshore grid construction. The TYNDP pre-set interconnectors are back in the graph and may be expanded as usual. Hybrid assets are excluded since wind farms cannot be clustered or chained. The market and investment results from this model run will reveal the added value of offshore topology optimisation. Special focus is drawn towards curtailment, not connected wind farms and link power ratings.

For a final model run, the power throughput limit for the onshore substations is lifted. This follows a notion of zonal copper plates. While onshore cross-zonal NTC is still constrained, the landing of offshore infeed at each zone is not. Such an investigation is expected to reveal the "true" value of the offshore topology, assuming that it would not need to address onshore congestion anymore. Wind power is then landed purely based on its added value on the energy market. The setup and characteristics of the investigated sensitivities is further elaborated in section 4.3.

4 Results

The analysis results are presented in three steps as summarised in figure 4.1. The first step addresses the GIS topology setup and reveals the initial graph with permissive links and hubs for the market model to iterate over. The second step represents a pre-solve of the actual market model. It is the warm start copper plate dispatch with no congestions onshore or offshore. Finally, the topology optimisation reveals the base case result for activated links, nodes and equipment. This third step is further divided in three sensitivities, which are overlaid with the base case results.

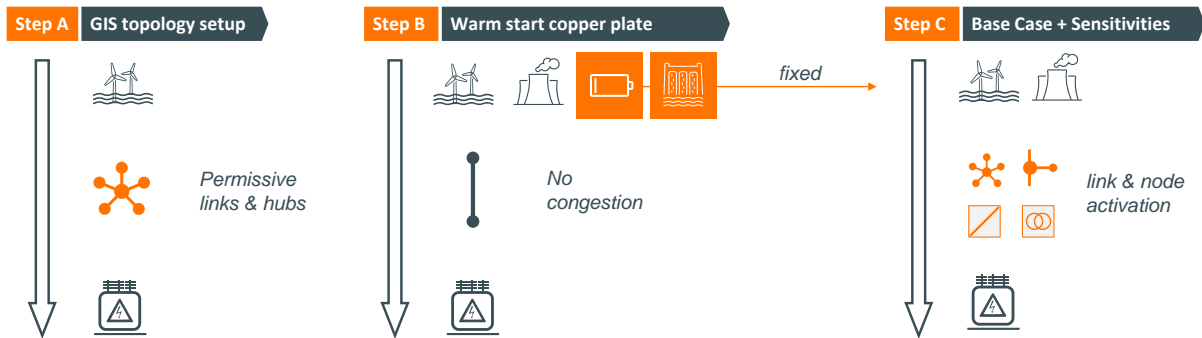


Figure 4.1: Overview on results categories.

Recap on the analysis scope

The following chapter is dedicated to presenting and explaining the results. The investigation and interpretation of the results should be conducted with the simplifications from the input data discussion in mind. They include an abstracted viewpoint with economic viability and operational feasibility of the identified offshore grid topology not being investigated. As seen from the model, the wind farms in question are fixed and come “for free”. Their business case and operation is not further analysed. All link and node activations in the model are based on a reduced set of time steps which are aggregated from one climate year. In addition, the offshore transmission assets are assumed to operate smoothly with each other, i.e. contingencies are not investigated. While the NTC based modelling accounts for congestion in the offshore topology, it does not co-optimize offshore with onshore grid capacity expansion. Internal bottlenecks per bidding zone are thus neglected and subsumed in the hosting capacity parameter of each substation. Onshore cross-zonal bottlenecks stem from the assumed NTC values between market areas (based on TYNDP) and are also not part of the optimisation.

With this recap on the analysis scope in mind, the results should be studied solely for illustration of the proposed framework for investigating a high-level offshore topology optimisation problem. Their purpose is to showcase what type of results and conclusions such an two-step analysis can deliver, given the choice of input data and parameters. They do not form an offshore grid outlook as such. Hence the feasibility and favourability of proposed, planned or approved transmission projects in the Baltic Sea as of date remains unquestioned in this analysis. Whenever trajectories are described and discussed, this follows the notion of an academic discussion from the Baltic InteGrid study. This notion is expanded in the discussion of chapter 5, which outlines the contribution and limits of this analysis and puts the findings of this thesis into the context of ongoing and future research.

4.1 Presolving topology and dispatch

4.1.1 GIS topology output

Wind farm clustering

The MiniMax group partitioning algorithm from chapter 2 organises the set of wind farms into clusters²⁰ and creates permissive hub nodes. The result is shown on the map in figure 4.2. Study the results in a layered logic. At the top level all wind farms are scanned for dense heap membership (yellow buffer circles). Up next, sparse heap membership (green buffer circles) and outlier condition (blue buffer circles) are tested and displayed. Finally tee-in prospects into interconnectors (red buffers) are investigated. Observe that while the wind farms are not displayed, examining the blue outlier buffer circles reveals their location implicitly. Each wind farm has per definition an outlier buffer to facilitate the outlier search in GIS. Its centroid is the wind farm.

Studying overlaps of different buffer circles reveals the mechanics behind the cluster creation. If an outlier buffer circle does not overlap with any other buffer circle, the wind farm has no prospect of clustering and is denoted as singular. Overlap of two or more outlier buffers reveals the first group of permissive hub nodes: Outlier hubs. They are created in GIS when either two (or more) outlier wind farms are density connected via an intermediate node. Or, when they link an outlier wind farm with a nearby heap. Heaps are either sparse (green) or dense (yellow) and contain hub nodes as obtained from the clustering algorithm. In many cases, such hub nodes of different categories overlap, hence redundancy filtering is applied to avoid an overhead of nodes in the final graph.

An example of strong redundancy filtering can be found in the Estonian EEZ. Two clusters of wind farms are identified: A two-wind-farm-cluster west of Saaremaa (in the map: D4) and a four-wind-farm-cluster in the Gulf of Riga (D5). Both clusters are characterised as dense heaps, i.e. a common centre point exists from which all heap members are directly reachable. The MiniMax algorithm consequently classifies this centre as permissive k-means hub and filters all redundant DBSCAN hubs and outlier hubs in the surroundings. The displayed buffer circles still signal their former existence in the pre-filtered set of points. Notice the minimising agent of the algorithm, trying to limit the solution space to absolute necessary nodes.

The opposite of redundancy filtering is the inclusion of outliers and neighbouring heaps. The elongated cluster north of Poland (B3) illustrates this. It is characterised by a long loose chain of wind farms. While k-means identifies only some hub nodes ambiguously, DBSCAN fills in the gaps. Finally, the search of outliers restores the chain-like structure of a sparse heap. It is achieved by the maximising agent in the MiniMax algorithm. The final result contains an exhaustive set of hub nodes and wind farm members which fulfil the permissive rules of direct reachability, density reachability and density connectivity respectively (c.f. section 3.1.5).

In a final step of node creation a re-scan for potential overlap of hubs or wind farms with interconnectors is conducted. If a hub node is located close to an interconnector its status is lifted to a tee-in hub. This is shown with a red stroke for the hub symbols in question. If an outlier is tied into an interconnector, an extra node is created. Study the interconnector from Güstrow (DE) to Bjærverskov (DK) for an example. Note, that crossing of the planned interconnectors between Germany, Sweden, Poland and Denmark also creates a potential interface which is modelled as a tee-in hub in this analysis.

²⁰In this section a cluster is the general term for any kind of grouping.

In conclusion, the wind farm clustering reveals regions of high wind farm density and regions with a lack thereof. The largest share of offshore wind power capacity (40 GW) has at least one prospect of clustering. Hence the identification of synergies in offshore grid planning is prevalent almost everywhere across the water body. Twelve clusters are identified as highlighted in the map of figure 4.2. While five of them show a dense setup with a single centre (k-means hub), most other clusters are arbitrarily shaped with several sub-centres (k-means, DBSCAN or outlier hub). Four clusters benefit from at least one potential tee-in prospect into an interconnector, where the Kriegers Flak area (B2 & A2) between Denmark, Sweden and Germany contains the bulk of it. From the complete set of 71 wind farms, only twelve remain singular in the analysis, which amounts to 12 % of offshore wind power not clustered.

Understand that this finding does not necessarily reveal a forecast of future offshore grid focus areas. Nor does it suggest a concentration of future offshore wind infeed beyond the prevalent time correlation of availability. It does however indicate without complex modelling, which synergies can be obtained from the geodata hidden in the sea. The results serve as an intermediate step from the initial set of wind farms towards future connection prospects of them. The next sections reveal how the singular wind farms without clustering prospects turn out as the missing link in completing the offshore topology network of the Baltic Sea Region.

Linking clusters and wind farms

Following the link creation procedure from section 3.1.5, the initial graph topology is created in GIS. The resulting network of permissive links and hub nodes is shown on the map in figure 4.3. Most wind farms are not displayed for simplicity. Refer to figure 4.4 for a cascading disaggregation of all link types for better readability. It starts from the shortest hub-spoke links and finishes with the most extended wind farm and hub chains. Understand that such a cascade is manually generated for ease of understanding. The GIS generates all links simultaneously in one single network.

The visual representation of all permissive links completes the picture of the potential future offshore grid in the Baltic Sea. Two main conclusions can be drawn from it. First, all previously identified clusters are linked with their closest neighbours at least once. Second, the outliers from the MiniMax clustering are also linked with each other and to their closest cluster neighbours.

The resulting permissive graph topology creates a pan-Baltic network where each node is at least indirectly connected to every other node. For each pair of nodes, an ordered set of chained links can be found to connect them. Such a connection is denoted as a path. In contrast to the complete graph, each connection is no longer represented with an individual link. Instead, bundling of transmission paths is applied. Recall figure 3.4 to understand the similarities and differences from the complete initial graph and the pre-processed one.

The interconnection of clusters is realised with a wide range of link types. Notice that they complement each other depending on the spatial features of the region in question. South of Åland for instance (E4), where no clustering is done in GIS, mainly wind farm connectors (OWF chains) realise a link from the southern Baltic Sea into the Gulf of Bothnia. For the Baltic states and Poland, hub connectors (hub chains) dominate the picture with few detours into the Gulf of Riga and to the southern shore of Sweden. The link creation is calibrated such that all clusters are connected at least once. Observe that the depth of connection inside each hub rarely exceeds one. In other words, two clusters are usually connected via their mutual closest hub member and not any other member further inside the cluster. The connection paths to inner heap members are thus routed via outer members. Note, that this underlines the notion of a path-wise connection logic as opposed to direct links.

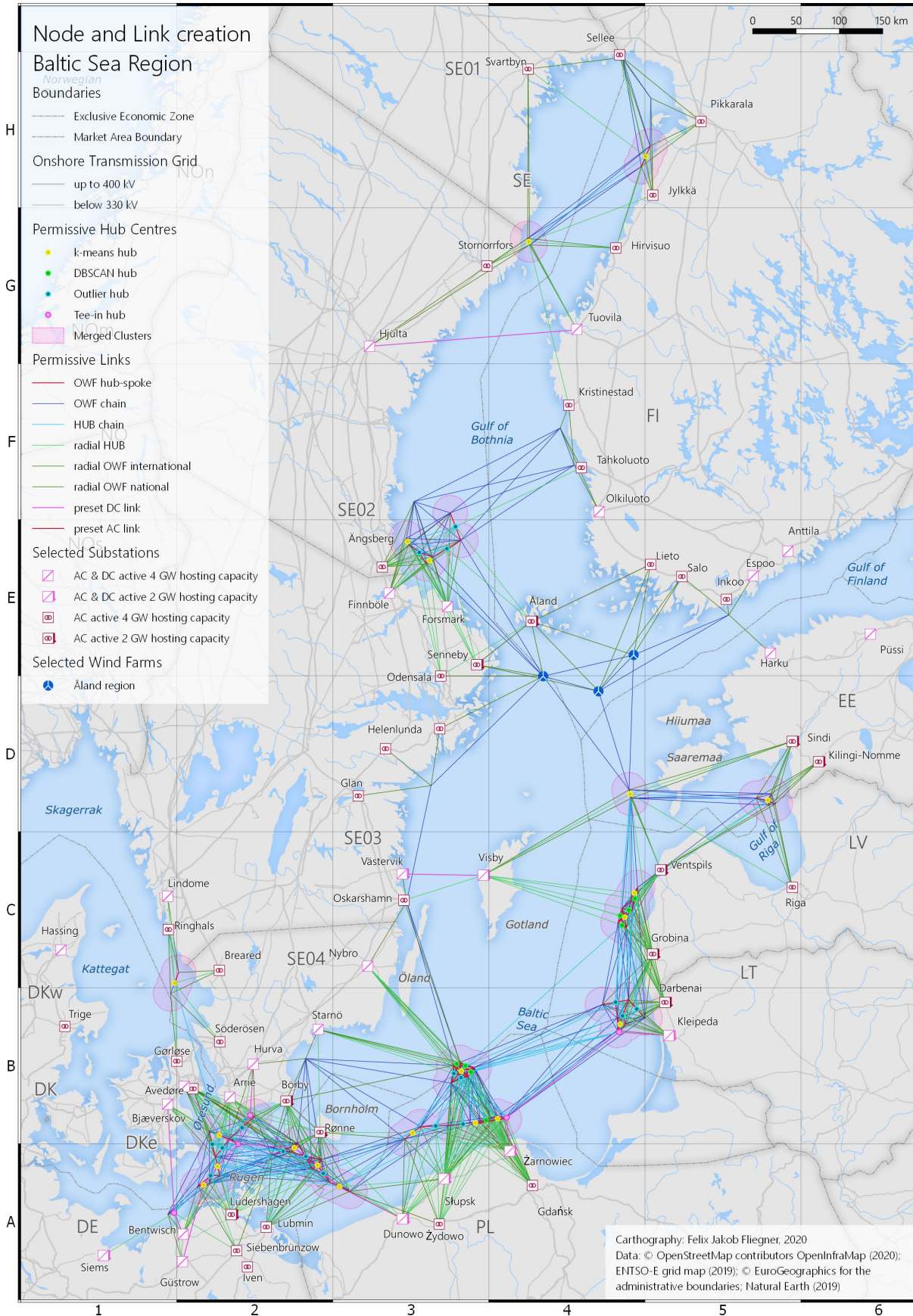


Figure 4.3: Map of permissive links in the Baltic Sea Region.



Permissive links Baltic Sea

- OWF hub-spoke — radial HUB — preset DC link
- OWF chain — radial OWF international — preset AC link
- HUB chain — radial OWF national

0 100 200 300 km

Cartography: Felix Jakob Fliegner, 2020
Data: Own Analysis

Figure 4.4: Permissive link types in the Baltic Sea Region.

The radial connection of wind farms or clusters to the shore is realised mainly to the first layer of substations. In Poland, Germany and Sweden, the second layer is sometimes included as well in the network. Since the onshore grid is aggregated into single market areas, the choice of an onshore connection point in the first or second layer does not matter for the market model. It is only relevant in light of the exogenous limitation of connection capacity per landing point as introduced in section 2.2.2. The distinction between national and international radial wind farm connection is only relevant for the sensitivity analysis. In the main model, those links are included equally. Hence their symbols are not coloured in separate colours on the map.

Observing the created graph topology several additional interconnection prospects beyond the presets from TYNDP can be found. In fact, almost every cluster is connected to more than one shoreline, creating an abundance of hybrid asset opportunities. Besides, even preset interconnectors are flanked by several other path options, which could lead to parallel or partly parallel interconnectors in the final topology. Remember that such an observation does not hint towards the profitability of any displayed link or path. It is the mere satisfaction of the introduced permissive rules that reveals many possible synergies in offshore grid development.

Leveraging the path logic leads to a substantial reduction in generated links. For illustration, study the connection from the three wind farms south of Åland (E4) to the Danish substation Bjærverskov (B1). In a complete graph for each of these wind farms, a direct link would exist to represent a connection to Denmark. The pre-processed graph, however, does not contain such long direct links crossing the entire Baltic Sea. Instead, a stepwise path can be found, which links the wind farms first with the nearest hub east of Saaremaa (D4), before spreading out to many more hubs further to the west. Ultimately the path ends in Denmark. Repeat this exercise with any other pair of nodes and end up with the displayed network. A discussion on strengths and ramifications of this observed GIS output follows in chapter 5.

The calibration of the GIS algorithm is designed to generate just enough links in the entire Baltic Sea region to link each cluster and a remote wind farm with their neighbours. This calibration allows the optimiser to connect any wind farm with any onshore substation in scope via paths, while still leveraging a substantially reduced graph topology. Remember the underlying notion of permissive links and intermediate hubs when investigating the map in figure 4.3. For two arbitrarily chosen nodes to be connected it is sufficient to find a chain of reachable nodes to “jump” over from node to node.

Linking neighbouring clusters with each other creates longer chains of links, which could ultimately represent a backbone for an offshore grid. The GIS output hints towards three approximate trajectories of permissive backbones in the southern Baltic Sea. Originating from the coasts of Finland and Sweden in the Åland region (E4), one route heads south towards the clusters offshore Saaremaa, Estonia (D4) and Ventspils, Latvia (C4). Here it splits into one central part, which heads directly to Börby, Sweden (B2) via the Swedish-Polish cluster (B3) in the central Baltic Sea and into an eastern part which continues via Lithuania and Poland to Germany. Ultimately both parts rejoin in the Kriegers Flak area (B2) west of Denmark. The third route follows the south coast of Sweden (C3) before rejoining the other two routes offshore Poland again. In the Gulf of Bothnia, a northward extension of these backbones is permissive (F4). Similarly a western extension is identified from Kriegers Flak into the Kattegat crossing the Øresund (B2). Mind that the mere density of links in the south does not imply superiority of any potential backbone trajectory there. At this stage of analysis, the southern backbone is equally feasible and permissive as its counterparts in the middle and along the northern coastline. In order to investigate the obtained topologies for feasibility and optimality, the dispatch results are introduced up next.

4.1.2 Warm start for market model

A pre-solved result is given to the final topology optimisation, to simplify the hourly time coupling for hydro reservoirs and other storages. It is labelled as warm start for its pre-definition of the generation and demand variables for all storages and hydro reservoirs. While the warm start is mainly conducted to fix the reservoir and storage variables, the other results are displayed as well for a preview on the final market model results.

The warm start results are summarised in table 4.1. A comparison to the TYNDP scenario report values is provided as well. It reveals a close match of the simulation results, which validates the model calibration of this analysis. Note that the warm start results are displayed and discussed for the Baltic Sea Region for RES generation levels, storage charging and demand respectively. While the WEST and SOUTH node are part of the simulations as well, their results are not of interest here and not displayed in the figures and tables.

Table 4.1: Yearly BSR energy outputs from copper plate model in TWh/ year

	Warm Start	TYNDP (comparison)
Wind (everything but BSR offshore)	529	450
Hydro	260	275
Solar (PV)	144	128
Other RES	96	97
Wind Offshore (BSR only)	158	84
Residual (thermal)	84	96
Demand BSR	1374	1365
- Of which storage (charging)	53	n.n

The demand time series shown in figure 4.5 emphasises the dominance of German energy consumption in the group of all BSR states. In relation to the comparatively low wind power capacity in the German Baltic EEZ (c.f. figure 2.3), it will be valuable to investigate how this asymmetry is reflected in the grid infrastructure of the Baltic Sea offshore grid. Besides this finding, the plot shows the usual weekly pattern of higher load during weekdays and a dip each time the weekend is reached. Summertime load is lower than in winter, and peak demand is reached during the coldest winter days in February.

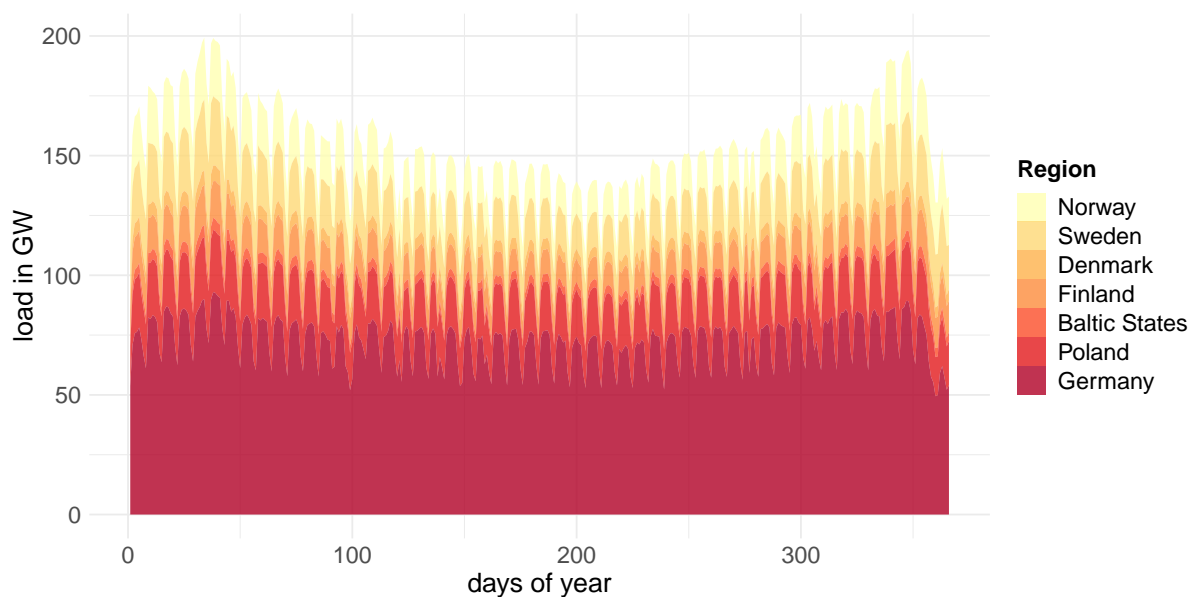


Figure 4.5: Daily mean demand Baltic Sea Region for 2040.

The warm start RES dispatch displayed in figure 4.6 reveals a high dominance of onshore and offshore wind energy in the system in 2040. Cumulated with photovoltaic and other RES generation, they cover the demand of the entire region for almost all hours of the year. The model dispatches 158 TWh of offshore wind energy in the Baltic Sea alone. Mind that due to the cost assumptions, onshore wind and PV are curtailed first, resulting in no Baltic offshore wind curtailment in the warm start. The offshore time series further reveals a less volatile profile than its onshore counterpart. It remains to be seen if this observation benefits the grid topology in a high cable utilisation per wind farm connection.

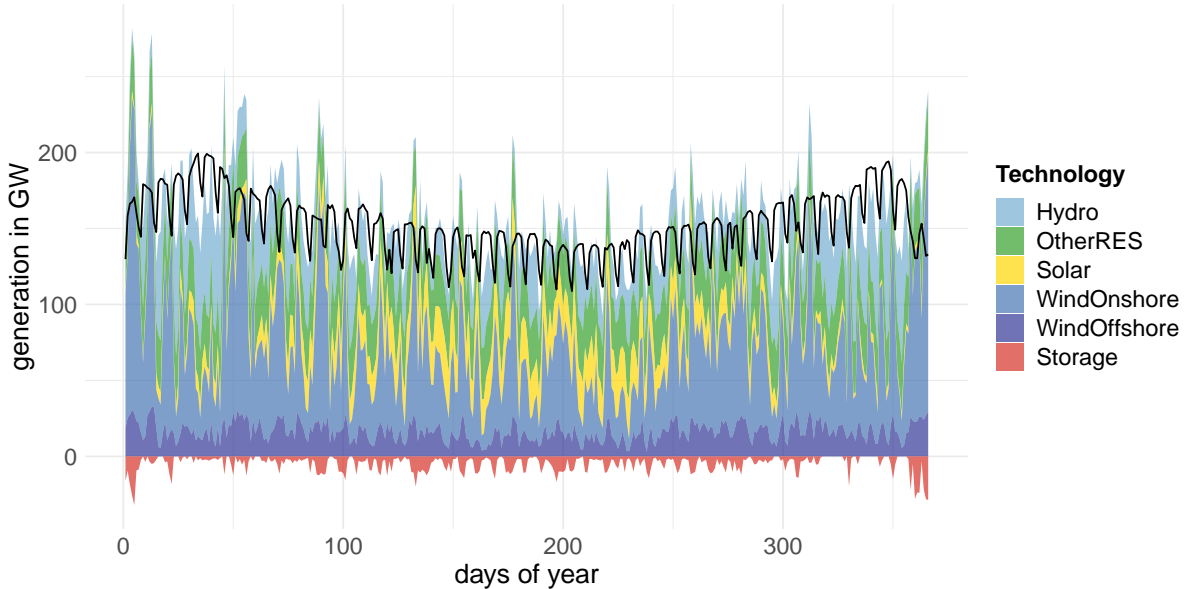


Figure 4.6: Daily mean RES generation and total demand Baltic Sea Region for 2040.

The storages in the model create a complement for the RES infeed. Since the model operates with perfect foresight, storage charging and discharging is allocated optimally throughout the year, to shift RES energy in time. This observation is also denoted as valley filling and peak clipping, since it buffers the volatile infeed from RES, reducing curtailment and dispatch of expensive thermal units respectively. Charging of storages occurs only in hours of RES oversupply, which underlines their complement nature once more.

For the modelled climate year, no long term storage needs seem to arise on a pan-Baltic level. Sequences of hours where demand is not met with RES hardly ever exceed the time horizon of days. A critical exception are two weeks in February, where a cold spell leads to a peak demand of 212 GW. At the same time, onshore wind infeed is exceptionally low, leading to high discharging from hydro reservoirs and other storages. The residual load is covered by thermal generation. Notice that the Baltic offshore wind infeed is less prone to such long periods of low infeed.

While on a regional level longer shortages of RES might still occur, in the big picture, energy volumes from renewable energies overwhelmingly dominate the dispatch. The topology results in the next sections are benchmarked against this warm start. It is of interest, to which extent an efficient offshore topology can fulfil the findings from the simplified and optimistic pre-analysis.

4.2 Base case topology optimisation

4.2.1 Grid topology result

The base case result for activated links and nodes is shown in the topology map of figure 4.7. It includes all wind farms under consideration, the onshore substations in scope of analysis and the onshore transmission grid for illustration. Pre-existing interconnectors and wind farms are not shown for simplicity. Refer to the map 2.5 for their display. Note that the substation status (AC, DC) represents the initial setup before topology optimisation. By that, it can be compared which substation changes its status and which substation is fully equipped to its hosting capacity limit of 2 GW and 4 GW respectively.

Red lines and pentagons represent AC systems, while blue symbols denote DC systems. Pentagons with a white centre dot denote a hub node which is only performing switching tasks. No converters or transformers are installed there. Dashed lines illustrate links not utilising their full cable capacity. Their cable and fixed nodal costs apply as if the full cable capacity rating would be built, but variable costs apply only to the extent of actual installed capacity. Study the interconnector leaving the Danish substation Bjæverskov to the south for illustration (B1). The link is dashed blue, meaning that it is a DC system which could handle up to 2 GW before a second system would need to be installed in parallel. Installed in the model are indeed just 0.7 GW. This logic represents the introduced stepwise installation cost accumulation from section 3.2.2. Solid lines represent links at full or almost full cable capacity. Several solid lines in parallel denote more than one cable system installed on the same link.

Chained wind farms and hubs

The map reveals that all 71 wind farms are connected to the grid. Six of them are connected radially, while the majority is either clustered into hubs (common centre nodes) or chained. While most clustered wind farms are connected with short distance hub-spoke links on an AC basis, the voltage type is switched to DC on the hub platforms in most cases. Chained wind farms are either AC or DC connected.

Chaining of wind farms and hubs can be understood as a set of hubs next to each other, where each hub is stepwise connected to the next one. The result is a DC or AC chain describing a path from one end to the next. If the chain has several ends or branches in between the chain bundles several paths into one transmission system.

In many cases, wind farms in a chain serve as intermediate hubs themselves before forwarding the energy to the next hub or wind farm node. Note that for the power flow, it does not matter if the path is routed via wind farm nodes or additionally installed hub nodes. The difference lies in the activation cost, which is higher for the new hub nodes than for wind farms since the wind farms are preset for the model.

When a chain connects to exactly one shoreline, the connection system is following a radial path, while leveraging synergies of a common path for all chain members. The bundling of energy flows into common paths, and reduction of parallel links is evident here. Study the AC chains south of Åland (E4) and in the north of the Gulf of Bothnia (H4) for illustration.

When a chain connects to two or more shorelines a hybrid asset is created, meaning that in addition to the wind power evacuation, the linked marked areas are interconnected for mutual transmission as well. Most chains in the base case have two or more ends, resulting in a variety of paths to transmit energy between countries and evacuate wind power to multiple market areas.

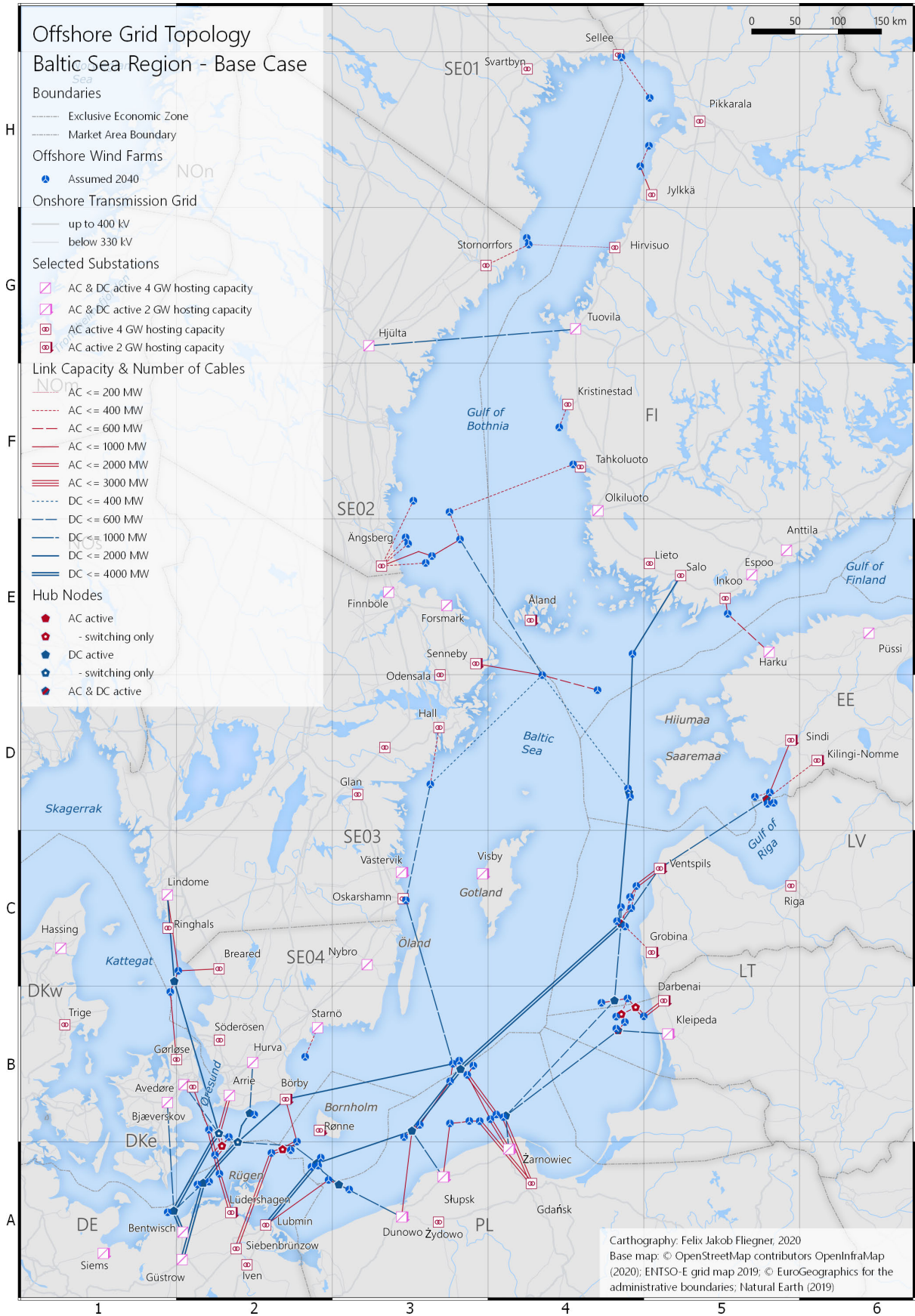


Figure 4.7: Map of topology results – Base case.

AC hybrid assets are realised in the model each time the distance to the opposite shoreline is short enough. In the Kriegers Flak and Bornholm area, two independent AC chains are created. The western chain links Sweden and Denmark with Germany, creating a tri-leg which collects all Kriegers Flak wind farms. The eastern chain links Sweden with Germany while teeing in the northern cluster of the Bornholm region. Observe that both chains are independent to the extent that no galvanic connection exists to the overlaying DC offshore links in the region. Even though the model routes the Swedish leg of the AC chain via a DC hub (B2) it is denoted as a switching station only, meaning that no conversion takes place there. This is another example of how the model applies the path logic of the GIS topology graph in order to connect remote nodes with each other, while not physically activating each intermediate node if not needed for the transmission task.

AC radial chains with just one connected shoreline are realised in regions where the opposite shore is too far away. Observe this along the coasts of Poland, Lithuania and Latvia. In contrast to the AC hybrid assets from above, they do not operate independently from the remaining DC offshore grid. They share common DC hub nodes where a connection from the AC grid is realised to the DC grid.

The DC chains are the enablers of the pan-Baltic offshore grid. In this case, no independent chains with two or three ends can be identified. Instead, many crossings of DC links are realised as hubs. DC links connect wind farms across distant heaps with each other, with several “third legs” to multiple shorelines. By that an overlaying grid topology can be identified which is supplemented by short distance branches either in AC or DC technology. Remote wind farms are chained directly, meaning that the wind farms serve as an intermediate hub themselves. Wind farms belonging to heaps are frequently clustered into a common central hub, which is itself part of a DC chain. Notice that the singular wind farms south of Åland (known from the GIS topology results) are thus becoming part of the long path from Finland south to Germany.

Asymmetrical capacity rating

Studying the subsections of the created paths reveals an asymmetrical capacity rating. One end of the path is usually stronger than the others, meaning that its installed capacity is increased. In the case of radial chains, the links closer to the shore get stronger, since they need to handle the accumulated power infeed from more and more wind farms along the path. In the case of hybrid assets, the end reaching towards the higher demand market area is realised strongest. Observe this with the DC and AC paths terminating in Germany and Poland, the two market areas with the highest power demand in the model.

The preset interconnectors from TYNDP also show up in the model results with asymmetrical capacity. While they are activated for each section at least with the given capacity rating from TYNDP, some sections are strengthened to bundle additional transmission tasks on their links as well. The interconnectors entering Germany, for instance, are strengthened towards the German side. The interconnector departing from Żarnowiec, Poland splits up into the preset path to Klaipėda, Lithuania and an additional northern path to Latvia. The interconnector from Sweden to Finland is not expanded. Yet, the net transfer capacity between both countries is still increased via the hybrid assets in the north (Stornorfors-Hirvisuo) and south (Ängsberg-Tahkoluoto).

Cross-national connections

Clustering and chaining of wind farms are employed across jurisdictional borders almost everywhere in the Baltic Sea Region. In many cases, central hub nodes are activated at the EEZ boundary, which cluster wind farms from two or more countries into one node. The energy is then evacuated from the hub to the countries where the wind farms belong to or entirely to other countries if the connection to the national border is suboptimal. In the latter case wind energy is generated nationally but consumed

internationally. Study the Estonian DC cluster west of Saaremaa (D4) for illustration. While the wind power is generated in the Estonian jurisdiction, it is evacuated towards Finland, Sweden and Latvia, depending on the respective direction of power flow in the available links. While on balance the generated electricity might still reach Estonia via other links it is first “exported” from Estonia in to the offshore grid.

An example of a shared connection to an international cluster is the Swedish-Polish cluster (B3). It groups most wind farms into one centre DC hub, before distributing the energy into four directions, namely Sweden, Latvia, Poland and Germany. Notice that the total connecting capacity of the links to Poland is not large enough to connect all Polish wind farms of that cluster fully. Similarly with the Swedish wind farms. Here the interconnection towards the neighbouring clusters of Latvia (C4) and Bornholm (A2) is therefore not only an additional trade opportunity for the wind farms. In the model it is indeed required if all wind farms happen to feed in at rated capacity at once to evacuate the total wind power.

Realisation of backbones

The most noticeable effect of bundling links into common transmission paths is the realisation of backbones in the offshore grid. The base case reveals two of such concentrated paths, i.e. chains of links with a high capacity rating compared to the branching links to shorelines and other hubs along the way. One backbone departs in Salo, Finland (E5) and follows the coast of the Baltic states, passes by the Swedish-Polish cluster (B3) and Bornholm before terminating in Lubmin, Germany (A2). It has a minor counterpart originating north of Åland, following the Swedish coast, intersecting with the major part at the Swedish-Polish cluster (B3) before taking a detour north of Bornholm via Börby, Sweden (B2) and eventually terminating in Güstrow, Germany (A2). The Second major backbone Starts in Lindome, Sweden (C1) and crosses the Øresund before approaching Kriegers Flak and eventually reaching Bentwisch, Germany (A2).

From an energy market perspective, the effect of the backbones is threefold. First, they facilitate long-distance transmission from bulk wind power infeed to bulk consumption via bundling of several paths into one route of links. Second, they create the opportunity of various interconnection paths beyond the preset and enhanced interconnectors from above. With many intermediate branches, that link several DC chains among each other, offshore meshes are created. Additionally, “third legs” are realised, each time the backbones are linked to a shoreline nearby. Third, they sometimes signal onshore grid congestion which is relieved with offshore grid expansion. While grid congestion per market area is neglected, it can still occur in the model between bidding zones and at each onshore substation. The latter is enforced by the hosting capacity parameter for each substation.

Detours and onshore congestion relief

While the model cannot expand onshore grid links, it can account for onshore constraints by alternating the offshore topology accordingly. One example of onshore congestion relief is the DC chain from Lindome (SE03) to Bentwisch. As seen from the model, a shorter link from Bentwisch to Arrie (SE04) would be beneficial, since it saves on cable length. The onshore power flows between SE04 and SE03 are, however, congested with the given assumptions on NTC values in TYNDP. This enforces a trade-off. Either the model chooses not to connect additional capacity to Sweden, or it accepts to build longer cables, which would signal highly efficient connection to Sweden even with suboptimal connection prospects being present.

Offshore Poland some wind farms are part of a chain that is connected at both ends in the Polish market area (B3). The purpose of this chain is hence not healing onshore grid congestion between market areas. As seen from the model, the wind energy is integrated into the Polish onshore grid either way. The

chain results from a split-up of wind power infeed across various substations to address the tight hosting capacity limit in the model for the onshore substations along the Polish coastline. Notice that such a topology entirely results from the parametrisation and a non co-optimised onshore grid.

The split-up of the DC backbone from the Swedish-Polish cluster towards Germany (Güstrow and Lubmin) north and south of Bornholm signals a similar type of congestion. As seen from the model, this time, the substation of Lubmin would be the favourable point of connection for power import from the east. Still, the station is limited to 4 GW of power throughput. If the model wishes to import more power into the German bidding zone, another substation needs to be chosen. While Lüdershagen or Siebenbrünzow would be distance-wise next-best solutions, they are also congested already. Hence Güstrow is the final option for connection at the cost of a much longer DC link.

Thus the first realisation of the study of the base case grid topology is, that the offshore transmission grid reveals a tendency to a DC dominated overlay network. Some strong backbones bundle bulk transmission paths into one route, while branches and crossings create multiple hybrid connection opportunities of wind farm connectors and interconnectors. The offshore grid is expanding strongest in its North-South direction, with several detours in the southern parts to reflect the tight onshore substation hosting capacity limits. Note that this finding is only a preliminary one, since the onshore grid is not co-optimised in this model. Yet, further drivers for such a topology finding can be identified with an investigation of concentration of wind power infeed and evacuation to the shore.

4.2.2 Concentration of grid infeed

Net-infeed per substation

The high concentration of power infeed from the Baltic offshore grid into the onshore grid is further illustrated in map 4.8. For each activated onshore substation in the model, it displays in red shades how large the net-infeed is over the entire year in TWh. It is defined as the difference of all imports and exports per substation with respect to the offshore grid. Dark colours represent a much larger import from “the sea” than export into “the sea”. White colours represent a negative net-infeed, meaning that the substation is exporting more into the offshore grid than it is importing from it. Two triangles per substation further disaggregate this information for the direction of power flow. Bottom left-facing triangles scale in size and denote the total annual energy throughput that is imported from the offshore grid. Top right-facing triangles conversely denote total energy throughput that is exported into the offshore grid.

The observation from the topology study of high infeed concentration in Germany and Poland is confirmed with the power concentration analysis. On balance, Germany is by far importing the largest amount of energy from the Baltic offshore grid, followed by Poland and Sweden. Notice that this observation correlates with those three countries being the largest consumers of energy in the Baltic Sea Region as well. Thus, integrating wind energy in those market areas is most beneficial for the model with regards to the objective function improvement on the dispatch cost side. Notice that the Polish substations import at their capacity limit. If the stations were not restricted to 2 GW throughput, Poland would import even more energy from the sea. The added value of RES supply originates from the merit order of the Polish power market which in the model still contains high shares of (more expensive) thermal generation (c.f. figure 2.8). Offshore wind could replace it to some extent.

Denmark is mainly exporting energy into the offshore grid. This represents an abundance of offshore wind energy from the North Sea and onshore Denmark already. On balance it is exported from Denmark throughout the entire year. Figure 4.9 illustrates this net negative position of Denmark in the context of all other Baltic Sea states. Be careful when interpreting the results in that graph, since it only shows the aggregated yearly net-infeed per country. There are several hours of the year, where Denmark, for instance, is still importing energy from the sea, as can be seen on the map at the Danish substations.

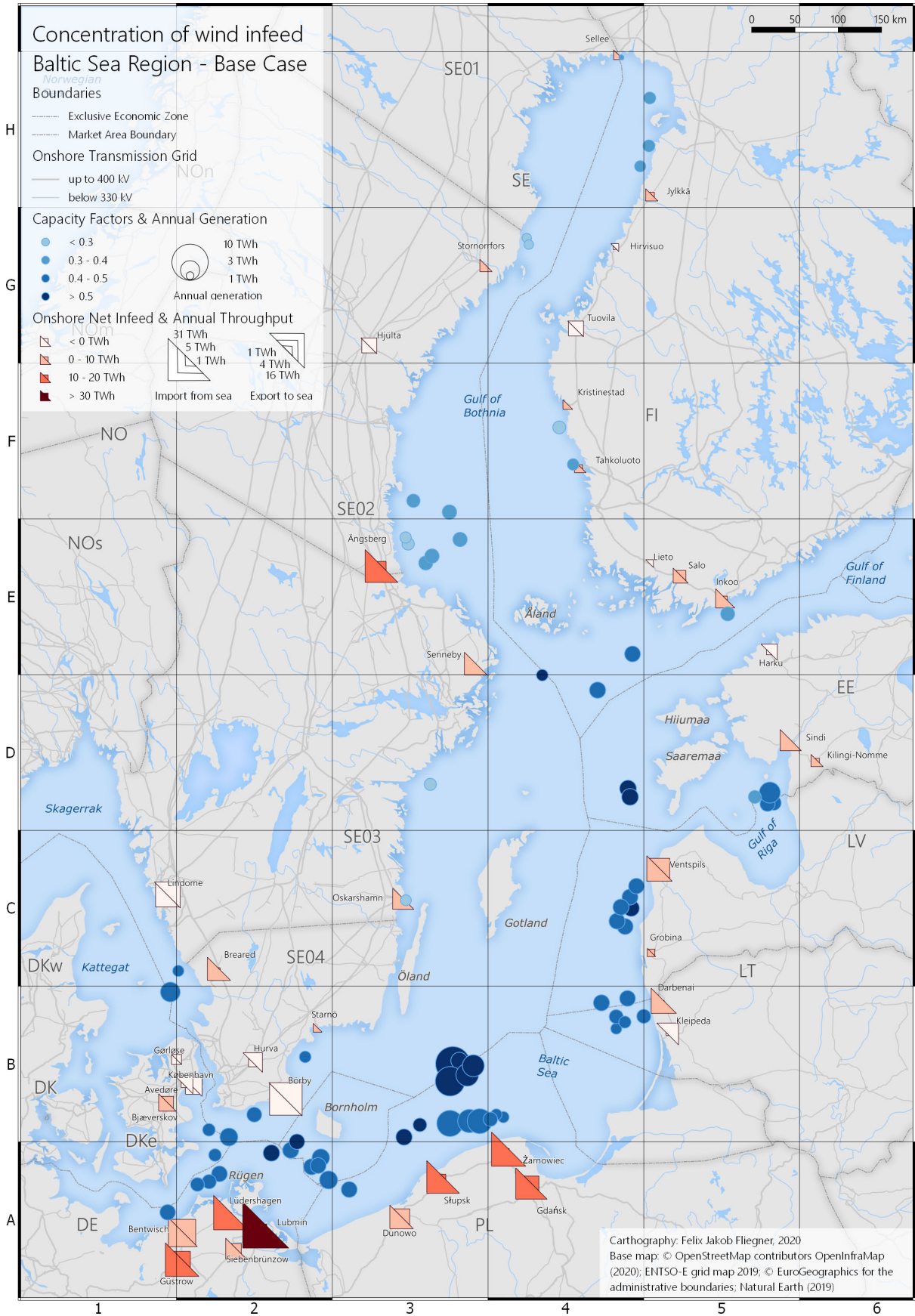


Figure 4.8: Map of wind concentration and distribution of energy landing per substation – Base case.

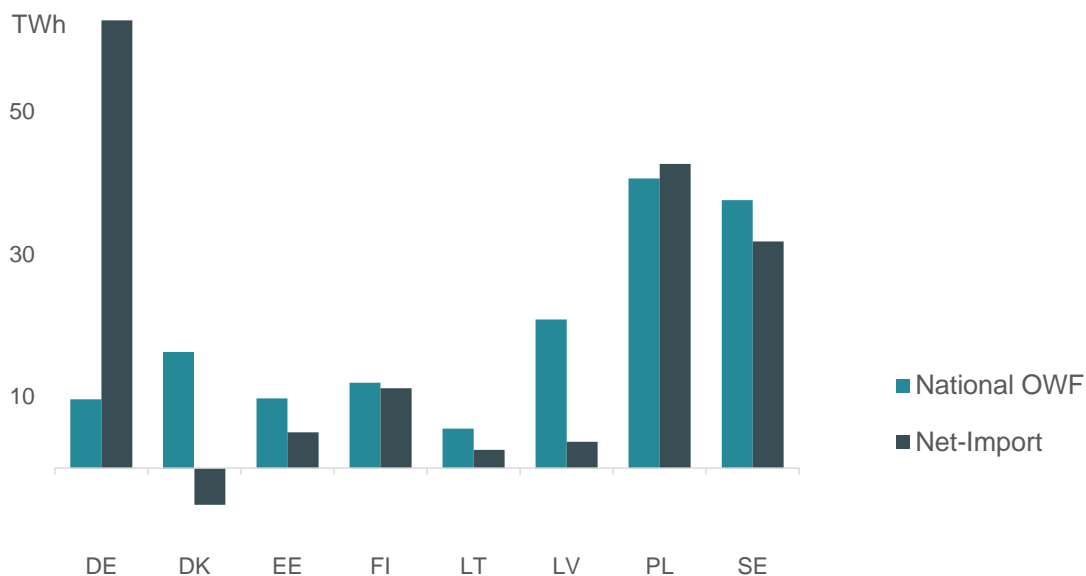


Figure 4.9: Net-infeed and total wind farm generation per jurisdiction per year

Comparing the net-import per country and the offshore wind power generation per jurisdiction in the Baltic sea reveals that all countries except Denmark are net importers of energy from the Baltic offshore grid. Notice that the net-infeed of all countries combined equals the total generation of all wind farms combined. On balance, Germany and Poland import more energy from the offshore grid, than they export. The graph does, however, not allow the simplified conclusion that Germany on the left imports all the leftovers from the right bars. It is an aggregated view which by design mixes infeed from the offshore grid that infeed originates from wind farms (wind power integration) and infeed from it that originates from another market area (cross border exchange). Latvia is with Denmark the largest net exporter of energy, meaning that those countries on balance import only small fractions of their offshore wind energy into their national grids. Both countries share almost 100 % RES and low demand in 2040 compared to the rest of the Baltic Sea Region. Hence, the integration of much additional offshore wind at the cost of transmission capacity is not seen beneficial by the model.

Spatial concentration of power generation

Similarly to the concentration of landed wind energy onshore, the offshore grid needs to cope with a spatial concentration of wind power generation. It is shown as shaded blue circles in map 4.8 as well. While dark colours represent higher capacity factors, the diameter scales with the annual generation per wind farm.

The map reveals that overall wind conditions are attractive in the Baltic sea. The capacity factors of most wind farms in the model are above 40 %, with lower values in the Gulf of Bothnia due to cold climate conditions. Some sites are particularly well suited with capacity factors of up to 54 %. On balance the yearly output of the wind farms per jurisdiction mirrors the installed capacity, meaning that those countries with the highest installed capacity also generate the most (c.f. figure 2.3).

The highest concentration of wind power infeed is found in the Swedish-Polish cluster (B3) both, for its favourable wind conditions (high capacity factors) and large wind farms (high annual output). According to the model, other good wind locations are east of Bornholm (A2), Saaremaa (D4) and Latvia (C4). Even some nearshore wind farms around southern Sweden perform well judging from the capacity factors, while their yield is lower for their smaller size.

Notice that the most attractive wind power sites are usually also furthest away from the coast compared

to all other wind farms. They are less influenced by shading from rough land areas compared to less rough sea surface. Besides, the shortest distance to any shore is often enough not belonging to the same jurisdiction where the wind farms are located in. The cross-national and protruding nature of the Baltic offshore grid becomes evident in this observation once again.

In conclusion, the analysis of power generation and evacuation concentration reveals two further insights on the base case topology. The offshore transmission grid not only needs to evacuate large amounts of wind energy from most remote offshore sites. In fact, it also needs to transmit energy from the northern parts into the south since consumption and generation are displaced from each other. Notice the dual transmission purpose in these findings.

4.2.3 Utilisation and redundancy

The visualisation of power flows refines the previous findings on concentrated infeed and utilisation of the grid. Map 4.10 aggregates the power flows on all links into arithmetic mean values. They represent the average of all positively and negatively counted flows throughout the year. Links with high average power flow signal both, high installed link capacity and one predominant flow direction during most parts of the year. Low mean power flows signal two different situations. Either, the link is indeed a small one with low installed capacity. Alternatively, positive and negative flows are almost equal over the entire year regardless of actual link capacity. Low mean power flow can, for instance, be observed on most radial wind farm connectors. Since only one direction is possible on those links, the value directly correlates with the mean wind farm infeed.

Bidirectional use of links

Some parts of the identified major backbone paths show low mean power flow values as well. Study the northern part of the Finish backbone (D4) or the northern part of the Øresund backbone (B2) for illustration. On average, the power flow is below 0.4 GW on those links, while still facing southbound on most sections. Knowing that the link capacity on those backbones is above 1 GW such a low mean value signals a bidirectional use of some paths in the grid. While on average more energy is transmitted south, there is still a significant amount of energy going north instead. Compare with the substation throughput in map 4.8 for verification.

The bidirectional use shows up mostly on the northern ends of the paths. This finding correlates with the vast storage potential of the Nordic countries, which is used for temporal storage during hours of high RES supply in the Baltic Sea Region. Mind that the Norwegian storage potential is largest in the south (NOs) and indirectly reachable via Denmark (DKw) and Sweden (SE03). The Swedish storage potential is largest in the far North (SE01). In consequence, the offshore grid topology is connecting market area SE03 strongest for its intermediate “bypass” purpose on the way North. Going further south, the predominance of southbound power flow increases, which partly hides reverse power flows in the yearly aggregation. In combination with increased link capacities, this underlines the previous observations of bulk import of energy into Germany and Poland from figure 4.9.

The examined importance of interconnectors towards the Nordic storage potential is further elaborated with map 4.11. It shows the relative link utilisation, which is defined as the ratio of absolute annual power flow (regardless of direction) to the theoretically possible annual throughput at rated capacity. Darker colours denote higher utilisation, which in some cases reaches up to 98 %.

Revisiting the connecting links towards SE03 and Finland, the low mean power flow values from above are now facing high link utilisation rates of 61 % to 86 %. This proves the observation from above of bidirectional use of many hybrid assets across the water body. The remaining offshore grid shows high utilisation of cables as well, which is always above 40 %.

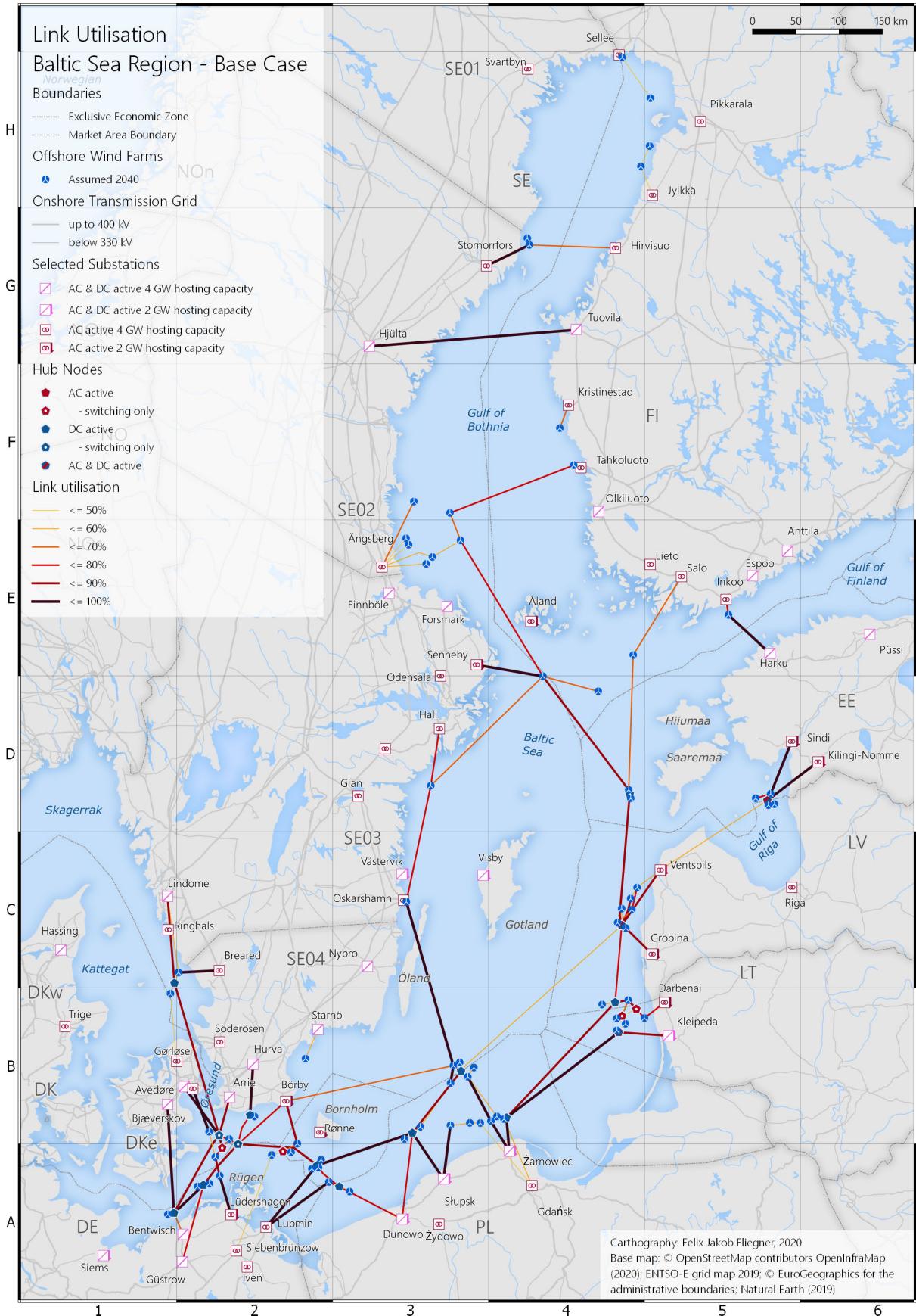


Figure 4.11: Map of utilisation per link – Base case.

Low redundancy

The connecting capacity towards single wind farms (end of a chain, radial link or hub-spoke link) is always lower than the rated capacity of the wind farms. It illustrates the underlying trade-off between investment cost into the “last” gigawatt of capacity and the added value it has on the dispatch side. Since the wind farms are rarely generating at full capacity, the model decides to clip those hours when they do. This increases the utilisation rate of the transmission system during the rest of the time horizon. Study the direct radial wind farm connections east of Ängsberg, Sweden (E3) for illustration. The utilisation rates reach values of more than 50 % while the capacity factor of the wind farms remains below 40 %.

The undersizing of wind farm links can be applied to wind farm chains as well. If a wind farm is connected into multiple directions, no single link capacity would be sufficient to evacuate the total wind power being generated at full infeed. Unless wind power is curtailed, the cumulative capacity of all connected links to the wind farm is required to evacuate the power. In other words, the hybrid asset can only offer the trading capacity to the market during hours of medium or low wind infeed if wind power curtailment is to be avoided. Consequently, the offshore grid is built with minimal redundancy to the extent that the dual purpose of hybrid assets, namely interconnection of market areas and wind power evacuation to the shore, is indeed not enabled simultaneously but rather sequentially. Sequential use of bundled transmission paths thus leads to the high utilisation rates displayed in map 4.11. Notice that this observation is not precisely accurate for every chained wind farm. Especially not for those, being part of a stronger backbone which serves bulk transmission tasks as identified above. Investigating the ratio of total installed wind power and total landing capacity of the offshore grid reveals, however, the overall low level of redundancy of the offshore grid in the model.

Figure 4.12 shows the installed wind farm capacity and offshore grid connection capacity per jurisdiction and aggregated for the entire Baltic Sea Region. While the ratio is very different for each country, it reaches almost 1:1 on an aggregated pan-Baltic level. The figure also depicts once more the high importance of bulk transmission from the north and east towards the south. Oversupply with offshore wind in Denmark, Sweden and Latvia (high onshore RES) and Poland (tight hosting capacity limit) are visible alongside with higher imports into Germany than is installed around it.

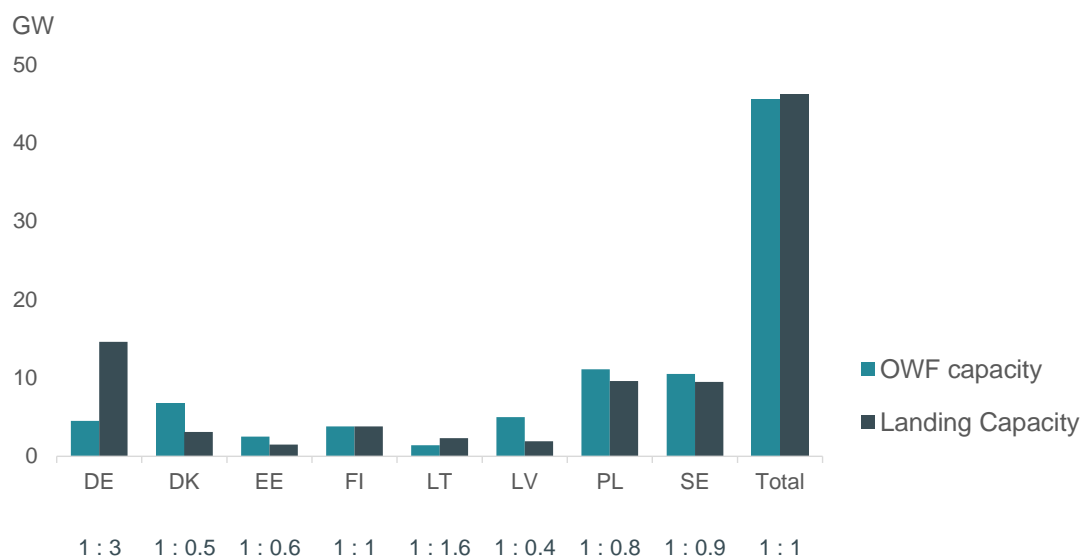


Figure 4.12: Ratio of total installed wind farm capacity and total landing capacity per jurisdiction.

The major takeaway from the utilisation study of the base case topology is that bundling of transmission tasks into many hybrid assets not necessarily leads to an overall increase of landing capacity onshore.

While the total installed capacity of all links exceeds the 45 GW of wind power by far, the actual landing capacity of the grid is almost of the same size. On a pan-Baltic level, wind power evacuation from the sea and interconnection of market areas is enabled via bundling of transmission corridors. The dual purpose of the transmission is, therefore, not reached by maximising cable capacity but instead maximising utilisation rates over time.

4.2.4 Investment cost breakdown

The total investment taken by the model amounts to 57 bn € and is distributed among different AC and DC technologies, as shown in figure 4.13. The largest shares of cost amounts for cabling. It also includes miscellaneous equipment such as reactive power compensation for AC cables. Notice that DC and AC cable cost are almost equal in total. With 4600 km DC cables with up to 6 GW and 3800 km AC cables with up to 4 GW being installed, it reveals the relative cost-benefit of DC cables over AC cables. This benefit is outweighed on the nodal cost for DC equipment, namely AC-DC converters and DC circuit breakers. Compared to the DC nodal costs the AC equipment and platform investment costs are dwarfed.

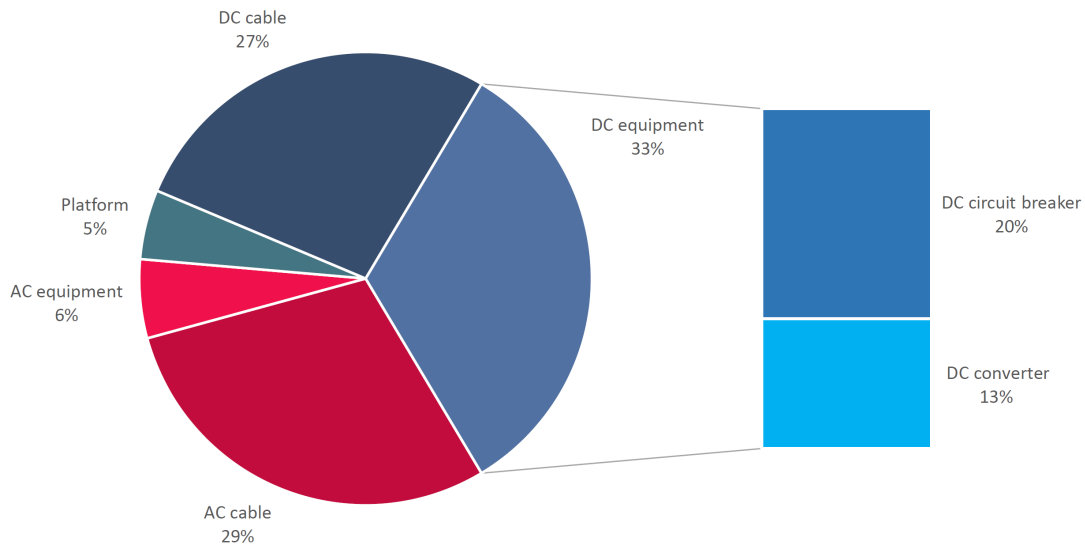


Figure 4.13: Cost breakdown of offshore grid investments – Base case.

Notice that the low platform and low AC equipment cost partly results from the underlying notion of pre-activated nodes and links. For each wind farm node that is serving as its hub the node activation, i.e. building the platform and activating it for AC or DC conversion, the activation costs are zero. This is following the notion that as seen from the model, the wind farm is built either way. Hence its capability to feed-in AC or DC power is not explicitly installed and invested by the model. Since 38 out of 71 wind farms are part of chains, the intermediate hub platforms and wind farm transformers or converters come to the model “for free” as long as the wind farms are connected to the offshore grid. In other words, on most chains only switchgear and cables add activation cost to the objective function value.

On the contrary, most additionally installed hubs are in DC technology, meaning that neither platform nor node equipment is preset at zero investment cost. While the 27 of 71 wind farms of such clusters again are equipped with “free” equipment the central hub needs to be invested at full cost since it is an entirely new node in the network. This logic leads to high DC cost compared to the AC cost, even though physically way more AC transformers are present in the topology. Most of them just happen to be outside the boundary of analysis as elaborated in section 2.2.1 already.

In conclusion, three types of takeaways can be identified from the base case results.

Wind farm connections: The model connects all wind farms but slightly undersized with reference to the wind farm capacity. Most wind farms are either clustered into hubs based on the GIS permissive hubs or chained next to each other based on GIS permissive links. Clustering and chaining of wind farms lead to a high concentration of grid infeed, both offshore and onshore.

Topology characteristics: The offshore grid is realised with strong backbones from North to South and East to West. Most chains are created with asymmetrical capacity rating, where the stronger end reaches towards the high demand side. The model creates offshore detours to relieve onshore grid congestions between market areas or at overfull substations.

Utilisation: The mean power flow through the offshore grid is from North-East to South-West. Reverse flows occur especially towards the Nordic countries, mainly via Sweden SE03. They signal storage usage during times of high RES supply. The bundling of transmission tasks into common paths, as suggested by the GIS topology setup leads to maximised link utilisation. The interconnected chains of several hybrid assets allow maximum wind power evacuation and international trade opportunities without building redundant capacities. The utilisation for hybrid assets is optimised for sequential use, meaning that cross border trade mainly occurs during hours of low wind infeed.

4.3 Sensitivity of topology and dispatch

The base case topology results are investigated for robustness with the help of a sensitivity analysis. Its purpose is to identify the most influential constraints and their impact on the optimal solution when lifted. This thesis chooses three topological constraints which are sequentially analysed and discussed in this section. They include a removal of all preset links, denoted as “no interconnectors” (No IC); an enforced national radial connection of the wind farms without clustering or chaining, denoted as “radial”; and removal of the hosting capacity limit for all substations, denoted as “strong grid”. They are summarised in figure 4.14.

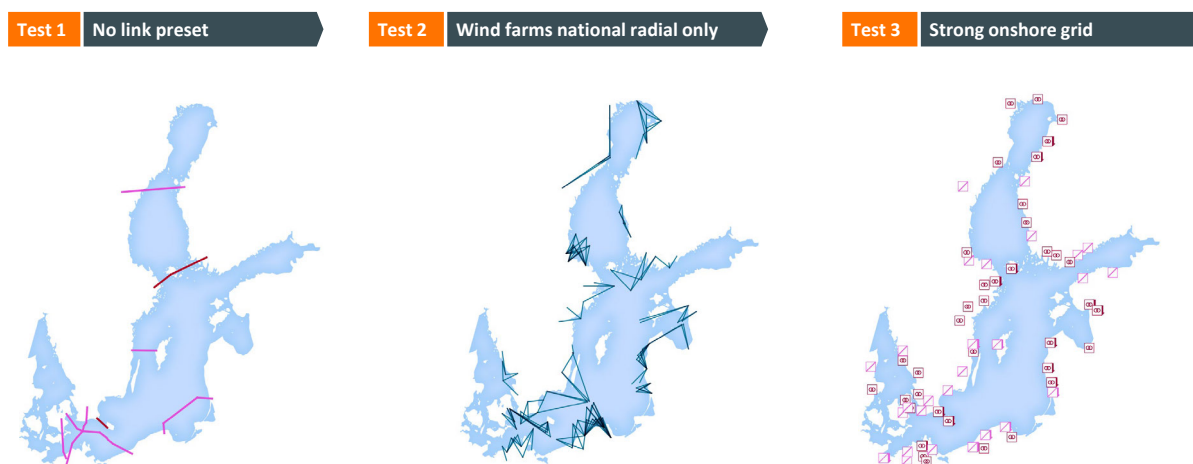


Figure 4.14: Sketched sensitivity analysis overview

While technical limitations and cost parameters are also sensitive inputs, a detailed technical and economic discussion is still out of scope of this report and therefore neglected. The subsequent discussion chapter provides some remarks towards operability and economic feasibility to trigger further discussions beyond this work.

The expected outcome of the sensitivity analysis is besides changing topology results a set of aggregated

indicators that describe the grid performance. They include curtailment of wind energy, total link lengths and the connection types for the wind farms. They are discussed alongside the topology results where appropriate.

For the **“no interconnectors”** sensitivity all links from the GIS topology setup are still permissive in the model, but their initial capacity is set to zero. While the previously pre-activated interconnectors links can still be built, the model needs to identify all transmission needs between countries on itself. Connecting the previously preset countries with each other now results in a slightly higher cost since the first couple of gigawatts of transmission capacity are no longer “for free”. The purpose of this sensitivity is to investigate the bias imposed on the model when predefining sets of links. The underlying question is first, whether the transmission capacity is still realised between the countries and second, whether the trajectory of the interconnectors changes and whether different wind farms and clusters are teed in along the way. Finally, it is of interest if other transmission corridors change in size and trajectory as well, once the pre-existing docking options for bundling of transmission paths is no longer given.

In the **“radial”** sensitivity wind farms must be connected to the same jurisdiction they are located in. Besides, no clustering or chaining, i.e. bundling of wind farm connectors is allowed. The preset interconnectors from the base case are back in the model and additional interconnection between countries, including the formation of backbones, is still allowed. Hybrid assets, by definition, cannot be built, since wind farms must not be clustered or teed in. While this sensitivity appears rather strict and unfavourable, it is the most commonly realised offshore topology as of date. Wind farms are usually connected to the country they “belong to” and interconnectors between countries are planned and optimised separately. The purpose of this sensitivity is hence, to showcase the benefits arising from an interconnected offshore grid with hybrid assets as opposed to radial connections only.

The third sensitivity is denoted as **“strong grid”** since it tries to address one blindspot in the base case analysis, namely the onshore grid. The base case results reveal a binding constraint of the onshore substation hosting capacity in the form of long detours along the coasts of Sweden, Poland and Germany. While this constraint is meant to illustrate the power handling capacity of the onshore grid, a sensitivity is conducted assuming that the onshore grid would yet be stronger and could integrate more wind power per substation. The hosting capacity is lifted to infinity, while the onshore cross-zonal capacities from TYNDP remain in place. The expected result is the removal of detour links and the “true” value of offshore wind power connection for each country. Mind that this sensitivity is incorporating a bias for integrating too much wind energy in each national grid. Since the onshore grid expansion is introduced at no cost for the model, the actual trade-off between grid expansion investment and dispatch improvement from the base case is no longer valid. Besides, not co-optimising cross-zonal capacities still faces the optimiser with some onshore congestion which might alter the topology findings as has been shown in the base case results already.

4.3.1 No preset interconnectors

The map in figure 4.15 shows the topology results, with removed interconnector presets. It reveals that most interconnectors from TYNDP are confirmed in their cross-border capacity. Due to the model focus on bundling, tee-in and clustering their trajectory is, however, slightly shifted. In the southern Baltic Sea the four interconnectors between Germany, Sweden, Poland and Denmark are, for instance, routed via two DC chains, where the first one connects Arrie, Sweden (B2) with Bentwisch, Germany (A2) and the second one Avedøre, Denmark (B2) with Słupsk, Poland (A3). This finding supports the notion of ever more bundling of transmission tasks into common paths.

Removing the preset links also changes the onshore substation choice in the model. While the *Hansa-Power-Bridge 2* from TYNDP connects Hurva, Sweden with Güstrow, Germany it is now adjusted to Arrie – Bentwisch in the model. Notice that this change does not originate from any onshore grid analysis, since the model cannot distinguish between the physical strengths of any substation in a given market area. The reason here is that Arrie and Bentwisch are closer to their respective shorelines, hence chosen first before other substations further into the market area are connected by the model. Distance and power throughput limit are the paramount criteria the model can investigate. Hence it always connects the first row of substations in the solution space. Observe a similar finding with the Swedish-Finish interconnector which is not built as such. Its transmission capacity is realised via the previously identified link from Stornorrfor to Hrivisuo north of it for its shorter total distance it needs to bridge.

The interconnector from Żarnowiec, Poland to Klaipėda, Lithuania is both rerouted and landed differently. Leaving the Polish coast, it is first clustered slightly further west into the Polish cluster before heading east. In Lithuania, an enforced AC branch connects to Klaipėda, while the main DC chain continues further north until it merges with the German-Finish backbone. Notice the slightly more centralised grid topology compared to the base case.

While the offshore grid is more centralised than the base case, it still faces congested landing points with the substations of Poland and Germany. Hence the detour split-up of the German-Finish backbone still occurs with one Lubmin-leg and one Güstrow-leg. In contrast to the base case, this split up now happens on Bornholm, saving on the former DC hub node offshore south of Bornholm. This shift in space signals an impact of the interconnector assumptions on the resulting offshore topology. The formerly preset interconnector between Denmark and Poland biased the model towards more tee-in opportunities along its trajectory. Those opportunities are still permissive but more expensive now since they would require full cost for the interconnector cables. Thus, the splitting hub and intersection are shifted to a shore, here, the natural Island of Bornholm. Notice that the Danish-Polish path still crosses with the German-Finish path. The crossing is just shifted to a more favourable (onshore) location which saves fixed investment cost. Repeat this observation with the formerly northern detour of the German-Finish backbone from the Swedish-Polish cluster via Börby, Sweden to Güstrow (c.f. map 4.7). One additional offshore DC hub can be saved if this path is bundled in Bornholm as well. As a result, the German-Finish backbone is now more readily visible and “cleaned up”.

The connection types of all wind farms are untouched by this sensitivity. Similar to the base case, most wind farms are chained or clustered, as figure 4.16 summarises. Substantial changes in the connection of wind farms occur in the subsequent two sensitivities where either all wind farms are connected radial (“radial”) or ever more centralisation of wind power infeed in clusters is optimal (“strong grid”).

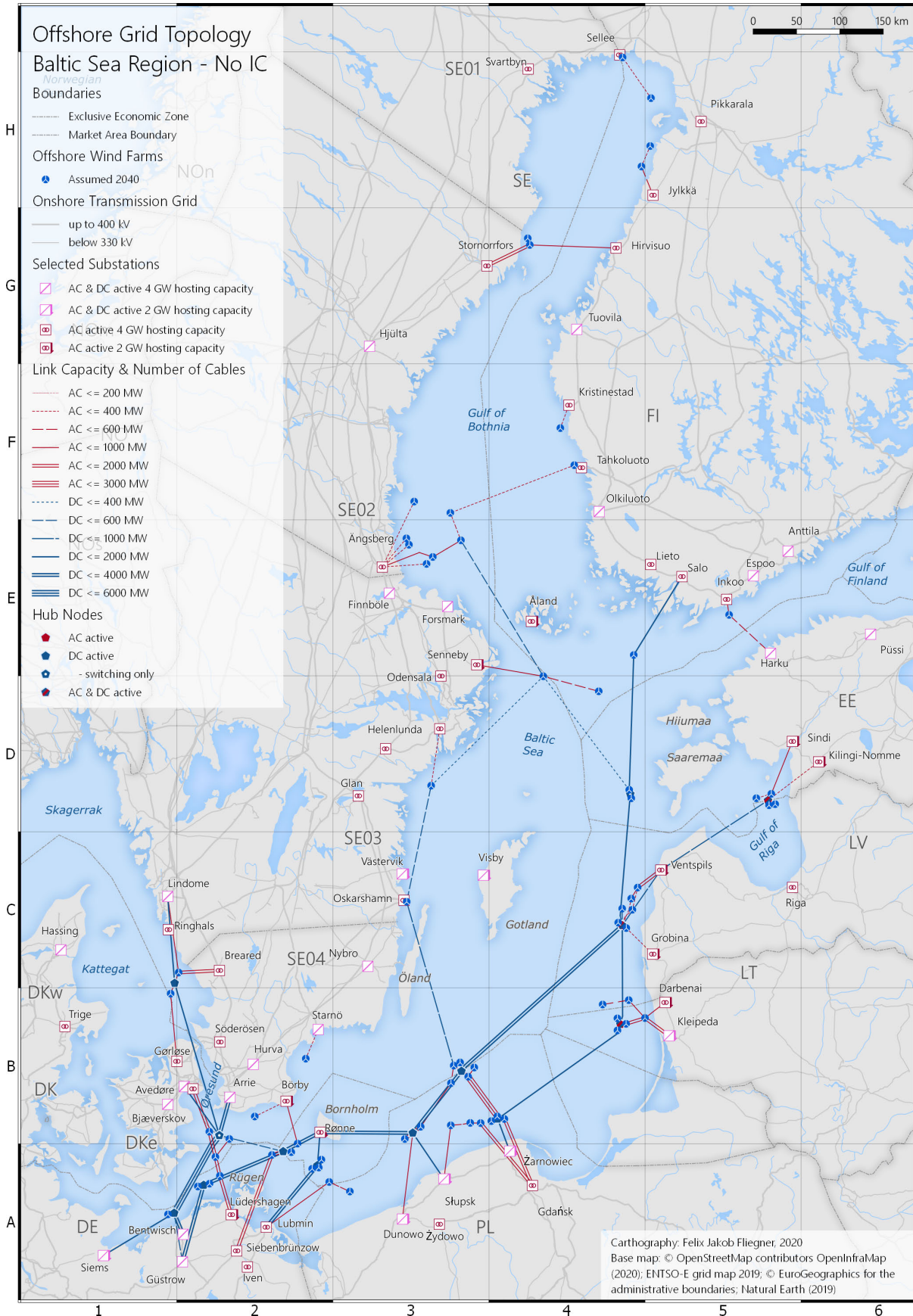


Figure 4.15: Map of topology results – No interconnectors sensitivity.

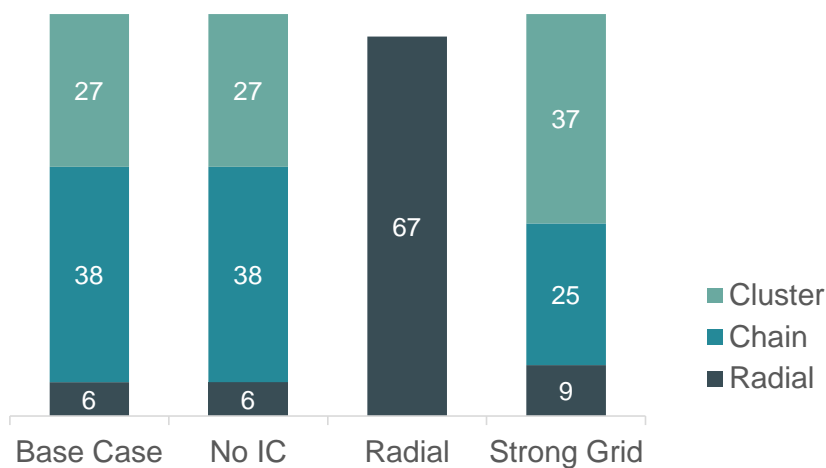


Figure 4.16: Number of wind farms per connection type (total: 71).

The conclusion from this sensitivity is that removing preset links in the model impacts topology results. While the trans-Baltic transmission needs identified by the model remain mostly unchained from the base case they are realised in a different layout. The enforced bundling of links due to higher utilisation prospects and saved cable lengths can act even stronger, resulting in a more centralised and “tidy” offshore grid. This observation also signals that exogenous information on the location of preset links, hubs and indeed wind farms is an influential input parameter on itself. It underlines the introduced notion of grid investment being residual to generation investment and is discussed further in the next chapter.

4.3.2 Wind farms connected national and radial only

Enforcing national radial wind farm connections leads to suboptimal connection prospects. Since some wind farms are located closer to foreign countries, their national connection systems now require costly cables. Due to this observation, four wind farms are not connected at all, leading to a loss of 3.5 GW offshore wind capacity in this sensitivity. Besides, an increasing number of distant wind farms is now connected with DC links for the considerable distance they are offshore. Study the Swedish-Polish cluster (B3) in figure 4.17 for illustration of both findings and compare with the base case. Notice that the distance criterion is indeed paramount here. It is not the least attractive wind power locations with small capacity factors, which are spilt here. In fact, the model does not connect two Swedish wind farms (B3), which used to perform best in the base case.

The suboptimal connection layout is evident in the presence of many interconnectors being built in parallel to the radial wind farm connectors. While bundling of interconnection paths is still possible and often adopted by the model, hybrid assets cannot be built. Hence clustering of wind farms and chaining is not found anymore. Notice that the exclusion of wind farm chains shortens the German-Finish backbone substantially, since building a long link to the north without leveraging synergies from integrating wind energy along the way is now suboptimal. Instead, the Øresund backbone is enforced even stronger still to reach some parts of the Nordic storage potential.

The formerly installed AC chains are no longer present since those chains usually originated from wind farms being connected with each other. On the DC side, the former cluster hubs are now switching hubs only, since no wind power is integrated along the way. Intersections of DC chains are created for switching and rerouting of power flow only. Detours and split-ups are still created with the same reasons as in the base case.

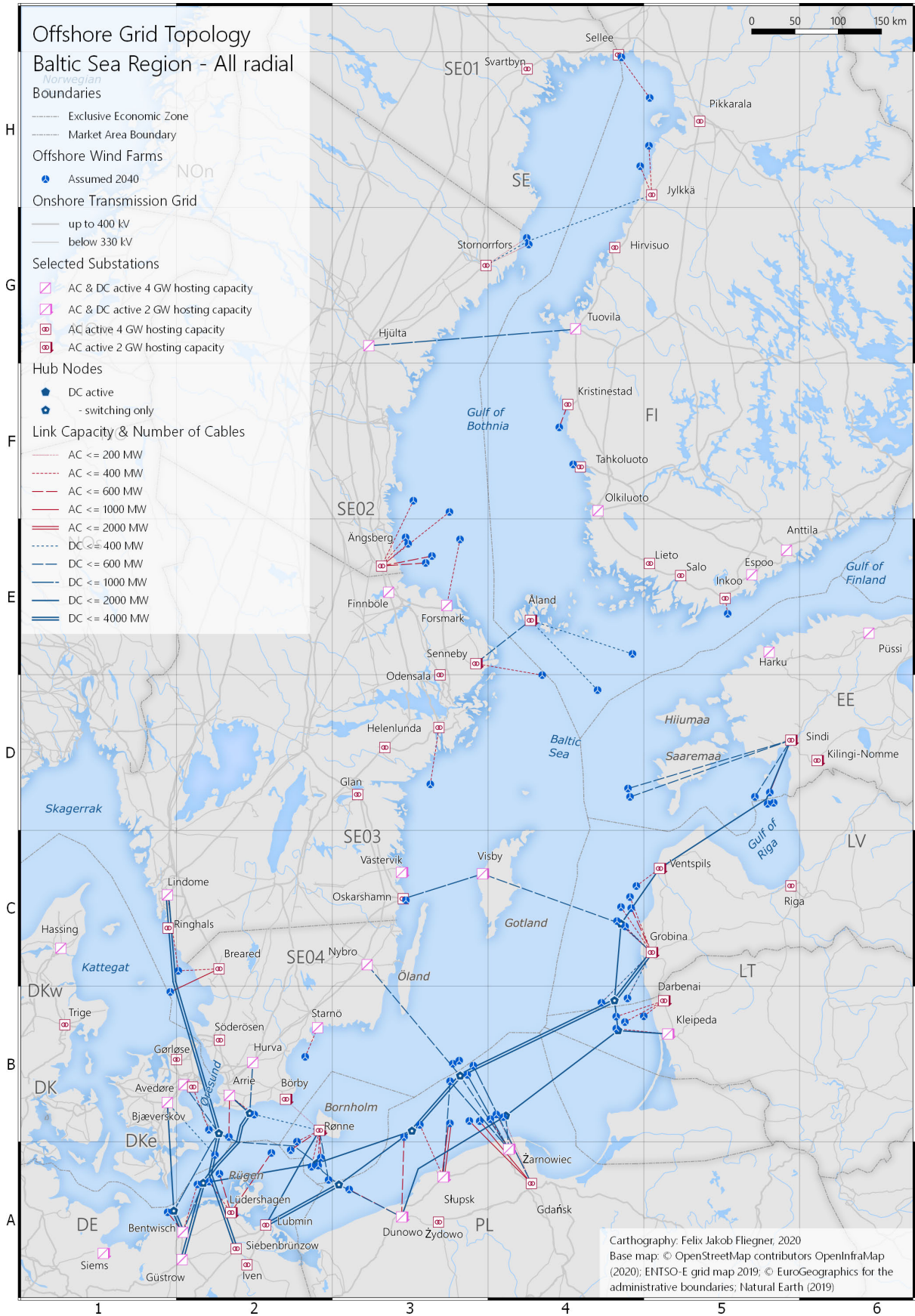


Figure 4.17: Map of topology results – Radial sensitivity.

The wind farms linked to Bornholm are technically connected nationally since the Island belongs to the jurisdiction of Denmark. At the same time, a strong DC link from Bornholm is activated, which evacuates the landed energy straight back to Germany, where it used to land in the base case before. Observe that the connecting capacity for the Bornholm wind farms and many other wind farms is reduced compared to the base case. The high investment into doubled transmission capacity and cable kilometres challenges the cost trade-off between investment and dispatch and leads to an overall reduced connected wind farm capacity. Repeat this observation around the Åland region with Finish wind farms being connected indirectly to Sweden.

One consequence of undersized cabling is increased curtailment of wind power. Figure 4.18 compares the average curtailed wind power and yearly curtailed energy from in the Baltic Sea region. While overall curtailment is small in all cases, it experiences its maximum in the radial sensitivity. 5% of the yearly Baltic Sea power generation from the warm start results are curtailed in the radial sensitivity, as opposed to 3.5% in the base case and less than 1% in the strong grid sensitivity.

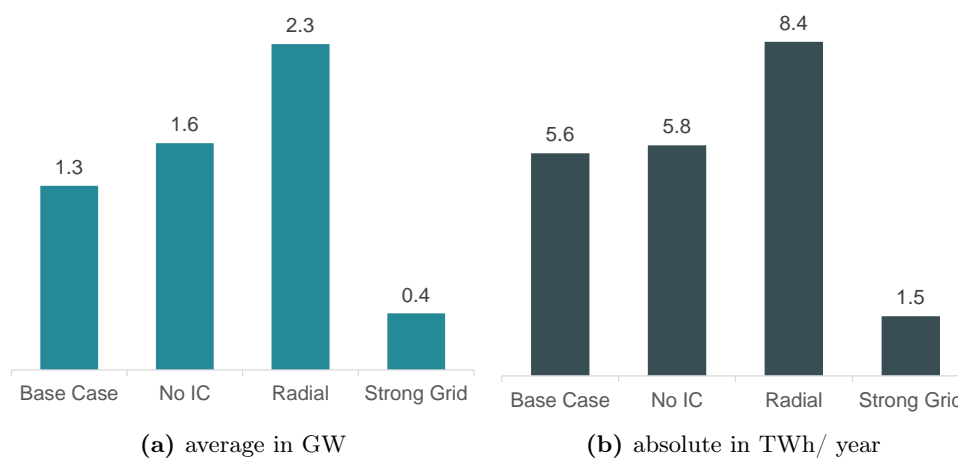


Figure 4.18: Offshore wind curtailment

Despite being a suboptimal scenario, the radial sensitivity is a well-suited case study for the tipping point of cable length between AC and DC technology. Studying radial connections in the base case and the sensitivities reveal a tipping point from AC to DC at about 80 km link length, which is in agreement with the input data discussion. Mind that this finding should be interpreted with care since this analysis is not a technical simulation of the offshore grid as such. Furthermore, the distance of a given link is not the only criterion to choose AC or DC. In many cases, it is also the context of power transmission that decides on the voltage type of a given link. The strong DC links in the model, for instance, do not change their voltage type in between just because the distance is short enough between two nodes. When additional conversion with expensive equipment can be avoided, the model tries to stick with one voltage type as far as possible for a given path.

4.3.3 Strong onshore grid

With a hypothetical strong grid behind, the offshore grid does not need to install split backbones and detours any longer. Study in the figure 4.19 the most centralised and “clean” offshore grid in this analysis. Its purpose is now mainly wind power evacuation and cross-national trade and not the relief of substation congestion. Observe, that the offshore grid is still used to address onshore cross bidding zone congestion, which is the only option for the model, since it still does not co-optimize the onshore grid. The Øresund backbone is still present on the map. The German-Finish backbone, on the contrary, is simplified into one path without a Swedish counterpart and a split up in the Bornholm region.

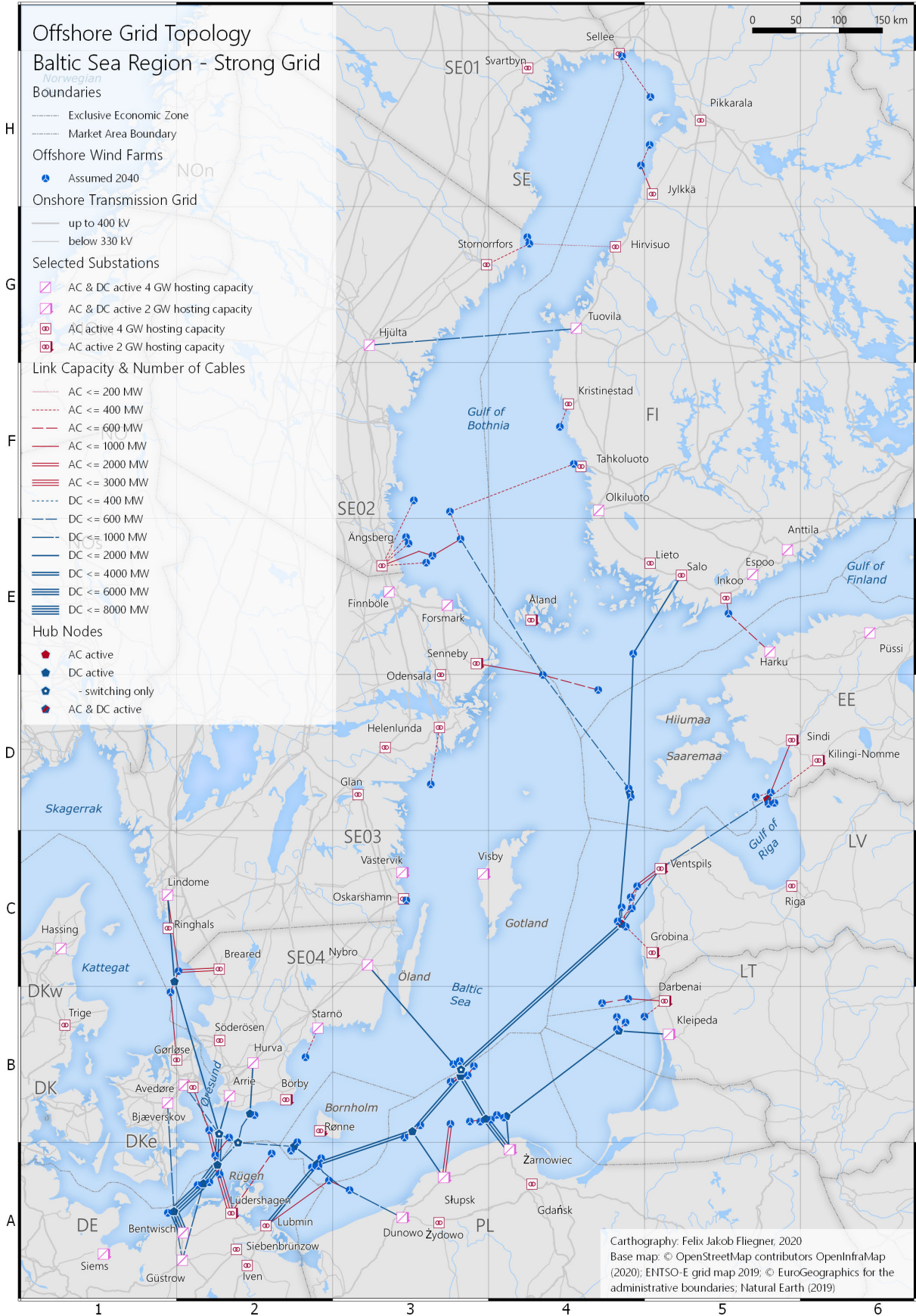


Figure 4.19: Map of topology results – Strong grid sensitivity.

The total landing capacity of the offshore grid in Germany is slightly smaller, signalling a shift of wind power integration towards the East. Poland and Lithuania are integrating more of their nationally generated offshore wind power since the onshore grid congestion is lifted. Latvia, on the contrary, still exports most of its offshore wind generation. This observation is evidence of a high dominance of onshore RES supply at comparatively small demand. Given the tight cost trade-off in the model Latvia does not have an added value in integrating ever more offshore wind into its grid. In the model, it is more beneficial to still export the energy northbound or southbound even with unrestricted onshore connection points nearby. Note that this finding might turn out differently with other objectives being included in the optimisation problem.

The bundling of energy flows in the offshore grid is maximised in this sensitivity. The number of clustered wind farms increases from 27 to 37 (out of 71), while AC chains of wind farms are reduced. Notice that both the AC chain west of Bornholm (A2) and the AC chain from the Swedish-Polish cluster (B3) to Poland are replaced by DC clustering and tee-in into DC backbones. Besides, all backbones are now landing in the first row of substations being closest to the shoreline. As seen from the model, all substations are now equally well suited as long as they are part of a given market area. Study this finding at the substations of Gdańsk (A4), Siebenbrünzow and Güstrow (both A2). Understand that Güstrow is still connected to the offshore grid since the *Hansa-Power-Bridge 2* preset link terminates there and is realised for its zero cost assumption.

An increased concentration of offshore wind farms into central hubs and backbones leads to a more prominent landing of power at the remaining substations. The maximum installed link capacity reaches power ratings of up to 8 GW on the DC side, meaning that on some chains four DC cable systems are installed in parallel. Study the DC chain from Bentwisch towards Kriegers Flak for illustration. It starts with 8 GW bundled capacity in the south and splits up into four legs on the northern end (Hurva, Arrie, Lindome and Avedøre).

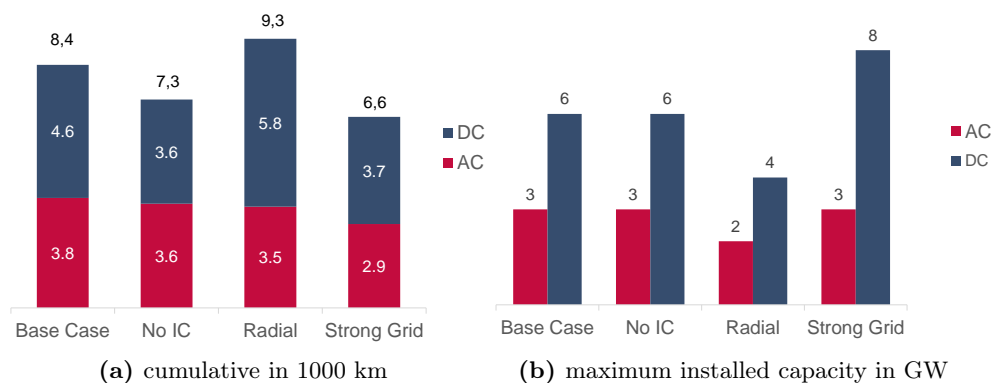


Figure 4.20: Cable lengths and strengths

Figure 4.20b compares this maximum capacity rating per voltage type of all model runs. While the DC backbone purpose is visible in all cases, it experiences a dip in the radial case for less energy being available for bundling and is highest in the strong grid scenario for the above-listed reasons. AC cable ratings hardly change since their purpose is almost always the same, namely short distance hub-spoke cabling and chaining of selected wind farms. The radial sensitivity does not allow AC chains. Hence the strong asymmetrical ends of those chains are not realised, leading to a smaller power maximum in that scenario.

Figure 4.20a shows the savings in cable length in the strong grid sensitivity compared to all other cases. While the AC link lengths do not alter a lot for reasons discussed above, the DC links have substantial differences in total length. Slightly shorter total DC cable length in the “no IC” sensitivity is evidence of

the less favourable trade-off for the model since no links are introduced for free. In the radial case, a high amount of redundant links is built, which is usually realised in DC for the long distances and high power ratings required. In consequence DC cable length peaks in this case.

The figure also delivers the concluding remark from this sensitivity: International wind farm connections and a strong onshore grid foster a centralised offshore backbone with minimised link length. Remember from figure 4.13 that saving on link lengths is most influential on the total investment cost. In other words, the “strong grid” sensitivity can also be regarded as an optimistic stance towards the future offshore Baltic offshore grid.

Closing the results chapter, the following insights can be drawn from the sensitivity analysis. Removing preset links from the solution space enforces the investment decision trade-off by removing free cables and platforms from the model. While exchange capacities between countries are almost unchanged and the type of connection for the wind farms remains stable as well the first tendency towards more centralised and bundled transmission paths can be seen.

Enforcing national and radial connection of wind farms even without national clustering or chaining leads to a highly redundant grid topology. Total cable length increases which drives investment cost the most. At the same time curtailment is highest in the set of analysed cases and some wind farms are not even connected to the grid for their suboptimal location for the jurisdiction they belong to. Even without the opportunity to realise hybrid assets with wind farms, the interconnection between countries remains high.

With a hypothetical strong grid, the offshore topology can mirror the centralised infeed from the wind farms best, by bundling energy flows even stronger. The backbones are confirmed from the base case but appear more readily on the map since their detours and split-ups are minimised or removed entirely. The Baltic states and Poland can integrate more of their wind power, while Latvia and Denmark are still exporting most of their energy into the grid. Even though total investment is smallest due to shortest cable lengths, this sensitivity ignores the cost of necessary onshore grid enforcement leading to a slight bias in the resulting topology.

5 Discussion

The modelling results reveal a wide range of storylines that can be created for the future Baltic offshore grid. This thesis does not attempt to rank them for favourability, relevance or indeed probability to be realised. Base case and sensitivities should be studied as four individual spotlights on selected characteristics of a high-level offshore topology and not regarded as a scenario for a deployment plan towards 2040. Purpose of this discussion chapter is, therefore, to illustrate the added value of the analysis from a methodological stance, not a strategic. It revisits selected considerations from the methodology and results chapter for discussion and prepares the concluding remarks and value drivers from this report. This chapter closes with a look ahead to identify aspects out of scope and emphasise a need for further research.

5.1 Contribution of this analysis

Endogenised identification of offshore transmission paths

The optimisation framework presented in this thesis makes the location, size and configuration of offshore hubs subject of optimisation, as opposed to defining them explicitly. This inverts the common practise approach of scenario-based analysis of manually pre-selected offshore hubs towards parametrised identification of permissive grid elements (GIS analysis) and mathematical optimisation of their characteristics (market modelling).

The analysis follows a modular approach with several abstract building blocks for offshore transmission assets. They represent the physical reality of the offshore grid and include various link types, bundling options and technology types. Based on the selection of considered building blocks and the level of detail they are modelled at, various model calibration options arise. Note that this thesis uses a simplified technical simulation, which results in a purely economic power flow analysis. Yet, it allows the analysis of transmission paths and their various purposes, namely bidirectional power transmission for wind power evacuation, market area interconnection and storage utilisation in the Nordics.

With a widespread permissive graph topology to perform iterations over the landing of offshore wind energy is more flexible. In contrast to the approach in the Baltic InteGrid study [7], transmission corridors are not fixed in trajectory and capacity. Besides, the bundling of transmission paths allows implicit expansion of cross border capacity wherever efficient. Notice that hybrid assets, therefore not need explicit proposal or pre-definition. They are created as a takeaway from bundled and chained transmission paths. On the contrary, non-bundled paths and non-hybrid assets, i.e. singular wind farm connectors and interconnectors can still be built if optimal. This is enforced by the integrated optimisation, which follows the trade-off between cable investment and dispatch cost improvement.

Pre-solve with GIS analysis

The GIS topology creation separates the initial optimisation problem into two parts. The link creation results in a striking reduction of the solution space. The computationally highly demanding practise of including all possible combinations is therefore avoided. The saved resources can be spent elsewhere to increase the complexity and granularity of the market model. Notice that the GIS pre-processing is the enabler of a strong focus on the combinatorial complexity of the high-level offshore topology. Since the GIS pre-processing is fast performing, it could also be used to create an abundance of high-level GIS pre-solves before selecting an “interesting” set for further investigation based on the research questions at hand. Thus, the first hints towards the final topology result are obtained in a lightweight and fast model without awaiting complex market model results.

GIS pre-processing obtains the topology bottom-up without heuristics or manual scenario building. Expanding SVENDSEN's clustering approach, it leverages various geodata sources which creates a uniform and validated point of departure for analysis (spatial analysis). With alternative calibration of the MiniMax algorithm for geometric clustering, several permissive graph topologies are obtained. The GIS analysis is, therefore, a parametrised first part of the toolchain, which maintains the analytical nature of the entire analysis.

Open source and open data

The optimisation in Julia and QGIS is setup entirely in open-source software. The licensed solver Gurobi can also be replaced by open-source alternatives [81]. Input data and information on future outlooks are retrieved from publically available data sources. No internal or indeed strategic insights from TSO level or offshore wind farm operator level are used for analysis.

5.2 Limits of the proposed framework

The results presented in this thesis do not allow strategic conclusion or inference of any stakeholder's positioning being active in the Baltic Sea Region. Findings and discussion are solely based on publically available data and should be treated as an entirely descriptive discussion of the matter. Beyond this legal disclaimer, further academic limits of the proposed framework are discussed in the following section.

5.2.1 Accuracy of GIS analysis

Weight of wind farm assumptions

The choice and number of wind farms in the model directly influences the final topology result. Observe this at the example of frequently mentioned chained singular wind farms. If they were not included in the initial set of permissive elements, the GIS clustering would require a different calibration to identify remote connection points still. Distance and density thresholds would then be higher. The value and level of detail of other geographic information also directly influences the pre-processed results. Observe this in the process of spatial analysis, where repositioning, filtering and estimation of wind farm locations is performed. Retrieving concrete value drivers or indeed the future of the Baltic offshore grid is consequently limited to qualitative trends. It showcases what topology trends can be seen, given a set of pre-defined wind farms and interconnectors.

Strong backbones showing up in the model results should not be confused with most likely backbones. Similarly, density and number of permissive links do not correlate with the superiority of a given path (c.f. GIS results). Understand that the realisation of many identified links crucially depends on the realisation of the chained and connected wind farms. For the analysis, they are fixed, i.e. assumed realised by design. Acknowledging the high uncertainty for the long time horizon in question, the topology results could look quite different with modified wind farm distribution and layout. The sensitivity analysis hints that slight changes in the initial setpoints result in a spread of topology results. Robustness of the GIS results is thus only maintained to the extent that the wind farms are indeed realised as listed at rated capacity and location.

Routing bias for long paths

The dominance of backbones and bundled transmission paths in the final topology partly stems from the GIS processing calibration. On the one hand, this introduces a bias into the model where remote locations are almost always connected via shared transmission paths with other points along the way being tied in. On the other hand, this bias can be regarded as a more accurate representation of the geographical

reality of the water body. Study figure 5.1, which revisits the Åland wind farms for illustration. It shows a hypothetical extreme case of remote connection from the Åland region to the Danish coast. In the unprocessed initial graph topology (“complete graph”), direct links exist from remote wind farms to the destination (straight violet lines). In the pre-processed permissive graph topology (“reduced graph”) these links are not part of the solution space. Instead, the connection is realised via a path, which is routed via a set of intermediate links connecting pairwise wind farms and hubs into a long chain (blue line with vertices). The green line denotes a hypothetical optimal (i.e. shortest distance) trajectory of an offshore submarine cable following the convex hull of the shoreline.

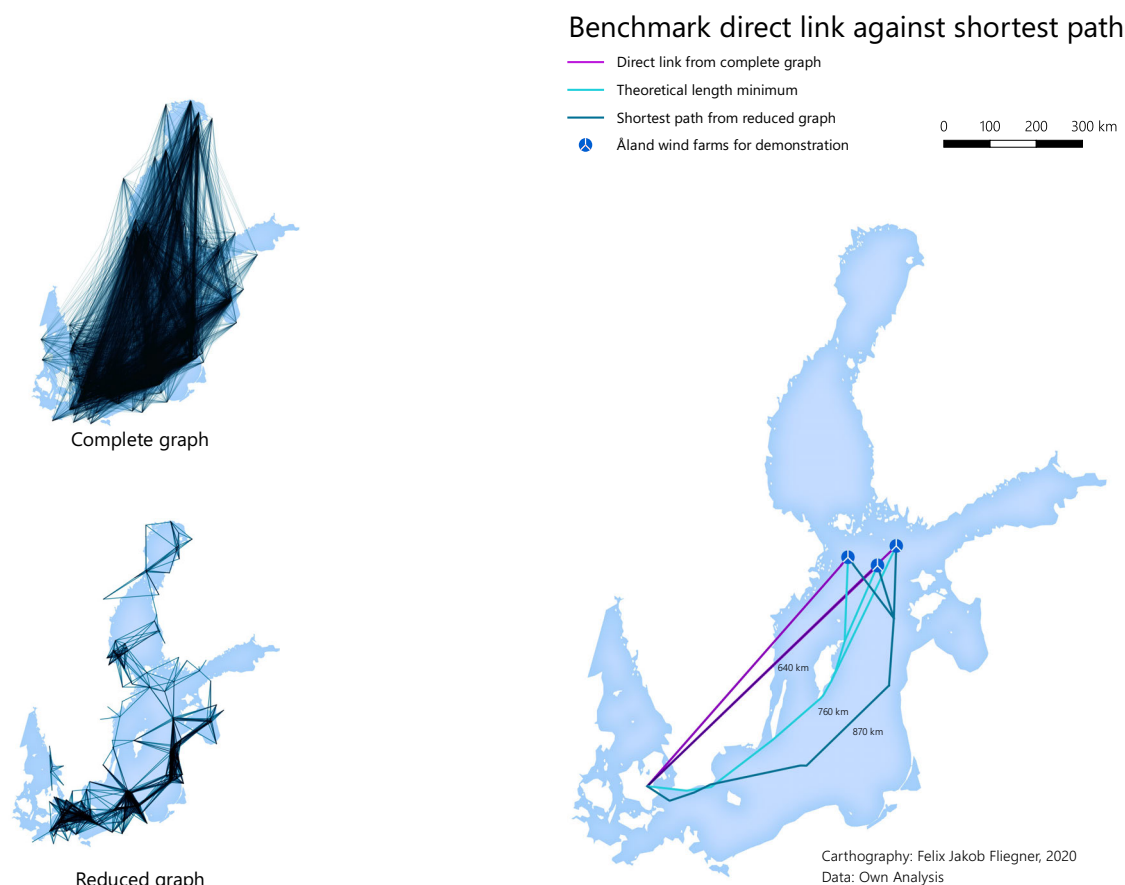


Figure 5.1: Benchmark link creation – Åland to Denmark path.

Neither the complete graph nor the reduced graph return the true link length of the optimal mutual connection of two arbitrarily chosen points. In this example, they diverge equally in either direction. While the complete graph tends to underestimate link lengths, the reduced one tends to overestimate them. Notice however that the overestimated path is at least physically realisable as a submarine cable. The former one is simply an infeasible and wrong solution, regardless of accurate length estimation or not. Besides, the “true” path in the middle is not necessarily optimal or even realisable.

While the reduced graph cannot identify the “true” link length, it obtains paths which can account for the geographical reality of the Baltic Sea. Notice the concave bend of the coastline from north to south, which can only be represented with a set of short distance straight links. Additionally, further improvements of the GIS tool could account for regional conditions such as water depth or maritime protection to reroute paths across the water body accordingly. Such granular calibration would not be possible in the unprocessed topology graph.

Solution space granularity

The concentration of permissive links into common paths (c.f. dark blue sections from figure 5.1) shifts a part of the bundling optimisation from the market model into the GIS pre-processing. Hence the market model does not need to identify all bundling options on its own but receives some pre-solved options instead. For the discrete decision making in the market model, this resolves the challenge of differentiating solutions which are very close to each other. Branching and pruning of paths in the search tree are only possible if the optimiser identifies large enough objective function improvements or bounds. If an abundance of redundant links next to each other results in link lengths which hardly diverge from each other, the model wastes resources in climbing down the search tree without solution improvement.

Pre-solving redundant links or bundling overlapping paths into common permissive and chained links is thus a valid relaxation of the initial problem. In fact, it is the only option to maintain solvability for the model, without increasing the optimality gap threshold too much. Remember that this pre-solve is based on parameters which are subject to calibration. Therefore, the optimisation remains analytical, which facilitates the sensitivity analysis in the end. In this model, the parameters are calibrated such that the search radius for neighbours and density clusters is just large enough to link the most remote wind farm at least once. Notice that such a calibration looks different for water bodies other than the Baltic Sea since their coastline might be shaped differently.

5.2.2 Accuracy of market model

Resolution of technical components and time

Similarly to the sensitive input geodata, there are uncertainties involved in market modelling as well. They address the level of technical detail on which the offshore grid building blocks are modelled. Remember from the input data discussion, that the physical reality is simplified significantly to the benefit of the discrete decision making in the model. Besides, energy losses during conversion and transformation cannot be modelled. Consequently, no real power flow is calculated. The transport model only accounts for NTC values on given links. The physical reality is thus simplified to the extent that loop flows in the obtained meshes cannot be modelled.

While this ramification is usually most critical when modelling AC dominated onshore grids, it is less pronounced in an offshore DC grid. With converters being present on most DC platforms in the base case load flow is physically directly controllable, meaning that the adoption of a transport model is accurate enough in this analysis.

The simplified solution procedure with a warm start, topology optimisation and rerun of the model reduce accuracy as well. While the actual dispatch both for warm start and final model run are at higher time resolution the topology optimisation itself is only obtained on a reduced time series of infeed and demand situations. Analysing a higher diversity of climate years and more different utilisation situations of the grid could make the topology results more robust. Remember that this pitfall is partly addressed by a time series reduction strategy, which reduces the entire year in 25 h steps. This allows at least acknowledgement of seasonal and weekly demand patterns.

Finally, the demand side is fixed with zero price elasticity, meaning that flexible demand reacting to low and high market prices is neglected. Even though the TYNDP foresees a high increase in flexible demand, it is still simplified since the focus of attention is limited to the offshore grid. Arguably large shares of flexible demand could have an impact on power flows and eventually the power rating of newly installed links. They are, however, likely to be seen on the onshore grid first, which is simplified into zones. Refer to the Flex4RES study [45] for an analysis of transmission expansion with increased flexibility for the Nordic Energy system.

One shot and stepwise optimisation

The market model solves the dispatch with perfect foresight. Time series for RES infeed, demand and storage inflow are known in advance, which allows to match storage discharge and charge optimally with volatile generation and demand peaks. This creates a bias which utilises the storages more efficiently than would happen with stochastic operational planning. In addition, the hydro reservoirs are simplified quite substantially for the limited scope of this analysis. HÄRTEL & KORPÅS [39] provide a comprehensive overview of how to model hydro reservoirs adopting the water equivalent method. Such a model would be a desirable extension of the framework presented in this thesis for its relevance of bidirectional use of some parts of the offshore grid.

Perfect foresight is particularly enforced with the one-shot optimisation of the topology. The target year 2040 is chosen as a reference where all investments are made in. This assumption oversimplifies the true nature of offshore grid development for three reasons. First, some wind farms are scheduled for commissioning in 2030 already, meaning that their connection system is likely to be built before connecting wind farms in the timeline past 2030. Second, building the offshore grid at once is merely infeasible from a resource availability standpoint. BEMIP [11] estimates the workforce and material efforts required for a pan-Baltic offshore grid and results in several years of workforce required for realising such vast infrastructure investment. Third, the institutional framework for renewable energy targets and the investment climate is likely to change over time, as the past 20 years revealed in the German or Danish case, for instance.

Even when neglecting all these ramifications, one additional drawback remains unanswered by this thesis, namely the timely interdependency of grid investment. If the topology optimisation were performed stepwise in five-year intervals, for instance, it would be interesting to investigate if the final topology is still similar to this one-shot result. The underlying question is, whether the observed utilisation maximisation of links is of such high impact that the model makes no anticipatory investment. Hence, converters or links needed in later stages would not be built in advance for later stages to be utilised. In other words, a new trade-off is imposed, which weighs the costs from stranded assets in one stage against the benefits of “free” preset assets in subsequent stages.

With a sequentially and stepwise decision making, residual investment opportunities change over time, hence the permissive graph topology changes with it. Following the notion of the “no interconnector” sensitivity, this would impose a cascading preset of links until the final topology is reached. The sensitivity result suggests that indeed this could turn out as a different offshore grid. PROMOTION and GEA-BERMEDEZ et al. [72, 30] confirm this notion at the example of future north sea grid prospects.

Concluding the section on model limitations, the simplified nature of a linear cost model is emphasised. The nature of linear constraints and stepwise linear cost functions biases the model into extreme situations. The high link utilisations in the base case are one example of this. Simply put, the optimiser chooses one feasible solution and runs with it until another constraint becomes binding. If the model activates a link, it will be used as much as possible before another link is built. While this reflects the natural observation of bundling and leveraging of synergies, it may lead to a slight underestimation of actual investment cost. Actual cable lengths and investment cost should therefore be handled with care when comparing exact numbers with other analysis which used different parametrisations and cost function models. Besides, parameters which are not monetised cannot be taken into account by the market model. This includes contingencies, interoperability and indeed economic viability. Further aspects out of scope are discussed in the final section of this discussion chapter.

5.3 Rescope and further research need

Onshore grid

Internal congestion in the onshore grid is neglected in the analysis. Since each market area is aggregated into one bidding zone, only the cross-zonal bottlenecks appear in the model. Remember from the investigation of the two Swedish market areas SE04 and SE03 that such cross zonal bottlenecks can impact the resulting offshore topology significantly already. Not accounting for internal congestion within zones is therefore likely to overestimate the physical strength of the onshore transmission grid in 2040.

Aggregation of the German market area into one zone, for instance, neglects the strong need for North-South onshore reinforcements by 2040. As seen from the model, the total German load is connected directly to the onshore substations of Lubmin, Güstrow and others. Besides, the model cannot distinguish between the physical strengths of each onshore node beyond the hosting capacity limit of 4 GW or 2 GW, respectively. While Güstrow is physically the stronger node for its link to southern Germany [3], Lubmin and Bentwisch are located closer to the shoreline. Since the model merely accounts for distance and power throughput limit per node, Güstrow will always be connected “last”. For future improvements of the model, it should be investigated how the onshore landing of offshore infeed moves further inside the country when the onshore substations are modelled more accurately.

More accurate onshore grid modelling includes the opportunity to expand the grid either cross zonal or even internally. While cross zonal expansion options are easy to implement an accurate onshore grid modelling would face the challenging physical reality of an AC dominated system. Improving the transport model to sufficiently represent the onshore grid is hence far out of scope for its high computational complexity it would introduce into the problem. Modelling the offshore grid at the high granularity and simplifying the onshore grid into zones is considered a valid simplification for the demonstrational purpose of this thesis.

A first best improvement of the model could be to allow cross zonal capacity expansion. Thus, the initial cost trade-off between wind energy integration and line investment is restored onshore as well. An expected finding would be a slightly less centralised offshore topology. When the model needs to start paying for onshore grid reinforcements, some offshore transmission paths from the base case might be shifted onshore or removed entirely. In the most extreme case, the model might even “return” to more radial connections of wind farms since the bundling and concentration of onshore generation cannot be easily landed onshore anymore. Another finding could be increased curtailment or more not connected wind farms if internal onshore congestions are too high.

Including onshore grid reinforcement will also allow an investigation of the robustness of offshore interconnectors. The Øresund backbone relieves onshore congestion between SE04 and SE03 in all studied cases. If onshore grid expansion is allowed by the model and the Øresund backbone remains in the picture, it would signal a high added value to the offshore grid beyond mere interconnection of two onshore neighboured onshore market areas. Hence (cross zonal) onshore grid modelling allows to challenge the findings in this thesis for robustness.

Technical interoperability

The modular offshore transmission asset modelling allows fixed cost and variable cost accumulation in the objective function. By design, this leads to decimal units of Megawatts installed capacity of cables or converters, which diverges from reality where only discrete (integer) steps of ratings are available. Notice that such a notion of standardised assets is still included in the model with the offshore building blocks and a stepwise cost function to activate them. Due to the variable power rating, however, it leaves the discrete solution space and is relaxed into a continuous solution space. A follow up cost-benefit analysis

of actual installable equipment is, therefore, necessary to identify the “true” capacities per link and node and translate the continuous results back into discrete units of equipment.

Beyond the accuracy of component modelling, their interoperability is assumed without hurdle and power losses. The interoperability of DC chains with branches and “third legs” is yet to be proven for the offshore grid. Besides, interfaces from AC grids to overlaying DC grids are complex both in design operation. Refer to the studies of PROMOTION and MADARIAGA et al. [71, 49] for further elaboration on the technological trends and barriers for the realisation of complex offshore grid topologies. They also address the high uncertainty of available DC circuit breakers with such high-power ratings as required in the transmission grid. Alternative platform designs are discussed for alternative platform setups where switching is always done on AC side (no DC switching anymore) at the cost of much more converters being installed. Remember from the cost breakdown in figure 4.13 how these two components drive total equipment cost on the DC side.

Addressing interoperability also requires a contingency (n-1 cases) analysis of offshore transmission assets. This thesis assumes hubs and cables being available without interruptions. The system is rendered at a stable operation, and faults are neglected. Additionally, the model is allowed to operate links at rated capacity, meaning that no reliability margin is imposed for security. Acknowledging such parameters in the model is likely to result in less installed total transmission capacity compared to the base case since OPEX enter the cost trade-off. Besides, meshing might occur more frequently to create more redundancy for operational uncertainties. Find in GOMIS-BELLMUT et al. and VAN HERTEM & GHANDHARI [33, 79] for a comprehensive discussion of multiterminal transmission topologies for offshore grids.

For the connection of wind farms, this thesis allows AC and DC connections equally. As of date, there is, however, still a strong tendency to stick with AC systems for their lower technical complexity. With new stakeholders entering the market and new countries collecting first experience with offshore transmission assets it is yet to be seen if they indeed install DC systems from the beginning on or start with an AC infrastructure and expand from it. Lastly, new initiatives are announced recently to replace transmission cables entirely with a non electrical evacuation of wind power.²¹ It bases the energy evacuation on the Power-To-Gas technology. Electrical energy is converted offshore with electrolyzers into chemical energy (hydrogen) and exported by ship or pipeline [38]. Investigating the tipping point between cable systems and pipelines, i.e. switching from electrons to molecules, hence results in a separate offshore story to be investigated.

Economic feasibility

This thesis optimises a high-level offshore topology based on a pan-Baltic integrated optimisation. The resulting interconnection of market areas is therefore optimised from a European perspective, minimising the total cost. The impacts on welfare and other distributional aspects are out of scope in this analysis. Notice that the cost minimisation model is close to mimicking a welfare maximisation but not replicating it precisely. It merely investigates investment (CAPEX) into transmission assets and dispatch of power plants. Transmission OPEX, cost of redispatch and investment into generation capacity is excluded from the analysis. Hence, no true welfare gains can be derived from the results as such. Refer to [45] for an elaboration on distributional effects of large interconnection of the Nordics with the Baltic states.

Fixing the wind farms in the analysis implies their realisation at no cost as seen from the model. While the wind farm locations prove attractive from a resource potential point of view, their realisation is yet to be seen and only likely with revenues being high enough. An investigation of the revenues of offshore assets both for wind farms and cables can be found in TRABER et al. and RICHTS et al. [73, 61]. For Latvia and Denmark the benefit of installing offshore wind farms will crucially depend on the exporting

²¹three selected project initiatives: <https://bit.ly/3h1q4qc>, <https://bit.ly/32PwrYA> and <https://cnb.cx/3bpbuY1>

prospects into the future offshore grid. On the contrary, their existence is a crucial element in the link chains reaching out across the water body. Notice the interdependency of generation investment and transmission investment. The introduced notion that investment in grid usually follows investment in generation assets is, therefore questioned in this part. Nevertheless, the assumption of exact location and size of wind farms remains critical for the final topology results.

The realisation of wind farms and transmission assets happens in the context of an institutional framework and market conditions. Both are kept abstract in this thesis to the extent that a hypothetical party optimises the entire grid and assumes wind farms economically feasible in any case. Competing agents with cannibalisation of resources are ignored. Transnational barriers on the regulatory side are also assumed solved for each case where wind power is connected to a different jurisdiction from where it originates. In other words, permitting and operation of hybrid assets is not investigated in this thesis. Study DIWECON & NAVIGANT [32, 55] for an analysis of various operator models for offshore transmission assets. GERBAULET & WEBER and EGGERER et al. [31, 16] investigate the effects of different institutional frameworks on the investment climate and realisation of offshore grids.

When all wind farms in the analysis are indeed realised as listed, regions with high wind farm density experience cannibalisation of wind resources. PLATIS et al. and BALTICLINES [59, 14] reveal for the North Sea that wind farms cause widespread wake and shading. With predominating wind directions from west to east, wind farms in almost all clusters would face shading from previous clusters or individual wind farms further west. The estimation and implementation of wake losses in the availability time series are beyond the scope of this analysis. The latest they should be included in actual project-based cost-benefit and operation analysis.

Wrapping up the considerations on contribution, limits and further research needs, this thesis demonstrates the concept of pre-solving in the context of computationally complex, geographically large scale and technologically high-level transmission capacity expansion studies. A GIS analysis is introduced as an additional step in the commonly applied toolchain and the resulting topology results are discussed with respect to the toolchain performance and induced biases, given the set of parameters. While the results do not allow a derivation of future offshore grid deployment scenarios, they provide an insight of what the proposed toolchain is capable of. In addition, they pinpoint most crucial further research needs for future offshore grid development studies. Not least, the availability of input data both on assumed wind farm projects and national offshore wind power deployment strategies is identified as influential parameter. This thesis utilises a range of open-data sources both for geodata processing and market modelling and demonstrates which insights can be retrieved from it and where the limits arise. It stresses the rationale of a pan-European scope for future offshore grid studies and the benefit of cross-national cooperation when translating the climate protection targets into action.

6 Conclusion

Recap on the approach and scope of the thesis

Investigating the future offshore grid requires an analysis of wind farm locations, onshore landing prospects along with grid expansion needs and synergies that can be found when connecting both. On a high-level, the question arises which combination of offshore transmission assets is most beneficial to evacuate wind power to the shore and realise the interconnection of market areas. It leads to a twofold problem where the main part denotes a transmission capacity expansion problem, which is enhanced by a minor part projecting this problem into the physical reality of the water body with the help of a geographic information system (GIS). The purpose of this thesis is to demonstrate the performance of this twin-part division of the optimisation problem for the benefit of future offshore grid studies at the example of the Baltic Sea Region for 2040.

While most studies analyse the offshore grid scenario-based with predefined hubs, this thesis reverses this approach. Wind farms and onshore grid are fixed while the identification and connection to hubs are left to the model for optimisation. A mixed-integer linear problem (MILP) is set up, which makes discrete investment decisions for lines and hubs in the offshore region. They connect wind farms among each other, to additionally built hubs and eventually to the substations onshore. The level of complexity is limited to a high-level offshore grid topology. Its building blocks are activated on a modular basis while accumulating investment costs. The onshore grid expansion and detailed operational grid modelling are excluded from the analysis. The power flow is modelled as a transport model.

For the sizeable regional scope and the abundance of link combinations between wind farms and hubs in either voltage type, the solution space increases substantially. Joined with discrete decision investment making, the model quickly gets computationally infeasible to solve. Consequently, a presolve is introduced, which reduces the solution space while maintaining the analytical nature of the toolchain. The presolve is done in a GIS, which analyses the set of wind farms for density distribution and reachability among each other. A MiniMax group partitioning algorithm is presented, which structures and limits the solution space to a non-redundant set of permissive hub nodes for the clustering of wind farms. All nodes (wind farms, hubs and substations) are connected with permissive links, resulting in the final set up of a graph topology, which is substantially reduced in size and combinatorial complexity.

The linear market model adopts the graph topology. It iterates over the set of permissive links and nodes while activating them at a selected capacity wherever optimal. The optimality criterion is defined by a cost minimisation objective which enforces the trade-off between asset investment into the offshore grid building blocks and cost savings on the dispatch side. New lines and connections are built as long as they improve the objective function value. A sensitivity analysis investigates changes in the investment decisions when lifting three topological constraints which tighten the model solution space the most. They include assumptions on preset interconnectors, the strength of the onshore grid and enforcement of national radial wind farm connections.

Summary of the findings

In the Baltic Sea Region, most wind farms have at least one prospect of clustering. The GIS analysis reveals many permissive synergies for the future offshore grid topology. They include first, the centralised clustering of dense heaps with strong centre hubs, second, loose chains of wind farms and intermediate hubs in sparse heaps, and third, the connection of singular wind farms either radially or chained with neighbouring wind farms and heaps. Finally, planned but unbuilt interconnectors from TYNDP overlap with many heaps, resulting in an abundance of tee-in prospects for wind farms or intersections of two or more offshore interconnectors. The resulting permissive graph topology from the GIS pre-processing,

thus, reveals multiple prospects for future hybrid assets, pan-Baltic backbones or regionally limited chains of wind farms. At the same time, it “clears” the picture by reducing the complete graph topology to a light version for the benefit of subsequent discrete investment decision making in the market model.

Connecting wind farms into chains and clustering them into hubs is seen most optimal by the model. In the base case, all wind farms are part of the offshore grid, where only a minority is linked radially to the shore. This increases the concentration of wind infeed into the offshore grid beyond the mere locational and timely overlap of wind power generation. The offshore grid shows slightly undersized wind farm connections, meaning that the cable capacity is usually smaller than the rated wind farm capacity it connects.

Hybrid assets are installed in abundance across the water body. While AC chains are limited in regional scope, a pan-Baltic network of DC links is created. It is strongest on its North-South interconnection, reflecting mean bulk power flows from North to South. The capacity rating of most paths is realised asymmetrically with the stronger end facing towards the high demand side. Detours are created around congested onshore substations. Reverse power flows (South-North) signal utilisation of storages and reservoirs in the Nordics. The maximisation of wind power evacuation opportunities via hybrid assets is realised without redundant landing capacities. On balance, the landing capacity of the offshore grid is almost equal to the total installed wind farm capacity. Bundling of transmission tasks into common paths maximises link utilisation.

Removing the preset interconnectors from the solution space alters the topology towards a slightly more centralised topology design. The overall benefit of interconnecting market areas is, however, validated with similar cross border capacities between countries to the base case. Enforcing national radial connections for all wind farms tends to spill more offshore energy. It is either lost during operation with high curtailments or during installation, where the most remote locations are not connected at all. Redundant cable lengths and capacities dominate the picture. Simulating a strengthened onshore grid leads to a most centralised topology in this analysis. Cable lengths can be shortened with higher link-wise capacity ratings.

A high-level topology for the Baltic offshore grid is sensitive towards the exact location, capacity rating and generation profile of the wind farms in question. Its optimality crucially depends on the starting point of optimisation and planning horizon. Finally, the “first” binding constraints for the topology graph is the handling capacity of the onshore substations. For increasing the granularity of findings further research needs on interoperability, economic viability and regulatory feasibility of the future offshore grid are identified.

This thesis demonstrates that a twin-part division of the initial optimisation problem not only improves the overall performance of the toolchain. In fact, the pre-solve results allow first insights on future topology prospects without complex market modelling. The framework for offshore grid infrastructure optimisation, therefore, benefits from a thorough GIS pre-analysis for reasons of computational performance, data uniformity and parametrised scenario building. Not least does it reveal the benefit of leveraging hidden data in the sea for a large regional scope, such as the Baltic Sea Region. Optimising the future offshore grid is thus a quest of pan-European scale.

References

- [1] Baltic Sea, 2019. URL <https://www.britannica.com/place/Baltic-Sea>.
- [2] 3E, Dena, EWEA, and SINTEF. Offshore Electricity Grid Infrastructure in Europe. Technical report, European Commission, 2011. URL https://ec.europa.eu/energy/intelligent/projects/sites/iee-projects/files/projects/documents/offshoregrid_offshore_electricity_grid_infrastructure_in_europe_en.pdf.
- [3] 50Hertz, Amprion, TenneT, and TransnetBW. Netzentwicklungsplan 2030 V2019 Entwurf, 2019. URL https://www.netzentwicklungsplan.de/sites/default/files/paragraphs-files/NEP_2030_V2019_1_Entwurf_Teil1.pdf.
- [4] ACER and ENTSO-E. Joint task force cross border redispatch - Flow definitions, 2015. URL https://docstore.entsoe.eu/Documents/MC%20documents/150929_Joint%20Task%20Force%20Cross%20Border%20Redispatch%20Flow%20Definitions.pdf.
- [5] P. Ahlhaus and P. Stursberg. Transmission capacity expansion: An improved Transport Model. In *IEEE PES ISGT Europe 2013*, pages 1–5. IEEE, Lyngby, Denmark, Oct. 2013. ISBN 978-1-4799-2984-9. URL <http://ieeexplore.ieee.org/document/6695322/>.
- [6] N. Alguacil, A. Motto, and A. Conejo. Transmission expansion planning: a mixed-integer LP approach. *IEEE Transactions on Power Systems*, 18(3):1070–1077, Aug. 2003. ISSN 0885-8950. URL <http://ieeexplore.ieee.org/document/1216148/>.
- [7] D. B. Avdic and P. Ståhl. Baltic InteGrid review: towards a meshed offshore grid in the Baltic Sea. Technical report, Baltic InteGrid, 2019. URL http://www.baltic-integrid.eu/files/baltic_integrid/Arbeitspaket%202020/WP%203%20Development%20of%20the%20Baltic%20Grid%20Concept/3.7%20-%20High-Level%20Concept/Baltic%20InteGrid:%20towards%20a%20meshed%20offshore%20grid%20in%20the%20Baltic%20Sea_FINAL%20REPORT.pdf.
- [8] J. Bezanson, A. Edelman, S. Karpinski, and V. B. Shah. Julia: A Fresh Approach to Numerical Computing. *SIAM Review*, 59(1):65–98, Jan. 2017. ISSN 0036-1445, 1095-7200. URL <https://epubs.siam.org/doi/10.1137/141000671>.
- [9] R. Bill. *Grundlagen der Geo-Informationssysteme: 6. Auflage*. Wichmann, Berlin, 2016. ISBN 978-3-87907-607-9.
- [10] Bundesamt für Seeschifffahrt und Hydrographie, BSH. Flächenentwicklungsplan 2019 für die deutsche Nord- und Ostsee, 2019. URL https://www.bsh.de/DE/PUBLIKATIONEN/_Anlagen/Downloads/Offshore/FEP/Flaechenentwicklungsplan_2019.html.
- [11] COWI, THEMA Consulting group, and Ea Energy Analyses. Study on Baltic offshore wind energy cooperation under BEMIP: final report. Technical report, European Commission, 2019. URL http://publications.europa.eu/publication/manifestation_identifier/PUB_MJ0419544ENN.
- [12] Danish Energy Agency. Finscreening af Havarealer til etablering af nye hvymøllerparker med direkte forbindelse til land. Technical report, Energistyrelsen DK, 2020. URL https://ens.dk/sites/ens.dk/files/Vindenergi/1-0_finscreening_af_havarealer_til_ny_havvind_med_direkte_forbindelse_til_land.pdf.
- [13] K. Das and N. A. Cutululis. Offshore Wind Power Plant Technology Catalogue - Components of wind power plants, AC collection systems and HVDC systems. Technical report, Baltic InteGrid, 2017. 67 pp. URL https://backend.orbit.dtu.dk/ws/files/143240154/Technology_Catalogue_final.pdf.
- [14] Deutsche Windguard. Capacity densities of european offshore wind farms. Technical report, Baltic Lines, 2018. URL <https://vasab.org/document/capacity-densities-of-european-offshore-wind-farms/>.
- [15] I. Dunning, J. Huchette, and M. Lubin. JuMP: A Modeling Language for Mathematical Optimization. *SIAM Review*, 59(2):295–320, Jan. 2017. ISSN 0036-1445, 1095-7200. URL <https://epubs.siam.org/doi/10.1137/15M1020575>.

- [16] J. Egerer, F. Kunz, and C. v. Hirschhausen. Development scenarios for the North and Baltic Seas Grid – A welfare economic analysis. *Utilities Policy*, 27:123–134, Dec. 2013. ISSN 09571787. URL <https://linkinghub.elsevier.com/retrieve/pii/S095717871300060X>.
- [17] Energiföretagen Sverige. Kraftläget i Sverige Vattensituationen, 2020. URL <https://www.energiforetagen.se/statistik/kraftlaget/kraftlagets-arkiv/>. Library Catalog: www.nve.no.
- [18] ENTSO-E. Regional Insight Report - Focus on the Nordic and Baltic Sea. Technical report, 2018. URL https://eepublicdownloads.blob.core.windows.net/public-cdn-container/clean-documents/tyndp-documents/TYNDP2018/consultation/PCI%20Region/ENTSO_TYNDP_2018_Nordic_Baltic_Sea.pdf.
- [19] ENTSO-E. Position on Offshore Development. Technical report, 2020. URL https://eepublicdownloads.blob.core.windows.net/public-cdn-container/clean-documents/Publications/Position%20papers%20and%20reports/entso-e_pp_Offshore_Development_16p_200526.pdf.
- [20] ENTSO-E and ENTSO-G. TYNDP 2020 scenario report, 2020. URL https://www.entsos-tyndp2020-scenarios.eu/wp-content/uploads/2020/06/TYNDP_2020_Joint_ScenarioReport_final.pdf.
- [21] M. Ester, H.-P. Kriegel, J. Sander, and X. Xu. A Density-Based Algorithm for Discovering Clusters in Large Spatial Databases with Noise. *1996*, 96(34):226–231, 1996. URL <https://www.aaai.org/Papers/KDD/1996/KDD96-037.pdf>.
- [22] European Commission. 2050 long-term strategy, 2016. URL https://ec.europa.eu/clima/policies/strategies/2050_en. Library Catalog: ec.europa.eu.
- [23] European Commission. Introduction to MSP, 2018. URL <https://www.msp-platform.eu/msp-eu/introduction-msp>. Library Catalog: www.msp-platform.eu.
- [24] European Commission, COWI, THEMA Consulting group, and Ea Energy Analyses. Study on Baltic offshore wind energy cooperation under BEMIP: final report. Technical report, 2019. URL http://publications.europa.eu/publication/manifestation_identifier/PUB_MJ0419544ENN.
- [25] European Commission, European Parliament, and European Council. Communication from the Commission - The European Green Deal, 2019. URL <https://eur-lex.europa.eu/legal-content/EN/TXT/?uri=COM:2019:640:FIN>.
- [26] European Parliament and European Council. Directive 2014/89/EU establishing a framework for maritime spatial planning, July 2014. URL <http://data.europa.eu/eli/dir/2014/89/oj>.
- [27] European Parliament and European Council. Regulation 2018/1999 on the Governance of the Energy Union and Climate Action, Dec. 2018. URL <http://data.europa.eu/eli/reg/2018/1999/oj>.
- [28] EWEA. TradeWind – Developing Europe’s power market for large scale integration of wind power. Technical report, 2009. URL <https://backend.orbit.dtu.dk/ws/portalfiles/portal/195981748/Fulltext.pdf>.
- [29] Finnish Wind Power Association, STU. Wind power projects in Finland, 2020. URL <https://www.tuulivoimayhdistys.fi/en/wind-power-in-finland/wind-power-projects-in-finland/wind-power-projects-in-finland>.
- [30] J. Gea-Bermúdez, L.-L. Pade, M. J. Koivisto, and H. Ravn. Optimal generation and transmission development of the North Sea region: Impact of grid architecture and planning horizon. *Energy*, 191:116512, Jan. 2020. ISSN 03605442. URL <https://linkinghub.elsevier.com/retrieve/pii/S0360544219322078>.
- [31] C. Gerbaulet and A. Weber. When regulators do not agree: Are merchant interconnectors an option? Insights from an analysis of options for network expansion in the Baltic Sea region. *Energy Policy*, 117:228–246, June 2018. ISSN 03014215. URL <https://linkinghub.elsevier.com/retrieve/pii/S0301421518300934>.

- [32] Y. Girard. Market design for an efficient transmission of offshore wind energy. Technical report, DIW Econ, 2019. URL http://diw-econ.de/en/wp-content/uploads/sites/2/2019/05/DIW-Econ_2019_Market-design-for-an-efficient-transmission-of-offshore-wind-energy.pdf.
- [33] O. Gomis-Bellmunt, J. Liang, J. Ekanayake, R. King, and N. Jenkins. Topologies of multiterminal HVDC-VSC transmission for large offshore wind farms. *Electric Power Systems Research*, 81(2): 271–281, Feb. 2011. ISSN 03787796. URL <https://linkinghub.elsevier.com/retrieve/pii/S0378779610002166>.
- [34] J. Gorenstein Dedecca, R. A. Hakvoort, and P. M. Herder. Transmission expansion simulation for the European Northern Seas offshore grid. *Energy*, 125:805–824, Apr. 2017. ISSN 03605442. URL <https://linkinghub.elsevier.com/retrieve/pii/S0360544217302931>.
- [35] Havs- och Vattenmyndigheten. Havsplaner för Bottniska viken, Östersjön och Västerhavet: Förslag till regeringen, 2019. URL <https://www.havochvatten.se/download/18.4705beb516f0bcf57ce1b184/1576572386069/forslag-till-havsplaner.pdf>.
- [36] C. v. Hirschhausen. Green electricity investment in Europe - Development scenarios for generation and transmission investments. Technical report, European Investment Bank, 2012. 30 pp. URL <http://hdl.handle.net/10419/88100>.
- [37] H. Hirth. *Grundzüge der Finanzierung und Investition*. Oldenbourg Verlag, München, 3., überarbeitete und erweiterte auflage edition, 2012. ISBN 978-3-486-70211-8 978-3-486-70971-1. OCLC: 761830278.
- [38] P. Hou, P. Enevoldsen, J. Eichman, W. Hu, M. Z. Jacobson, and Z. Chen. Optimizing investments in coupled offshore wind -electrolytic hydrogen storage systems in Denmark. *Journal of Power Sources*, 359:186–197, Aug. 2017. ISSN 03787753. URL <https://linkinghub.elsevier.com/retrieve/pii/S0378775317306882>.
- [39] P. Härtel and M. Korpås. Aggregation Methods for Modelling Hydropower and Its Implications for a Highly Decarbonised Energy System in Europe. *Energies*, 10(11):1841, Nov. 2017. ISSN 1996-1073. URL <http://www.mdpi.com/1996-1073/10/11/1841>.
- [40] P. Härtel, T. K. Vrana, T. Hennig, M. von Bonin, E. J. Wiggelinkhuizen, and F. D. Nieuwenhout. Review of investment model cost parameters for VSC HVDC transmission infrastructure. *Electric Power Systems Research*, 151:419–431, Oct. 2017. ISSN 03787796. URL <https://linkinghub.elsevier.com/retrieve/pii/S0378779617302572>.
- [41] Isaac-Camilo Gonzalez-Romero, S. Wogrin, and T. Gomez. Proactive transmission expansion planning with storage considerations. *Energy Strategy Reviews*, 24:154–165, Apr. 2019. ISSN 2211467X. URL <https://linkinghub.elsevier.com/retrieve/pii/S2211467X19300227>.
- [42] Jan Rączka. Offshore Energy - Downwind or upwind? Technical report, Forum Energii, 2018. URL https://www.agora-energiewende.de/fileadmin2/Partnerpublikationen/2018/Forum_Energii_Offshore_Energy/Offshore_energy._Downwind_or_upwind_final_en.pdf.
- [43] Johannes Hüffmeier and Mats Goldberg. Offshore wind and grid in the Baltic Sea - Status and outlook until 2050. Technical report, Swedish Agency for Marine and Water Management, 2019. URL https://www.google.com/url?sa=t&rct=j&q=&esrc=s&source=web&cd=&cad=rja&uact=8&ved=2ahUKEwjev06Zx9fqAhXJsaQKHYWyAbUQFjAAegQIBhAB&url=https%3A%2F%2Fvasab.org%2Fdocument%2Foffshore-wind-and-grid-in-the-baltic-sea-status-and-outlook-until-2050%2F&usq=A0vVaw2XFLbUVJ9-aiKs_QJ2U4AJ.
- [44] D. Jovicic and K. Ahmed. *High-voltage direct-current transmission: converters, systems and DC grids*. Wiley, Chichester, West Sussex, United Kingdom, 2015. ISBN 978-1-118-84666-7.
- [45] Klaus Skytte, Claire Bergaentzlé, Felipe Junqueira Fausto, and Philipp Andreas Gunkel. Flexible Nordic Energy Systems - Flex4RES summary report. Technical report, Nordic Energy Research, 2019. URL https://www.nordicenergy.org/wp-content/uploads/2019/07/Flex4RES_final_summary_report_aug2019.pdf.
- [46] Kleipeda university coastal research and planning institute. Supplement of the general plan of republic of Lithuania by marine areas - Summar of strategic environmental assessment report, 2013. URL http://www.vpvb.gov.lv/data/files/Marine_Summary_of_SEA.PDF.

- [47] I. Konstantelos, D. Pudjianto, G. Strbac, J. De Decker, P. Joseph, A. Flament, P. Kreutzkamp, F. Genoese, L. Rehfeldt, A.-K. Wallasch, G. Gerdes, M. Jafar, Y. Yang, N. Tidemand, J. Jansen, F. Nieuwenhout, A. van der Welle, and K. Veum. Integrated North Sea grids: The costs, the benefits and their distribution between countries. *Energy Policy*, 101:28–41, Feb. 2017. ISSN 03014215. URL <https://linkinghub.elsevier.com/retrieve/pii/S0301421516306206>.
- [48] A. Korompili, Q. Wu, and H. Zhao. Review of VSC HVDC connection for offshore wind power integration. *Renewable and Sustainable Energy Reviews*, 59:1405–1414, June 2016. ISSN 13640321. URL <https://linkinghub.elsevier.com/retrieve/pii/S1364032116000940>.
- [49] A. Madariaga, J. Martín, I. Zamora, I. Martínez de Alegría, and S. Ceballos. Technological trends in electric topologies for offshore wind power plants. *Renewable and Sustainable Energy Reviews*, 24:32–44, Aug. 2013. ISSN 13640321. URL <https://linkinghub.elsevier.com/retrieve/pii/S1364032113001986>.
- [50] L. Meeus. Offshore grids for renewables: do we need a particular regulatory framework? *Economics of Energy & Environmental Policy*, 4(1), Jan. 2015. ISSN 21605882. URL <http://www.iaee.org/en/publications/eeeparticle.aspx?id=81>.
- [51] Ministry of Environmental Protection and Regional Development of the Republic of Latvia. Maritime Spatial Plan Latvia, 2019. URL http://www.varam.gov.lv/eng/darbibas_veidi/maritime_spatial_planning/.
- [52] Ministry of Maritime Economy and Inland Navigation of Poland. Spatial development plan for the internal sea waters, territorial sea and the exclusive economic zone - executive summary and provisions for neighbouring zones, 2019. URL <http://www.naturvardsverket.se/upload/stod-i-miljoarbetet/remisser-och-yttranden/esbo-arenden/polen-havsplan/6Executive-Summary.pdf>.
- [53] Ministry of Maritime Economy and Inland Navigation of Poland. Spatial development plan for the internal sea waters, territorial sea and the exclusive economic zone - general provisions, 2019. URL [MinistryofMaritimeEconomyandInlandNavigationofPoland](http://www.naturvardsverket.se/upload/stod-i-miljoarbetet/remisser-och-yttranden/esbo-arenden/polen-havsplan/6Executive-Summary.pdf).
- [54] A. Mitchell. *The ESRI guide to GIS analysis - Volume 3: Modeling Suitability, Movement, and Interaction*, volume 3. Esri Press, Redlands, Calif, 2012. ISBN 978-1-879102-06-4 978-1-58948-305-7.
- [55] Navigant. Connecting offshore wind farms - A comparison of offshore offshore electricity grid development models in northwest Europe. Technical report, 2019. URL <https://guidehouse.com/-/media/www/site/downloads/energy/2019/2019-navigant-comparison-offshore-grid-development.pdf>.
- [56] Noregs vassdrags- og energidirektorat (NVE). Magasin statistikk, 2020. URL <https://www.nve.no/energiforsyning/kraftmarkedsdata-og-analyser/magasinstatistikk/>. Library Catalog: www.nve.no.
- [57] Open Power System Data. Data Package Time series - Version 2019-06-05, 2019. URL https://doi.org/10.25832/time_series/2019-06-05.
- [58] S. Pfenninger and I. Staffell. Long-term patterns of European PV output using 30 years of validated hourly reanalysis and satellite data. *Energy*, 114:1251–1265, Nov. 2016. ISSN 03605442. URL <https://linkinghub.elsevier.com/retrieve/pii/S0360544216311744>.
- [59] A. Platis, S. K. Siedersleben, J. Bange, A. Lampert, K. Bärfuss, R. Hankers, B. Cañadillas, R. Foreman, J. Schulz-Stellenfleth, B. Djath, T. Neumann, and S. Emeis. First in situ evidence of wakes in the far field behind offshore wind farms. *Scientific Reports*, 8(1):2163, Dec. 2018. ISSN 2045-2322. URL <http://www.nature.com/articles/s41598-018-20389-y>.
- [60] Rahandusministeerium. Estonian Maritime Spatial Plan, 2019. URL http://mereala.hendrikson.ee/dokumendid/Eskiis/Estonian_MSP_draft_plan_ENG.pdf.
- [61] C. Richts, M. Jansen, and M. Siefert. Determining the Economic Value of Offshore Wind Power Plants in the Changing Energy System. *Energy Procedia*, 80:422–432, 2015. ISSN 18766102. URL <https://linkinghub.elsevier.com/retrieve/pii/S1876610215021785>.
- [62] Rolv Erlend Bredese, René Cattin, Niels-Erik Clausen, and Neil Davis. Wind energy projects in cold climates. Technical report, IEA Wind TCP, 2017. URL

- <https://community.ieawind.org/HigherLogic/System/DownloadDocumentFile.ashx?DocumentFileKey=04b5c3d8-9a6f-7d9a-c1d6-aa848027ca1d&forceDialog=0>
- [63] R. Romero, A. Monticelli, A. Garcia, and S. Haffner. Test systems and mathematical models for transmission network expansion planning. *IEEE Proceedings - Generation, Transmission and Distribution*, 149(1):27, 2002. ISSN 13502360. URL https://digital-library.theiet.org/content/journals/10.1049/ip-gtd_20020026.
- [64] S. J. Russell and P. Norvig. *Artificial intelligence: a modern approach*. Prentice Hall series in artificial intelligence. Pearson, Boston Columbus Indianapolis New York San Francisco, third edition, global edition edition, 2016. ISBN 978-1-292-15396-4 978-0-13-604259-4 978-0-13-207148-2. OCLC: 945899984.
- [65] H. Seifert. Technical requirements for rotor blades operating in cold climate. *Proceedings of Boreas VI*, Jan. 2004. URL https://www.researchgate.net/publication/266099142_Technical_requirements_for_rotor_blades_operating_in_cold_climate.
- [66] R. Sharma. *Electrical structure of future offshore wind power plant with a high voltage direct current power transmission*. PhD Thesis, Technical University of Denmark DTU, 2012. URL <https://orbit.dtu.dk/en/projects/electrical-structure-of-future-offshore-wind-turbine-farms-with-a>.
- [67] I. Staffell and S. Pfenninger. Using bias-corrected reanalysis to simulate current and future wind power output. *Energy*, 114:1224–1239, Nov. 2016. ISSN 03605442. URL <https://linkinghub.elsevier.com/retrieve/pii/S0360544216311811>.
- [68] H. G. Svendsen. Planning Tool for Clustering and Optimised Grid Connection of Offshore Wind Farms. *Energy Procedia*, 35:297–306, 2013. ISSN 18766102. URL <https://linkinghub.elsevier.com/retrieve/pii/S187661021301268X>.
- [69] Swedish Meteorological and Hydrological Institute SMHI. Ice conditions in the Baltic, 2017. URL <https://www.smhi.se/en/theme/ice-conditions-in-the-baltic-1.12257>.
- [70] TenneT, DNV-GL, Energinet, FGH, Tractebel, and Carbon Trust. Promotion D12.2 Optimal Scenario for the Development of a Future European Offshore Grid. Technical report, Promotion Offshore, 2020. 273 pp. URL https://www.promotion-offshore.net/fileadmin/PDFs/D12.2_-_Optimal_Scenario_for_the_Development_of_a_Future_European_Offshore_Grid.pdf.
- [71] TenneT, DNV-GL, and KU Leuven. Promotion D1.1 Detailed description of the requirements that can be expected per work package. Technical report, Promotion Offshore, 2016. URL https://www.promotion-offshore.net/fileadmin/PDFs/160415_PROMOTION_WP1_D.1.1_V1.0.pdf.
- [72] TenneT, Energinet, DNV-GL, Carbon Trust, Ørsted, Tractebel, and FGH. Promotion D12.3 Draft Deployment Plan. Technical report, Promotion Offshore, 2020. 195 pp. URL https://www.promotion-offshore.net/fileadmin/PDFs/D12.3_-_Draft_Deployment_Plan.pdf.
- [73] T. Traber, H. Koduvere, and M. Koivisto. Impacts of offshore grid developments in the North Sea region on market values by 2050: How will offshore wind farms and transmission lines pay? In *2017 14th International Conference on the European Energy Market (EEM)*, pages 1–6. IEEE, Dresden, Germany, June 2017. ISBN 978-1-5090-5499-2. URL <http://ieeexplore.ieee.org/document/7981945/>.
- [74] T. Trötscher and M. Korpås. A framework to determine optimal offshore grid structures for wind power integration and power exchange: A framework to determine optimal offshore grid structures. *Wind Energy*, 14(8):977–992, Nov. 2011. ISSN 10954244. URL <http://doi.wiley.com/10.1002/we.461>.
- [75] UBA. Potential der Windenergie an Land, 2013. URL https://www.umweltbundesamt.de/sites/default/files/medien/378/publikationen/potenzial_der_windenergie.pdf.
- [76] United Nations. Convention on the law of the sea: Part II Territorial sea and contiguous zone, Nov. 1994. URL https://www.un.org/Depts/los/convention_agreements/texts/unclos/part2.htm.
- [77] United Nations. Convention on the law of the sea: Part V Exclusive economic zone, Nov. 1994. URL https://www.un.org/Depts/los/convention_agreements/texts/unclos/part5.htm.

- [78] United Nations. Paris Agreement - Report of the Conference of the Parties on its twenty-first session, 2015. URL http://unfccc.int/files/essential_background/convention/application/pdf/english_paris_agreement.pdf.
- [79] D. Van Hertem and M. Ghandhari. Multi-terminal VSC HVDC for the European supergrid: Obstacles. *Renewable and Sustainable Energy Reviews*, 14(9):3156–3163, Dec. 2010. ISSN 13640321. URL <https://linkinghub.elsevier.com/retrieve/pii/S1364032110002480>.
- [80] A.-K. Wallasch, R. Borrmann, T. Künne, R. Weinhold, and C. Gerbaulet. Cost-benefit Analysis of an Integrated Offshore Grid in the Baltic Sea. Technical report, Baltic InteGrid, 2019. 64 pp. URL http://www.baltic-integrid.eu/index.php/download.html?file=files/baltic_integrid/Arbeitspaket%202/WP%203%20Development%20of%20the%20Baltic%20Grid%20Concept/3.6%20Cost%20Benefit%20Analysis/BIG_3.6_Cost-Benefit%20Analysis_final.pdf.
- [81] J. Weibezahn and M. Kendziorski. Illustrating the Benefits of Openness: A Large-Scale Spatial Economic Dispatch Model Using the Julia Language. *Energies*, 12(6):1153, Mar. 2019. ISSN 1996-1073. URL <https://www.mdpi.com/1996-1073/12/6/1153>.
- [82] WindEurope. Wind energy in Europe in 2019 - Trends and statistics. Technical report, 2020. URL <https://windeurope.org/data-and-analysis/product/wind-energy-in-europe-in-2019-trends-and-statistics/>.